Modelling and simulation of multitechnological machine systems

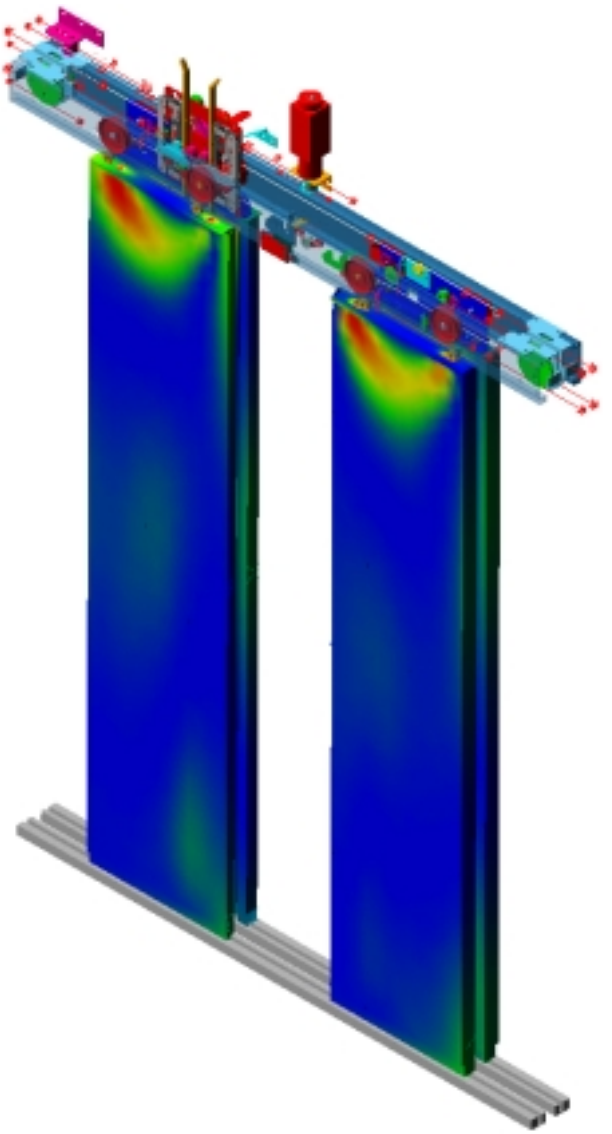

TECHNICAL RESEARCH CENTRE OF FINLAND ESPOO 2001

VTT SYMPOSIUM 209

Keywords:
smart machines, mechatronics, simulation, models, condition monitoring, machinery, vibration, noise reduction, sound transmission, hydraulic equipment

Modelling and simulation of multitechnological machine systems

Espoo, 30.11.2000

Edited by

Timo Holopainen

VTT Manufacturing Technology

Organised by

VTT Manufacturing Technology

TECHNICAL RESEARCH CENTRE OF FINLAND
ESPOO 2001

ISBN 951–38–5712–3 (soft back ed.)
ISSN 0357–9387 (soft back ed.)

ISBN 951–38–5713–1 (URL: http://www.inf.vtt.fi/pdf/)
ISSN 1455–0873 (URL: http://www.inf.vtt.fi/pdf/)

JULKAISIJA – UTGIVARE – PUBLISHER

Valtion teknillinen tutkimuskeskus (VTT), Vuorimiehentie 5, PL 2000, 02044 VTT
puh. vaihde (09) 4561, faksi 456 4374

Statens tekniska forskningscentral (VTT), Bergsmansvägen 5, PB 2000, 02044 VTT
tel. växel (09) 4561, fax 456 4374

Technical Research Centre of Finland (VTT), Vuorimiehentie 5, P.O.Box 2000, FIN–02044 VTT, Finland
phone internat. + 358 9 4561, fax + 358 9 456 4374

VTT Valmistustekniikka, Laiva- ja konetekniikka, Tekniikantie 12, PL 1705, 02044 VTT
puh. vaihde (09) 4561, faksi (09) 456 5888

VTT Tillverkningsteknik, Skepps- och maskinteknik, Teknikvägen 12, PB 1705, 02044 VTT
tel. växel (09) 4561, fax (09) 456 5888

VTT Manufacturing Technology, Maritime and Mechanical Engineering,
Tekniikantie 12, P.O.Box 1705, FIN–02044 VTT, Finland
phone internat. + 358 9 4561, fax + 358 9 456 5888

Text preparing Arja Grahn

Otamedia Oy, Espoo 2001

Preface

The goal of the Smart Machines and Systems 2010 (SMART) technology programme 1997–2000 was to help the machine and electromechanical industries in incorporating the modern technology into their products and processes. The public research projects in this programme were planned to accumulate the latest research results and transfer them for the benefit of industrial product development.

The major research topic in the SMART programme was called Modelling and Simulation of Multitechnological Mechatronic Systems. The behaviour of modern machine systems and subsystems addresses many different types of physical phenomena and their mutual interactions: mechanical behaviour of structures, electromagnetic effects, hydraulics, vibrations and acoustics etc. together with associated control systems and software.

The aim was to develop generic principles and methodologies to enable comprehensive simulation of machine systems for product development and condition monitoring needs within selected industrial cases. The actual research was carried out in three separate projects called Modelling and Simulation of Mechtronic Machine Systems for Product Development and Condition Monitoring Purposes (MASI), Virtual Testing of Hydraulically Driven Machines (HYSI), and Control of Low Frequency Vibration of a Mobile Machine (AKSUS).

This publication contains the papers presented at the final seminar of these three research projects, held on 30.11.2000 at Otaniemi Espoo. The papers highlight the latest research results. In addition to this seminar, tens of other papers were presented in several conferences, and published in journals or in report series. Also two doctor's theses and several master's and licentiate's theses were accomplished within these projects.

In this context, I would like to take the opportunity to thank all the people involved in these research projects at Helsinki, Lappeenranta and Tampere Universities of Technology, at VTT as well as at participating companies ABB Industry, KONE Elevators, Metso Paper, Nordberg-Lokomo, Plustech, Nokian Tyres and Valtra, for a very active participation and fruitful co-operation. By far,

the biggest part of the funding was provided by TEKES, the National Technology Agency, which, besides funding, deserves special thanks for a very active and supporting role throughout the whole research work.

Espoo 18.01.2001 Matti K. Hakala

Contents

Magnetic forces calculation for noise analysis of electrical machines

Anouar Belahcen
Helsinki University of Technology
Espoo, Finland

Abstract

This paper reviews the different methods for local force calculation in magnetised iron core and current carrying conductors in electrical apparatus. Three different methods are reviewed and the errors of each are discussed. These methods are implemented and applied to a simple model to verify them. To check the accuracy of the methods, the size and amount of elements in the FEM model are changed. The results of these computations are compared to such conventional methods as Lorentz forces and Maxwell stress tensor method. This paper also shows the theoretical equivalence between the methods discussed.

1. Introduction

The total force acting on any part of electrical apparatus can be easily calculated from the solution of the magnetic field using either the Maxwell tensor, the Lorentz formula or the virtual work method. [1]. These methods are well known and their accuracy is a reasonable statement. However, the analysis of vibrations and noise in electrical machines requires a detailed knowledge of the force distribution both on the surface of the iron and inside it. Many authors have worked with this subject and come up with different methods to calculate the nodal forces in magnetised iron cores [2–6]. These methods also show the forces on the interface between the iron core and air as well as the force acting on current carrying conductors. The purpose of this paper is to summarise the methods presented in the literature and use them as a simple model to show their equivalence. The paper, deals also with the error related to the calculation of nodal forces in respect to the error introduced by the finite element method. The

theoretical equivalence between the reviewed methods is also shown in this work.

2. Methods

2.1 Energy methods

Two energy methods can be found from the published literature. The first one (herein energy method 1) gives the magnetic energy of one element as:

$$W = \int_0^{\boldsymbol{B}} \boldsymbol{H} \cdot \mathrm{d}\boldsymbol{B}\, \mathrm{d}V_\mathrm{e} \tag{1}$$

And the contribution of the element to the nodal force as [3]:

$$F = -\frac{\partial W}{\partial s} = -\frac{\partial}{\partial s}\left(\int_0^{\boldsymbol{B}} \boldsymbol{H} \cdot \mathrm{d}\boldsymbol{B}\, \mathrm{d}V_\mathrm{e} \right) \tag{2}$$

The second one (herein energy method 2) gives the magnetic energy as [5]:

$$W = \int_0^{A} \boldsymbol{J}^\mathrm{T} \mathrm{d}\boldsymbol{A} \tag{3}$$

where $\boldsymbol{J}$ is the source term in the FEM equations: $\boldsymbol{M}\,\boldsymbol{A} = \boldsymbol{J}$

The nodal force is then [5]:

$$\boldsymbol{F} = -\frac{\partial W}{\partial \boldsymbol{s}} = -\int_0^{\boldsymbol{A}} \boldsymbol{A}^T \frac{\partial \boldsymbol{M}(\boldsymbol{A}, \boldsymbol{s})}{\partial \boldsymbol{s}} d\boldsymbol{A} \tag{4}$$

2.2 Tensor method

The tensor method is based on the Maxwell stress tensor. The tensor is defined as [4]:

$$\boldsymbol{T} = \left[H_i B_k - \delta_{ik} \int_0^{H} \boldsymbol{B} \cdot \mathrm{d}\boldsymbol{H} \right] \tag{5}$$

The contribution to the i[th] component of nodal force on the n[th] node from one element is [4]:

$$F_{ni} = -\int T_{ik} \partial_k N_n \mathrm{d}\Omega \tag{6}$$

2.3 Equivalence of the methods

The two energy methods and the tensor method are actually equivalents. To show this, let us take the incremental change of the energy density:

$$\delta W = \boldsymbol{H} \cdot \delta \boldsymbol{B} = \boldsymbol{H} \cdot (\nabla \times \delta \boldsymbol{A}) = (\nabla \times \boldsymbol{H}) \cdot \delta \boldsymbol{A} \tag{7}$$

Using

$$\boldsymbol{J} = \nabla \times \boldsymbol{H} \tag{8}$$

one gets:

$$\int_0^B \boldsymbol{H} \cdot \mathrm{d}\boldsymbol{B} = \int_0^A \boldsymbol{J} \cdot \mathrm{d}\boldsymbol{A} \tag{9}$$

The equivalence with the tensor method is demonstrated in Ref. [4].

2.4 Error induced by the method

In the standard formulation of the magnetic vector potential in the FE-method, the normal component of the magnetic induction is forced to be continuous while the tangential component of the magnetic field is not necessarily continuous. The ideal case is shown in Fig. 1. The discontinuity in the field across the element's boundary behaves like a current density according to Eq. (8) [7]. The extra current density introduces an error in Eq. (3). Hence, the error in the calculation of the forces.

Figure 1. Boundary conditions at element borders.

3. Application

The three methods mentioned above have been implemented and used in the following model. The model consists of a centre pole between yokes with a small gap. The geometry of the model and the FEM mesh are shown in Fig. 2. The calculated nodal forces are exactly the same for all three methods. The nodal forces for the FEM mesh of Fig. 2 are shown in Fig. 3.

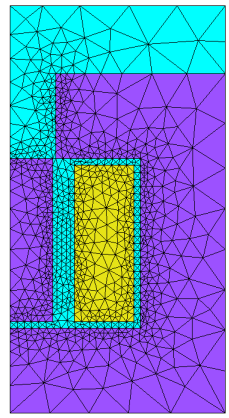

Figure 2. Geometry and FEM mesh of half the model.

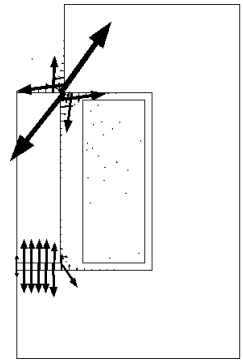

Figure 3. Nodal forces.

The mesh of Fig. 2 was adaptively refined. The total force acting on the iron pole and on the current currying conductor are calculated. The nodal force method and either the Maxwell stress sensor (for the iron pole) or the Lorenz

formula (for the conductor) are used. Fig. 4 shows a plot of the y-component of the total force vs. the number of nodes in the FEM mesh.

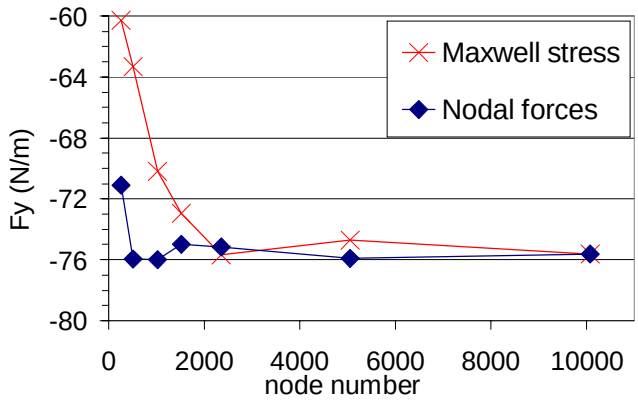

Figure 4. Y-component of the force on iron pole.

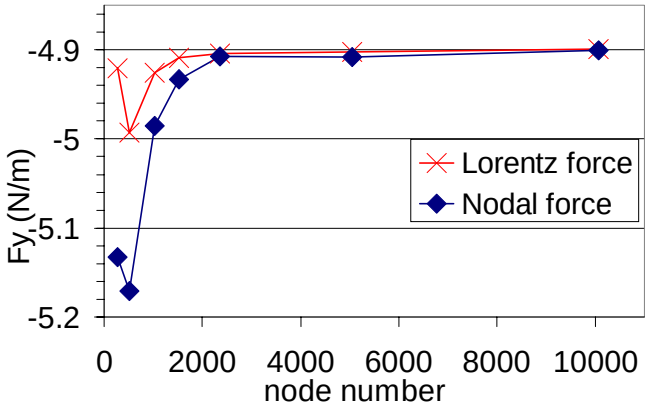

Figure 5. Y-component of the force on the current carrying conductor.

4. Conclusions

The three different formulations of the nodal forces are shown to be equivalent. The origin of the error related to the calculations of the nodal forces is explained. The methods are validated using FEM meshes of different densities.

In the case of current carrying conductors the force calculation is more accurate with the Lorenz formula when the FEM mesh is not dense enough. However, the difference with the nodal force is relatively small. In the case of magnetised iron the nodal force gives better accuracy than the conventional Maxwell stress method with coarse FEM mesh as well. With dense FEM meshes the total force is the same whether it is calculated with nodal forces or with either the Maxwell stress tensor method or the Lorentz formula.

The methods reviewed here can be used to calculate the excitation for structural analysis of electrical machines. The advantage of these methods is the fact that the nodal forces are found from the magnetic calculation. Hence the excitation term in the structural analysis does not need any additional integration. The verification of the validity of the reviewed methods at local level is, however, a difficult task that needs further elaboration.

References

[1] J. L. Coulomb. “A methodology for the determination of global electromechanical quantities from a finite element analysis and its application to the evaluation of magnetic forces, torques and stiffness”, IEEE Transactions on Magnetics, Vol. MAG-19, No. 6, 1983, pp. 2514–2519.

[2] G. Reyne. Anlyse theorique et experimentale des phenomenes vibratoires d’origine electromagnetique, these pour le titre de docteur de troisieme cycle, Grenoble France, 1987, 267 p.

[3] Z. Ren & A. Razek. “Local force computation in deformable bodies using edge elements. IEEE Transaction on Magnetics, Vol. 28, No. 2, 1992, pp. 1212–1215.

[4] A. Kameari. “Local force calculation in 3D FEM with edge elements”, International Journal of Applied Electromagnetics in Materials, No. 3, 1993, pp. 231–240.

[5] K. Delaere et al. “Coupling of magnetic analysis and vibrational modal analysis using local forces”, Proceedings of the Xth International Symposium on Theoretical Electrical Engineering ISTET'99, Magdeburg, Germany, 6–9 September 1999, pp. 417–422.

[6] P. Witczak. “Calculation of force density distribution in electrical machinery by means of magnetic stress tensor”, Archives of electrical engineering, Vol. XLV, No. 1, 1996, pp. 67–81.

[7] K. Reichert, R. E. Neubauer & T. Tarnhuvud. “A new approach solving the interface error problem of finite element field calculation methods by means of fictitious interface current sheets or interface charges”, IEEE Transactions on Magnetics COMPUMAG, Vol. 28, No. 2, 1992, pp. 1696–1699.

Vibration response and noise emission of electric generators

Paul Klinge
VTT Manufacturing Technology
Espoo, Finland

Abstract

This paper demonstrates how to calculate the vibration response and the noise emission of an electric generator beginning with the electromagnetic forces. The whole chain electromagnetic forces – stator core – stator frame – air is considered and it will be shown what can be done to reduce the vibration and noise emission at every stage.

1. Introduction

The usual sound sources of an electrical machine are the fan, the bearings and the sound radiation from the surface. The latter is the most important source of noise for electrical machines with six or more poles. This noise is usually found in the frequency range 0.5–3 kHz.

In an electric generator the magnetic field produces the circumferential forces required for the energy transfer. In addition, the field creates radial forces. These forces interact with the stator and excite it. The stator is in contact with the frame, which also is excited. The vibration of the frame accelerates the surrounding air, which is heard as noise. To avoid excessive noise the designer of the generators need methods to calculate the vibration and noise emission levels. This paper shows what kind of calculations are needed to assess the noise emission of an electric generator, starting from the electromagnetic forces, and what can be done to reduce the noise emission.

2. Electric generator

The main components of an electric generator are the stator, the rotor and the frame (Figure 1 and Figure 2). The energy is transmitted from the rotor over the air gap to the stator by the electromagnetic field. Electrical currents flowing in windings in the stator slots and on the rotor poles produce the magnetic field.

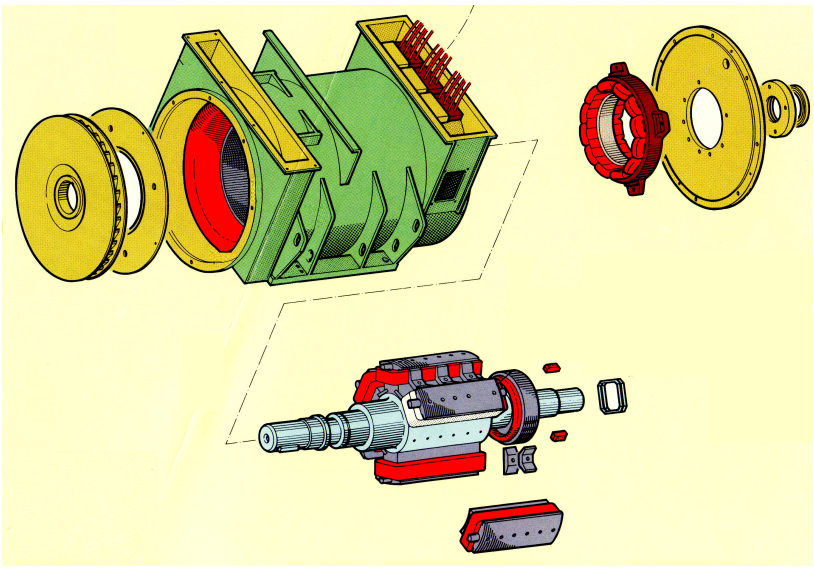

Figure 1. Components of a electric generator.

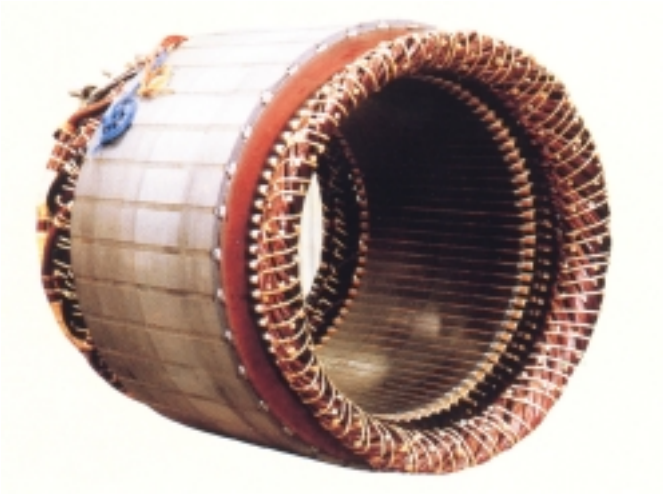

Figure 2. A stator, the core and the copper windings.

The stator core is made of 0.5 mm thick insulated steel sheet stampings layered over each other. They are assembled perpendicular to the shaft. The stampings have slots for stator windings. They are made of copper and electrically insulated from the core and from each other. Epoxy resin is used to impregnate the windings. In some stator models there are also air channels in the stator core for cooling.

The rotor poles are made of somewhat thicker steel sheets, typically 2 mm thick. The poles are fixed on the solid steel shaft. The copper rotor winding is made on the pole sides.

The stator frame is a coaxial cylindrical shell made of steel. It is connected to the stator core with longitudinal beams, which are welded to the stator core and the shell. This kind of frame forms air ducts for cooling the stator and keeps the stator packet together.

3. Magnetic forces

The magnetic field produces the circumferential forces required for the energy transfer. However, it also produces radial forces. The radial forces mainly cancel themselves out, but due to small asymmetries in the construction they may excite vibrations.

The magnetic field is usually calculated in 2D. This is a relatively good approximation, since the airgap is very small compared to the other dimensions of the generator. Another simplification usually made is to neglect the interaction between the magnetic field and the mechanical deformation. At higher frequencies where noise is mainly emitted the interaction is considered small. Because of this assumption, the magnetic forces can be treated like any external forces in mechanical calculations.

The magnetic field and forces are calculated by stepping in time. In Figure 3 the magnetic forces are shown at a time step. The figure shows how the magnetic forces concentrate at the tips of the stator teeth. The finite element mesh for the magnetic field calculations needs to be dense near the airgap, much denser than the mechanical element mesh of the stator. In this project the forces for every

tooth were summed up at every time step and the complex Fourier transformation was done on the calculations. This was considered the best way to transfer the calculated magnetic force data to the mechanical model.

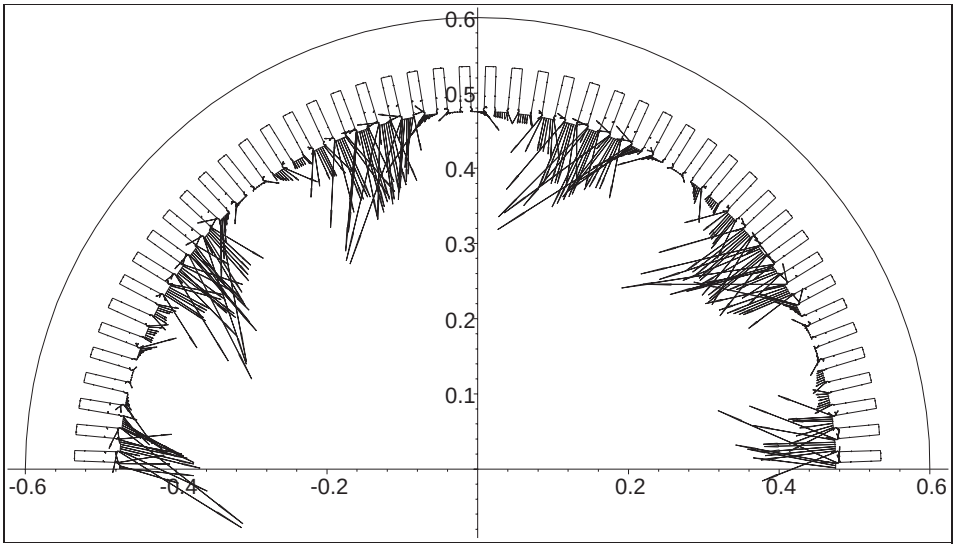

Figure 3. Magnetic forces at a time step.

Conventionally the calculated magnetic forces are presented as a Fourier series with two parameters, polar angle and time (Figure 4). Another way that the magnetic forces are usually presented is with waves rotating to the positive or negative direction. Commercial mechanical analysis programs do not understand these forms. They want the force data at a specific point on structure as a function of frequency or time. However, in harmonic response calculations a rotating force wave can be expressed as forces with phase differences. It corresponds to the above method.

An example of the radial force distribution of harmonic components is shown in Figure 5. Without calculating the response it is clear that a natural mode of a stator core with six waves would be strongly excited, if it were to appear at frequencies near this harmonic. By viewing the magnetic force distributions this way a mechanical designer can avoid resonant structural construction or the electromagnetic design can be changed to avoid resonances.

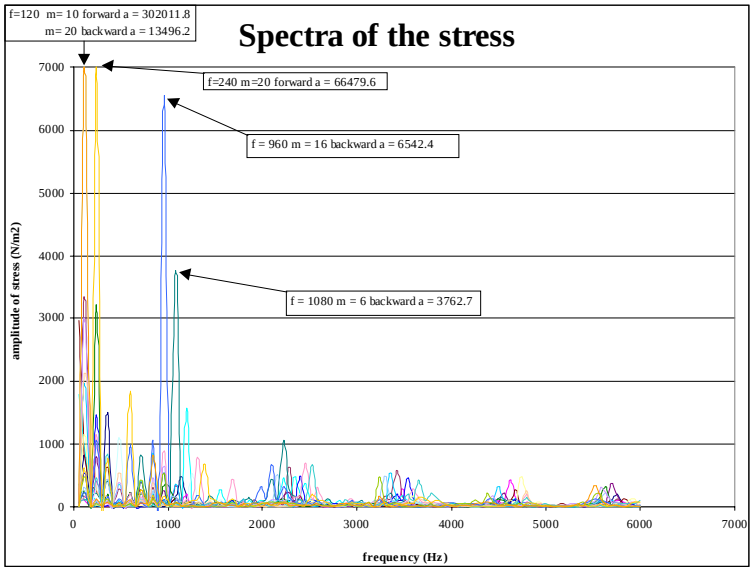

Figure 4. A double Fourier series presentation of magnetic forces.

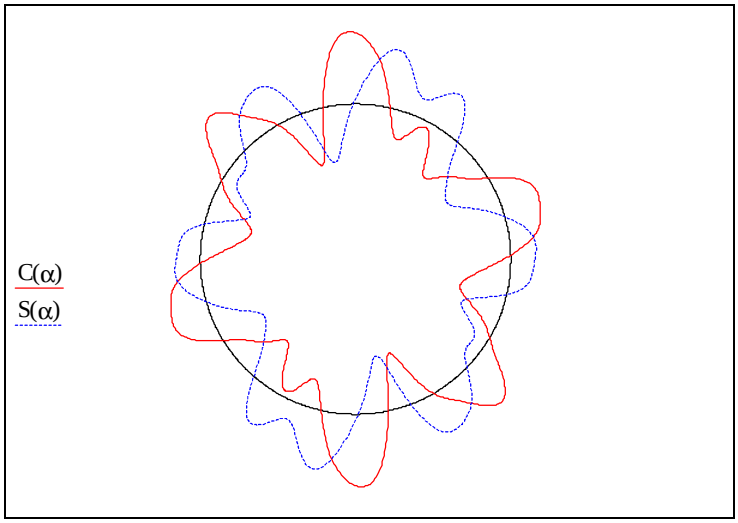

Figure 5. A spatial distribution of one harmonic component of radial forces.

4. Material model of the stator

It is impossible to model the stampings and their interaction exactly, therefore some kind of idealised model must be used. The most straightforward method is to model the stator geometry correctly and use an equivalent material model. Because of the structure of the stator core, the material model is orthogonal so that the cross-section is isotropic, but in the axial direction material properties are different.

The stator is composed not only of the steel stampings, but also of copper windings (Figure 2). The windings are even more difficult to model than the stator core. Furthermore, the connection between the core and the windings is vague. It is usually considered so weak that the windings can be left out of the model. However, the windings form a considerable part of the mass of the stator. If the generator is a part of a larger device, leaving out the mass of the windings may cause errors. That is why it is usually taken into account in the density of the stator core.

Structural damping is another difficult material parameter with the stator. Measured data is needed for determining both the damping and the other material parameters for the described equivalent material model.

5. Finite element model

The magnetic forces are practically always calculated in 2D. However, a 2D model cannot be used in the mechanical calculations. This is because the mechanical boundary conditions effect much more the natural modes and frequencies of the stator. Another important reason is the complex 3D behaviour of the stator frame, which cannot be taken into account with a 2D model.

In this project the stator core was modelled geometrically correctly with solid elements. By using the equivalent material model described above the mass of the copper windings was also included. The longitudinal beams were also modelled with solid elements and the frame was modelled with shell elements. The size of the elements was chosen so that natural modes near 1000 Hz could be correctly determined. The finite element model is shown in Figure 6.

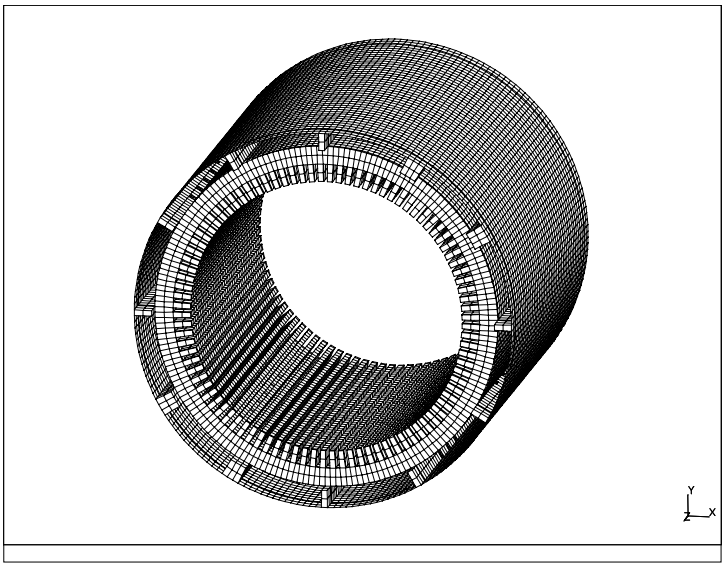

Figure 6. The finite element model of the stator.

There are problems with this kind of element model, when natural modes at high frequencies are calculated. The thin cylindrical shell of the stator frame will have more and more local natural modes the higher the calculation frequency is (Figure 7). In addition the teeth of the stator will have local natural modes. Since there are many teeth and they all have the same natural frequencies, it would be difficult to go above the first tooth frequency. However, it is not necessarily a realistic phenomenon, since the windings were not modelled. If the calculation frequency range includes the tooth frequencies, the modelling of the windings should be considered.

6. Mechanical response

The mode superposition method is normally used in response calculations. That is, the response is calculated as a linear combination of the calculated natural modes. Usually also the damping is given as a modal parameter. An equivalent viscous modal damping ratio is given to every natural mode.

The magnetic forces are calculated in 2D, because the force distribution in the axial direction is assumed to be constant. Thus the 2D forces are applied at all

node layers along the axis. In the 3D model there are thousands of nodes at the tooth tips and the magnetic forces act on each one. It is far too time consuming to feed in that much data manually. In the project a Matlab program was created, which transforms the magnetic tooth force data into an Ideas program file.

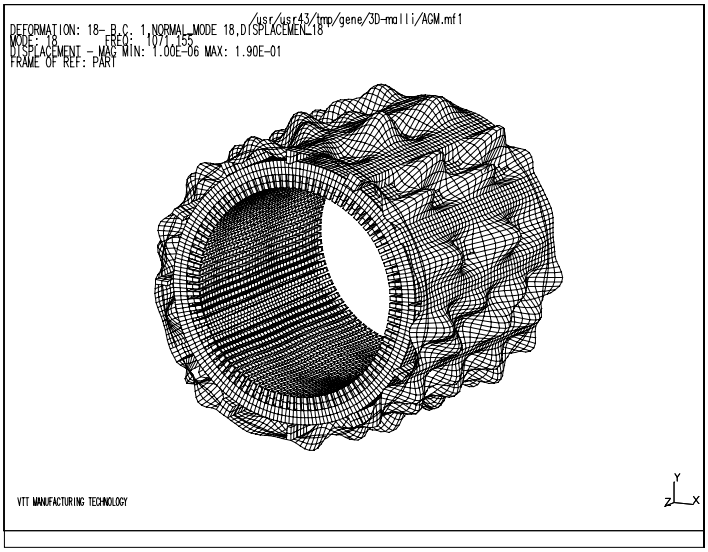

Figure 7. A local natural mode of the stator frame.

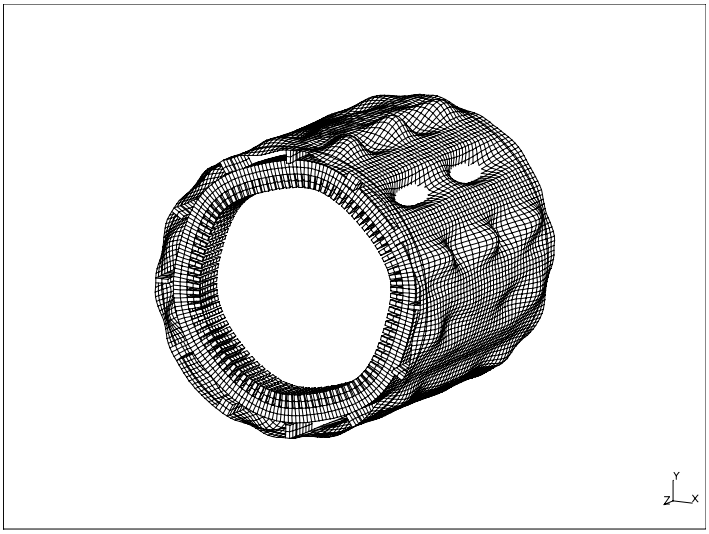

There are a lot of natural modes, because of the local modes of the stator frame (Figure 7). However, due to the constant force distribution along the axis only the lowest tube like modes of the stator core are excited strongly and dominate the response (Figure 8). The response of the frame depends on its coupling with the stator core. The response on the frame shell can be manifold compared to the core.

The excessive response levels are best avoided by checking the force distributions of the harmonic components of the magnetic forces. The structure of the stator frame should not be compatible with the strongest force peaks. This can be achieved for instance by using a suitable number of longitudinal beams. The coupling between the core and the shell can be controlled by changing the thickness of the shell.

7. Sound radiation

The usual sound sources of an electrical machine are the fan, the bearings and the sound radiation from the surface. Only the last one is excited by the electromagnetic excitation. It is also the most important source of noise for electrical machines with six or more poles.

Nowadays two powerful numerical methods are available for calculating the radiated sound, the finite element method (FEM) and the boundary element method (BEM). BEM is more suitable for pure sound radiation calculations. However, it is not necessary to calculate the sound pressure to assess the radiated sound power of the stator frame.

When the radiated sound power of a substructure is assessed by measurements, the following formula is used.

$$P = \rho c \sigma A \left\langle v^2 \right\rangle \qquad (1)$$

ρ is the density of air, c is the speed of sound in air, σ is the radiation index, A is the surface area and $\left\langle v^2 \right\rangle$ is the mean square velocity averaged over surface

and time. By calculating the response at some representative points and applying this formula the radiated sound power of the stator frame can be estimated.

The radiation index σ, which can be found in literature, is an important factor in the formula, since it is frequency dependent and takes into account the coincidence. Basically it is a situation where the wave on the structure and the sound wave in the air have same length and speed. The phenomenon is not very sharp, since the sound can radiate to a certain angle range. However, for every frequency there are conditions when the structure radiates sound most effectively. These conditions can be checked with the above method. The sound radiation may be considerably reduced by avoiding the coincidence type situation with structural modifications.

8. Conclusions

It has been shown how to calculate the vibration response of an electric generator starting from the electromagnetic forces and how to assess its noise emission. The whole chain electromagnetic forces - stator core - stator frame - air has been considered and it was shown what to do to reduce the vibration and noise emission at every stage.

ELECTROMAGNETIC DAMPING OF STATOR VIBRATIONS IN A CAGE INDUCTION MOTOR

Antero Arkkio
Helsinki University of Technology
Laboratory of Electromechanics
Espoo, Finland

Abstract

The electromagnetic damping of mechanical vibrations in a cage induction motor is studied herein. The analysis is based on time-stepping finite-element solutions of the magnetic field, voltages and currents of the machine. During a time-stepping simulation, the stator core of the machine is forced to vibrate, and the power transferred from the electromagnetic system to the vibrating mechanical system is analysed here. The power associated with damping is obtained from the product of the electromagnetic stress and vibration velocity. Both negative and positive damping powers were observed in the simulations. The damping forces are strongest at low vibration frequencies. At the higher frequencies typical for noise emission, the magnetic forces decrease, and the electromagnetic damping becomes smaller than the damping caused by mechanical sources. The method of analysis was verified by measuring the forces and damping powers acting on a cage rotor in whirling motion.

1. Introduction

In the conventional vibration and noise analysis of electrical machines, the chain from the electromagnetic excitation to sound radiation is usually treated as one-directional. The electromagnetic force is the source and there is no feedback from the vibration to this source. On the other hand, it is well known that an eccentric rotor produces a force between the stator and rotor. Thus, a rotor displaced from the central position or vibrating mechanically around it disturbs the flux distribution and generates magnetic forces. The aim of this paper is to study whether the two-directional electromechanical interaction is of such

strength that it should be taken into account in the vibration analysis of electrical machines, and more especially, if this interaction can cause significant damping of mechanical vibration.

The air gap of an induction motor is relatively small. The strains associated with vibration change the local radial air-gap length slightly, and the magnetic field crossing the air gap may also be affected. If the modified field causes additional losses in the machine, some damping of the vibration is to be expected. So, the key question is whether the vibration can cause significant electromagnetic losses in the machine structures. The potential types of electromagnetic loss are the resistive losses in the windings and iron losses in the core of the machine. The present paper focuses on the resistive losses in windings.

For a thorough study of the electromechanical interaction, a combined electro-magneto-mechanical model would be needed for the machine. However, valuable information can be obtained from an electromagnetic model, but only if the method is flexible enough to allow the electromagnetic modelling of forced mechanical vibrations of the machine structures. In this case, the work done or power displayed by the electromagnetic stress on the vibrating bodies can be calculated, and from the power, conclusions associated with the electromagnetic damping of the vibration can be made.

2. Method of analysis

2.1 Coupling between magnetic field and mechanical vibration

The results of Chapter 3 have been computed numerically, but to understand the physical phenomena, some analytical consideration is dealt with in this section. Früchtenicht et al. [1] derived an analytical model for the eddy-currents induced in the rotor cage when the rotor is in circular whirling motion. This type of motion can be taken as a special mode of vibration, and the equations derived can readily be generalised to fit other vibration modes. Basic results extracted and derived from the model of Früchtenicht et al. are briefly summarised below.

The stator displacement associated with a vibration mode is assumed to be

$$\Delta r(\phi,t) = \Delta_r \cos(q\phi - \omega_q t + \varphi_q), \tag{1}$$

where Δr is the radial displacement of the stator, Δ_r the amplitude of the vibration, q the wave number, ϕ the polar angle, ω_q the angular frequency of vibration, t the time and φ_q a phase angle. Equation (1) is only an approximation for a mode. An exact analysis would require a mechanical model to solve the mode shapes and natural frequencies. It is believed, however, that by forcing the stator to vibrate according to Equation (1) when solving the magnetic field, useful information of the electromechanical interaction can be obtained.

The radial air-gap length of a vibrating machine becomes

$$\delta(\phi,t) = \delta_{\mathrm{m}}\left[1+\frac{\Delta_r}{\delta_{\mathrm{m}}}\cos(q\phi - \grave{u}_q t + \varphi_q)\right], \tag{2}$$

where δ_{m} is the average airgap length. The non-uniform air gap generates two harmonic components into the airgap field

$$b_{p\pm q}(\phi,t) = B_{p\pm q}\cos\left[(p\pm q)\phi - (\grave{u}_1 \pm \grave{u}_q)t + (\varphi_p \pm \varphi_q)\right], \tag{3}$$

where p is the number of pole pairs of the machine and ω_1 is the supply frequency.

From Equations (1) and (3), it is easy to derive an equation for the electromagnetic power transferred to the vibrating stator. The flux density taken as the sum of the fundamental and vibration harmonics is substituted into the equation of the radial magnetic stress. The magnetic stress is multiplied by the velocity of the inner stator surface and integrated over the surface. The result is somewhat confusing. It shows that the average value of the energy transferred from the magnetic to the mechanical system vanishes, i.e., there is no electromagnetic damping.

The energy transfer is impossible because the magnetic stress and vibration velocity have a certain phase shift. The situation changes if the vibration

harmonic induces eddy-currents and losses in the machine structures. The field associated with the eddy currents is superposed on the vibration harmonic, and the phase of the harmonic is shifted. After the phase shift, power can flow between the magnetic and mechanical systems, and electromagnetic damping of vibrations becomes possible. The phase of the vibration harmonic is further discussed in Chapter 3.

The vibration harmonics induce eddy-currents in the rotor cage if the slips of the harmonics with respect to the rotor are non-zero; i.e., if the harmonics are time-dependent fields in the rotor frame of reference. The slips are

$$s_{p\pm q} = 1 - \frac{p \pm q}{p} \frac{\omega_1}{\omega_1 \pm \omega_q} (1 - s), \tag{4}$$

where s is the slip of the rotor with respect to the fundamental harmonic. The slips become zero at whirling frequencies

$$\omega_q = \frac{q - s(q \pm p)}{p} \omega_1 . \tag{5}$$

The slips of the vibration harmonics become zero simultaneously if the machine operates at the synchronous speed, and the vibration frequency is $q\omega_1/p$.

Another condition necessary for the eddy-currents to be induced into the rotor cage is that the slot pitch should not be a multiple of the wavelength of the vibration harmonic. All the lower vibration modes fulfil this condition.

The vibration may also cause resistive losses in the stator winding. This occurs if the winding factors associated with the vibration harmonics are non-zero. Figure 1 shows winding factors of a three-phase, one-layer stator winding for which the number of slots per pole and phase is three. The 15 kW induction motor studied in Chapter 3 contains this type of a stator winding. Only the vibration modes with wave numbers 0, 4, 8, can generate eddy-currents and losses in this winding. All the other modes of vibration are magnetically decoupled from the winding, and the winding does not dampen these modes.

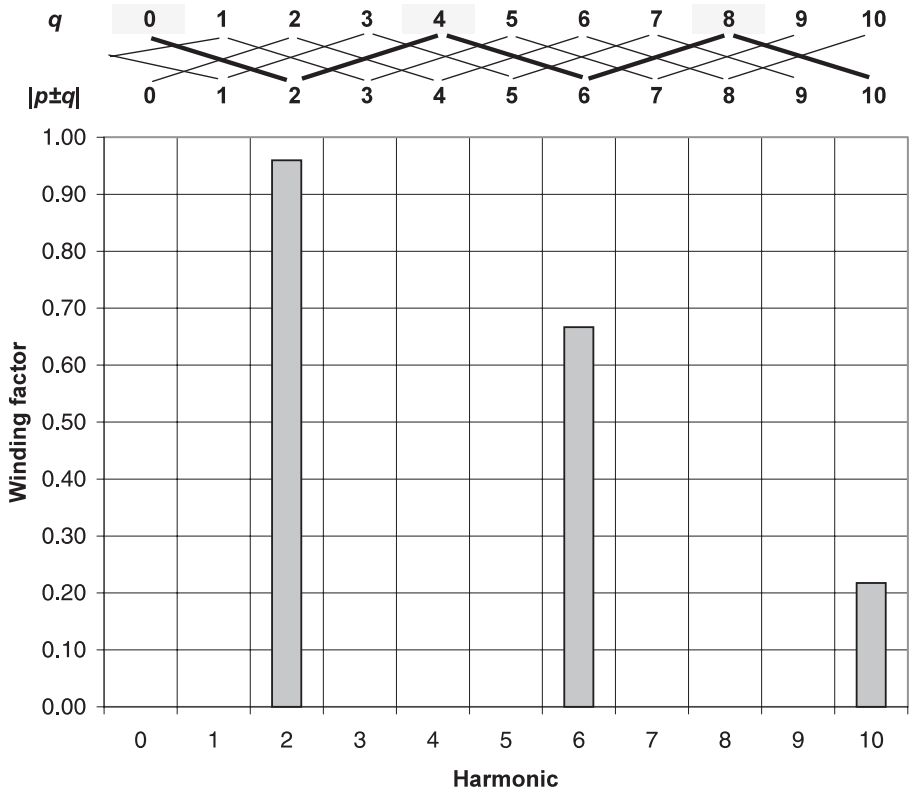

Figure 1. Winding factors for the lowest spatial harmonics of the airgap field. The winding is a one-layer, three-phase, four-pole winding with 36 stator slots.

Parallel branches in a stator winding or its connection may also affect the damping properties. Parallel paths may enhance damping by allowing circulating currents to flow between the branches. In a star connected winding, the sum of the phase currents must be zero. This means that an airgap field harmonic with a wave number which is a multiple of three cannot induce currents in a star connected three-phase winding. The delta connection puts no restrictions to the current flow. The motor used as a test machine in the next chapter is delta connected and has only one branch per phase winding.

The eddy-currents induced in the rotor or stator windings reduce the amplitude and modify the phase of the vibration harmonics. By doing this they affect the radial force. Depending on the phase angles, the magnetic forces may dampen or amplify the vibration.

2.2 Numerical analysis

The calculation of the magnetic field and operating characteristics of the machine is based on time-stepping, finite-element analysis. The details of the method have been presented by Arkkio [2]. The magnetic field in the core region of the motor is assumed to be two-dimensional, and the two-dimensional field equation is made discrete by the finite-element method. Constant end-winding impedances in the circuit equations of the windings are used to take approximately into account the effects of end-region fields. The field equation and the circuit equations are solved together as a system of equations. The time-dependence of the field is modelled by the Crank-Nicholson method. The rotor is rotated by changing the finite-element mesh in the air gap. The magnetic field, the currents and the potential differences of the windings are obtained in the solution of the coupled field and circuit equations.

A typical finite-element mesh for the cross section of the test machine contained about 3 000 nodes. First-order triangular elements were used.

Several simplifications have been made in order to keep the amount of computation at a reasonable level. The magnetic field in the core of the machine is assumed to be two-dimensional. The laminated iron core is treated as a non-conducting, magnetically non-linear medium, and the non-linearity is modelled by a single valued magnetisation curve. The unipolar flux that may be associated with the non-uniform air gap has been neglected. In spite of the simplifications, the method of analysis should model properly the effects of the eddy-currents, non-skewed slotting and magnetic saturation.

During a time-stepping simulation, the stator core is forced to oscillate according to Equation (1). The power that the electromagnetic field transfers to the vibrating stator core is obtained by integrating the product of the radial magnetic stress and vibration velocity along the inner surface of the core. The stress is obtained from Maxwell's stress tensor.

The fact that there are strong electromagnetic stress waves even in non-vibrating electrical machines (Figure 3) complicates the analysis. If such a stress wave coincides in wave number, frequency and phase with the forced vibration mode, a significant power is produced although the vibration may have nothing to do

with the stress. To banish this effect, the vibration modes were applied at four different phase angles, each differing by 90 degrees from the previous one. In this way, and assuming that the system is linear, the damping force can be separated from a primary electromagnetic force existing without vibration.

3. Results

3.1 Test motor

The method described above was used to study the electromagnetic damping of vibrations in a 15 kW four-pole cage induction motor running at no load. The main parameters of the machine are given in Table 1 and the cross-sectional geometry is shown in Figure 2.

As mentioned in the previous chapter, the magnetic field also generates radial stress waves in the air gap in normal operation (without the vibration) and one must be able to distinguish these primary waves from the ones associated with the vibration. The amplitudes of the primary waves (having wave number 4 and moving in the same direction as the rotor) are shown in Figure 3.

Table 1. Main parameters of the 15 kW motor.

Parameter	
Number of poles	4
Number of phases	3
Number of parallel paths	1
Outer diameter of the stator core [mm]	235
Core length [mm]	195
Airgap diameter [mm]	145
Radial airgap length [mm]	0.45
Number of stator slots	36
Number of rotor slots	34
Skew of rotor slots	0
Connection	Delta
Rated voltage [V]	380
Rated frequency [Hz]	50
Rated current [A]	28
Rated power [kW]	15

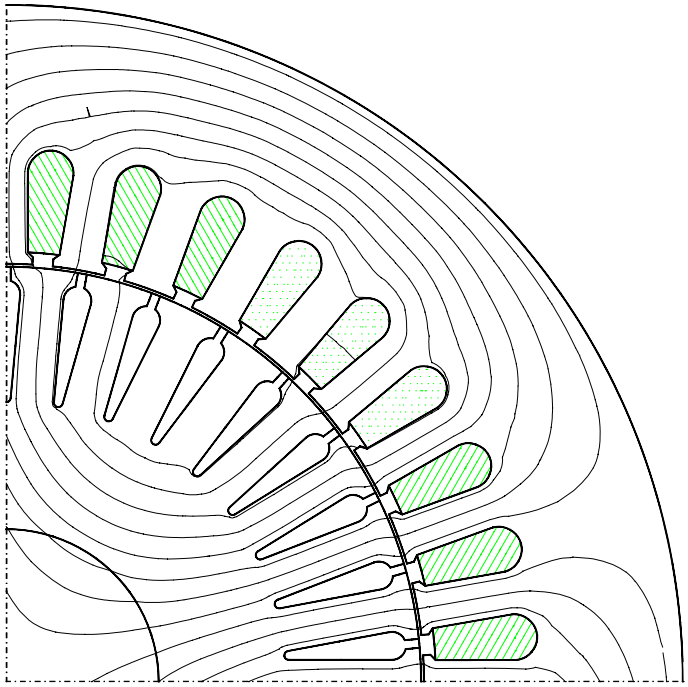

Figure 2. Cross-sectional geometry of the four-pole induction motor studied.

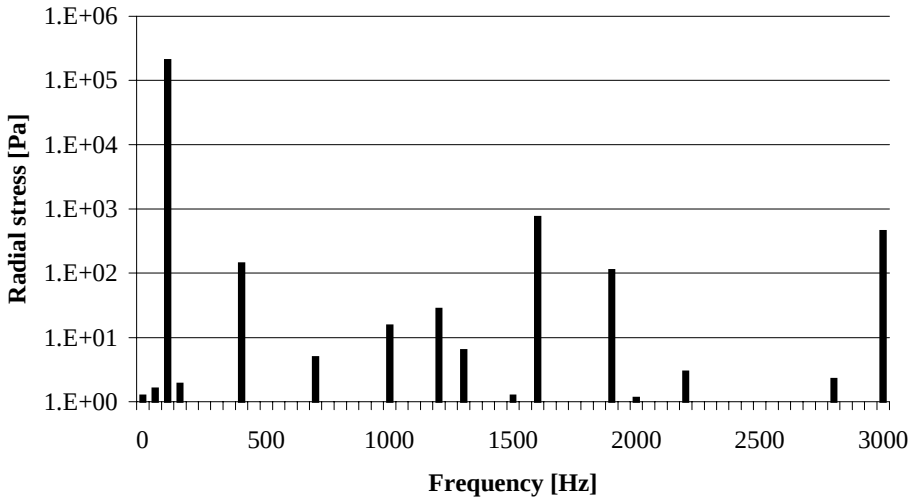

Figure 3. The amplitudes of stress waves having wave number 4 and rotating in the same direction as the rotor. These are the primary stress waves produced by the motor; i.e., they are not associated with stator vibration.

3.2 Results from Numerical Analysis

Figure 4 shows the power that the electromagnetic system absorbs from the stator core when the core vibrates according to the vibration mode with wave number q=4. These damping powers have been computed one by one in time-stepping simulations, changing the vibration frequency in steps of 10 Hz. The powers are the average values integrated over five periods of line frequency.

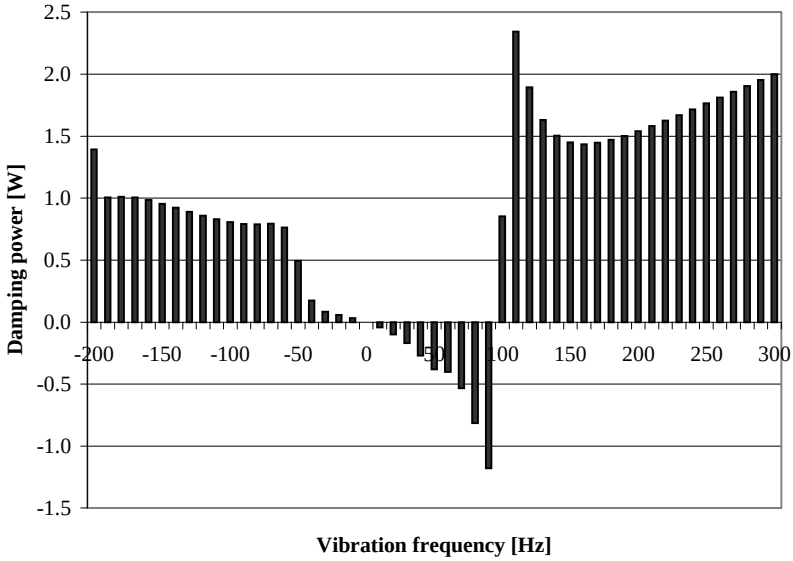

Figure 4. Electromagnetic power that dampens the radial vibration mode of wave number 4. A negative frequency means that the displacement wave associated with the vibration moves in the direction opposite the rotation of the rotor.

The negative power within the frequency range 0–100 Hz means that the electromagnetic field transfers more energy into the mechanical vibration. In other words, we have negative damping. Outside this range, the magnetic forces dampen the vibration.

The amplitude of the forced vibration was 45 μm, which is 10% of the radial air gap. Relatively large amplitude was chosen so as to be able to distinguish the damping forces reliably from the normal electromagnetic forces of the machine.

Simulations with varying amplitudes showed that the system is linear, i.e., the damping stresses increase linearly with the amplitude. Applying the linearity, the damping forces and powers obtained using the large vibration amplitude can be scaled to more realistic amplitudes.

As discussed in Section 2.1, vibration modes with wave number 4 can induce eddy-currents both in the stator and rotor windings. In order to study the contributions of the two windings separately, two additional simulations were made. Firstly, the rotor cage was removed from the machine. If there was damping, it must have been associated with the resistive stator loss. The result is shown in Figure 5. In the second simulation, the stator resistance was set at zero. This leaves the losses in rotor cage as the only source of damping. The damping power obtained in the second simulation is shown in Figure 6.

A third simulation was made for checking purposes. The stator resistance was set to zero and the rotor resistance to infinity. As the vibration cannot generate resistive losses in the machine, the time average of the energy flow between the electromagnetic and mechanical system should have been zero. The damping powers obtained in this case were about three orders of magnitude smaller than the powers shown in Figures 4–6.

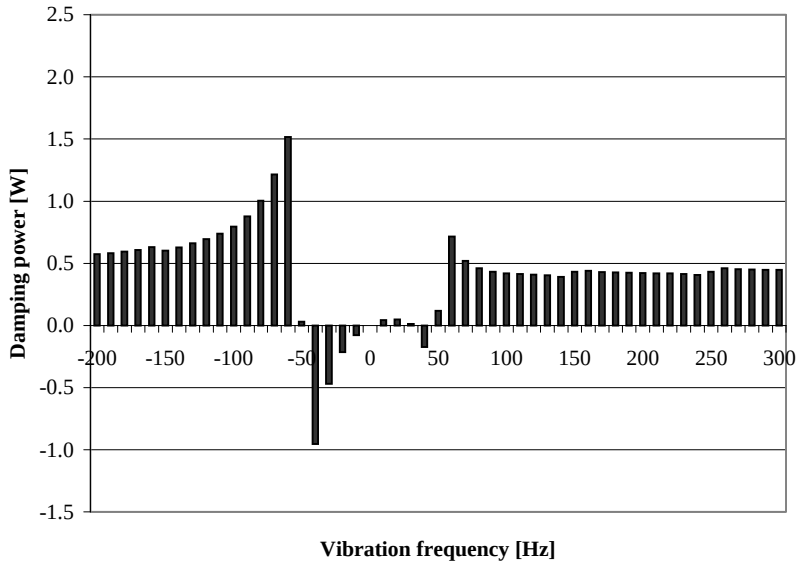

Figure 5. Damping power if the only loss is the resistive stator loss.

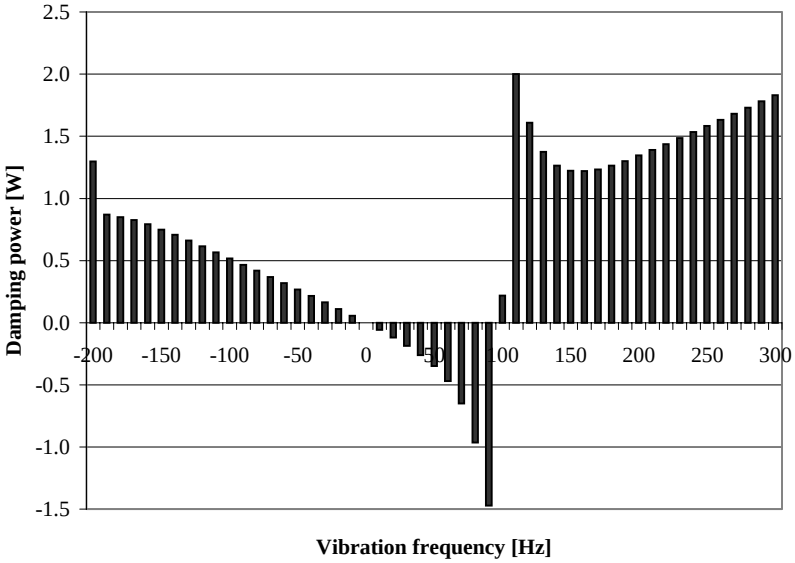

Figure 6. Damping power if the only loss is the resistive rotor loss.

Because the eddy-currents induced in the stator and rotor windings reduce the amplitudes of the corresponding flux-density harmonics, the direct superposition of the two sources of damping is not valid. From Figures 4–6, one can draw the conclusion that the stator and rotor windings are of about equal importance in the electromagnetic damping of vibration. This result applies only for the specific stator winding and the vibration modes with wave number 4. The stator winding studied can produce electromagnetic damping only if the wave number of a mode is a multiple of four.

Figures 7–9 show the amplitudes of the vibration harmonics in the airgap flux density, stator current and rotor current. In addition, the phase angles of the two vibration harmonics are shown in Figure 7. As a reference, the fundamental airgap flux density of the motor is about 0.95 T, the rated current of a phase winding about 16 A and the rated rotor-bar current about 320 A. The points in which a harmonic coincides with the fundamental harmonic have been excluded from the figures.

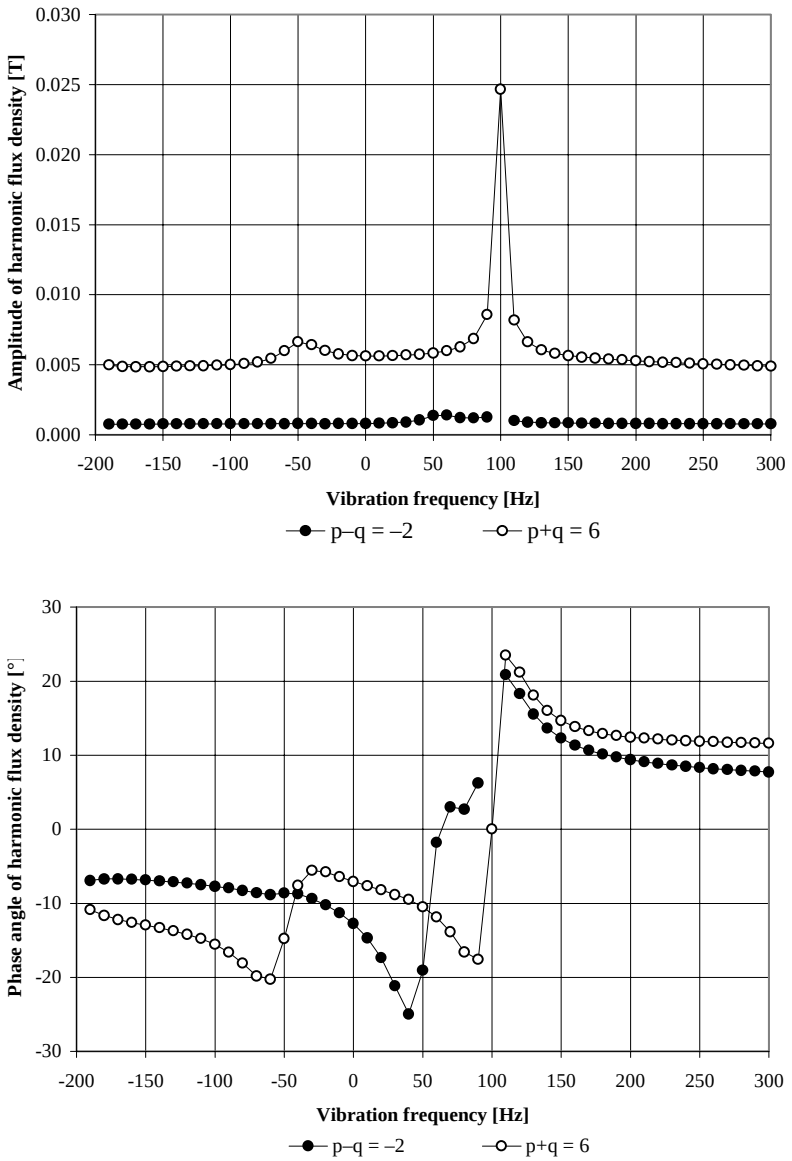

Figure 7. The harmonic components of the airgap flux density associated with the vibration modes having wave number q = 4. The upper figure shows the amplitude, the bottom figure the phase of the harmonic. The harmonic p – q = –2 coincides with the fundamental harmonic at vibration frequency 100 Hz. This point has been excluded from the figure.

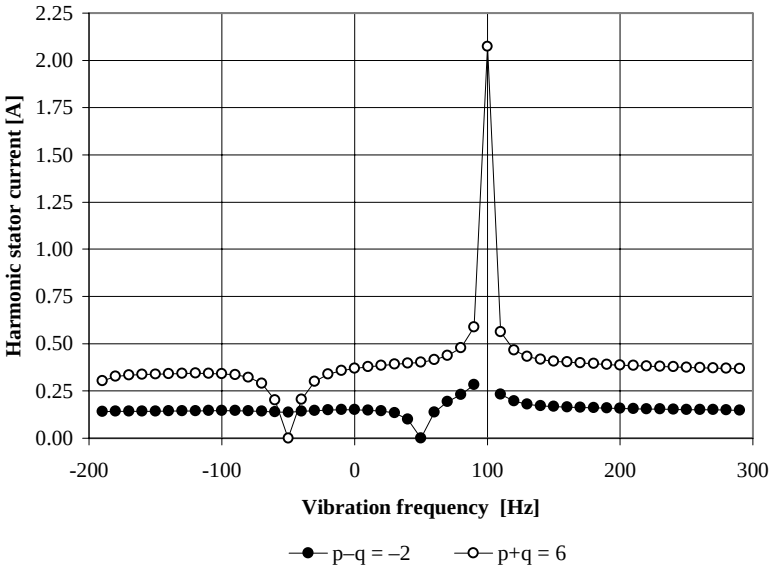

Figure 8. The harmonic components of the stator current associated with the vibration mode with wave number 4.

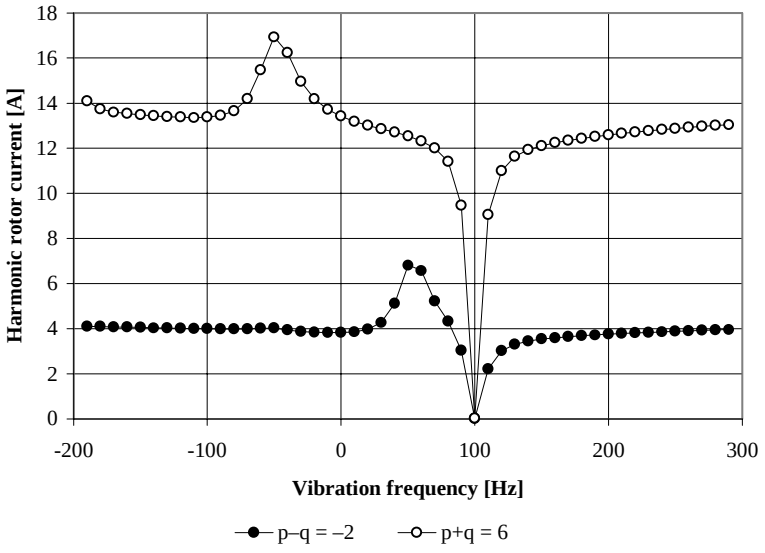

Figure 9. The harmonic components of the rotor current associated with the vibration mode with wave number 4.

As discussed in Section 2.1, the eddy-currents induced in the windings modify the phase angles of the vibration harmonics. This is shown in Figure 7. For instance, the phases of the harmonics are rapidly shifted when passing the frequency 100 Hz. At this frequency, the slips of the vibration harmonics with respect to the rotor become zero and change their sign (Equations 4 and 5). The abrupt phase shifts at ±50 Hz frequencies are associated with currents induced in the stator winding. A change in the phase angle causes a corresponding change in the damping power (Figures 4–6).

The couplings between the harmonics are also evident from Figures 7–9. For instance, the frequencies of the two vibration harmonics in the airgap field become zero at the vibration frequencies ±50 Hz (Equation 3). A d.c. field cannot induce harmonics in the stator current. As a result, the stator does not damp the airgap field harmonics, and both the airgap field and rotor current harmonics have local maxima at the ±50 Hz vibration frequencies. A similar situation occurs in the rotor frame of reference at the vibration frequency 100 Hz. Unfortunately, the maxima in the harmonics of the airgap field and stator current are masked behind the fundamental and third harmonics of these quantities, which are present in the machine even without the vibration.

Similar studies were done for vibration modes having different wave numbers. Typically, the damping power increases with the wave number of the vibration mode, and there always seems to be a region of negative damping between the angular frequencies 0 and $q\omega_1/p$. Simulations were also made for a loaded motor. According to the simulations, loading the machine by the rated torque affects the electromagnetic damping of vibrations only slightly.

3.3 Measured results

The damping powers obtained from the numerical model should be verified by measurements. Force and power measurements were made for a rotor in circular whirling motion [3]. From the point of view of the vibration harmonics, the whirling motion is closely related to the vibration mode which has wave number 1. In this whirling motion, the geometric centrelines of the rotor and stator are aligned but the former moves around the later in a circular orbit with a frequency (called whirling frequency) and with a radius (called whirling radius). In

addition to the whirling motion, the rotor rotates around its centreline in the normal way.

The 15 kW test motor was equipped with magnetic bearings. By proper control of the bearings, the centreline of the rotor was forced to follow a circular whirling path. In addition, the bearings were calibrated to measure the total force acting between the stator and rotor. The power damping or accelerating the whirling is obtained from the measured total force and whirling velocity. That said, it can also be computed from the electromagnetic stress as described in Section 2.2. Figure 10 shows the measured and computed damping powers.

In the measurements, the supply voltage of the machine had to be reduced to 230 V in order to keep the magnetic bearings within their linear range of operation. The amplitude of vibration, i.e., the whirling radius was set to be 11% of the radial air gap of the motor. In the computation algorithm, the forced motion of the stator core was changed from the flexible vibration described by Equation (1) to the solid-body motion associated with whirling.

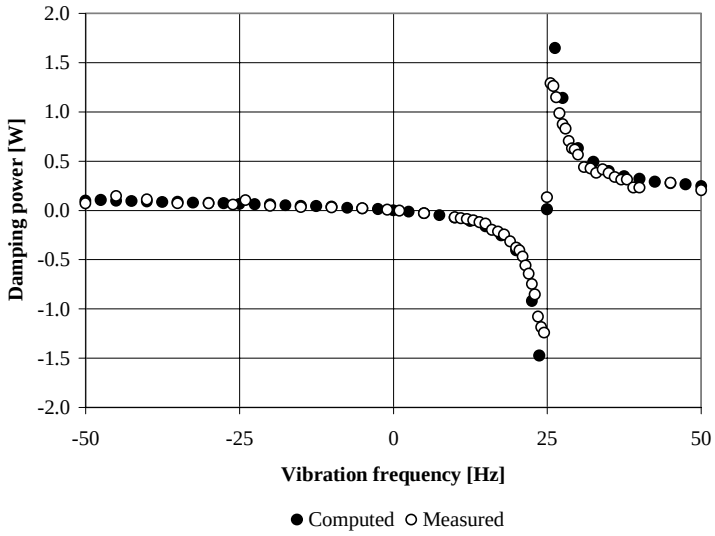

Figure 10. Comparison of the measured and computed damping powers for a rotor vibrating around its central position in a whirling motion.

The agreement between the measured and computed damping powers is satisfactory. Both results show a region of negative damping between the frequencies 0 and 25 Hz.

3.4 Magnitude of electromagnetic damping

One of the aims of the paper is to estimate whether the electromagnetic damping can affect the vibration characteristics of electrical machines. To achieve this aim, the damping powers given in Figure 4 should be related to parameters more commonly used in association with mechanical vibration.

An idealised, effective stress acting on the airgap surface of the stator and producing the same damping power as given in Figure 4 could be a useful quantity for comparison and evaluation purposes. Assuming that the effective stress τ has a sinusoidal space and time dependence and is in phase with the velocity associated with the vibration

$$\tau(\phi,t) = \tau_q \sin(q\phi - \omega_q t + \varphi_q), \tag{6}$$

the amplitude of the stress becomes

$$\tau_q = \frac{P}{\pi \omega_q \Delta_r \ell R}, \tag{7}$$

where ℓ is the length of the machine and R the airgap radius. The amplitude of the idealised damping stress for the vibration modes of wave number 4 is shown in Figure 11. The idealised stress changes sign at frequency $f = 100$ Hz ($= q\omega_1/2\pi p$), has its maximum amplitude on both sides of this frequency and starts to decrease when moving away from the frequency. The two flux-density harmonics, which the vibration generates into the air gap field, change their direction of rotation with respect to the rotor at the same frequency.

The stresses of Figure 11 should be compared with the primary stresses that occur in the induction machine without any stator vibration (Figure 3). In the comparison, one has to keep in mind that the damping stresses were computed for a large vibration amplitude 45 μm, and they are directly proportional to this

amplitude, whereas the primary stresses are independent of vibration. The largest peaks in the spectrum of the primary stress are much bigger than the corresponding damping stress. If a large primary stress excites a mechanical resonance, the electromagnetic damping is too weak to limit the vibration amplitude. On the other hand, many of the peaks in the spectrum of the primary stress are smaller than the corresponding damping stresses. In these cases, provided that the electromagnetic damping is positive, it may have a stabilising effect on the vibration behaviour of the machine.

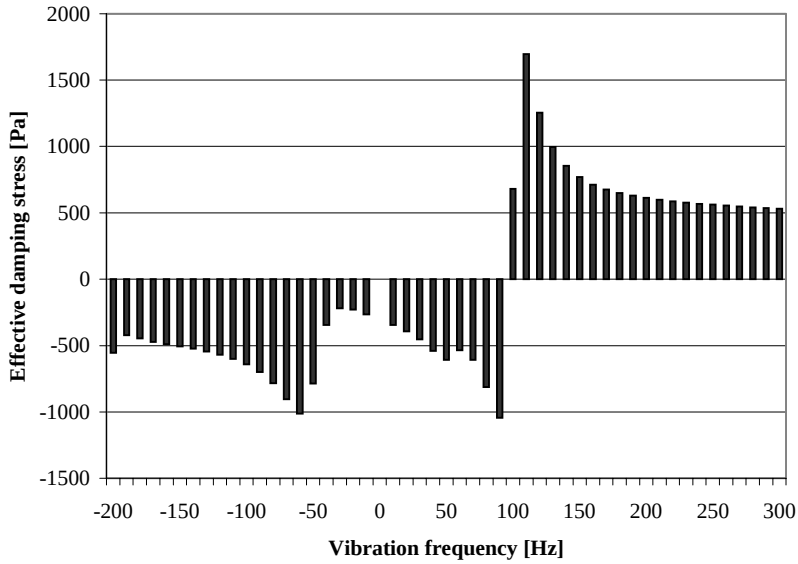

Figure 11. Effective stress that damps the radial vibration modes with wave number 4.

The damping ratio or relative damping factor may be a useful quantity for evaluating the significance of electromagnetic damping with respect to other, mechanical sources of damping. The damping ratio is defined as the ratio of the damping coefficient and critical damping. Assuming viscose damping, damping coefficient C can be derived from the damping power P

$$C = \frac{2P}{(\Delta_r \omega)^2}, \tag{8}$$

and the damping ratio becomes

$$\zeta = \frac{C}{2m\omega_{\mathrm{n}}} = \frac{2P}{2m\omega_{\mathrm{n}}(\Delta_r \omega)^2}, \tag{9}$$

where m is the mass associated with the vibration mode and ω_{n} is the natural frequency of the mode. The natural frequency ω_{n} brings the mechanical stiffness of the stator into consideration. To obtain this frequency, one needs either a mechanical model of the stator or measured results. As a rough estimate, the value $\omega_{\mathrm{n}} = 2\pi \cdot 1000$ Hz is used for the natural frequency, and the mass m is taken to be equal to the mass of the stator core. Figure 12 shows the damping ratio.

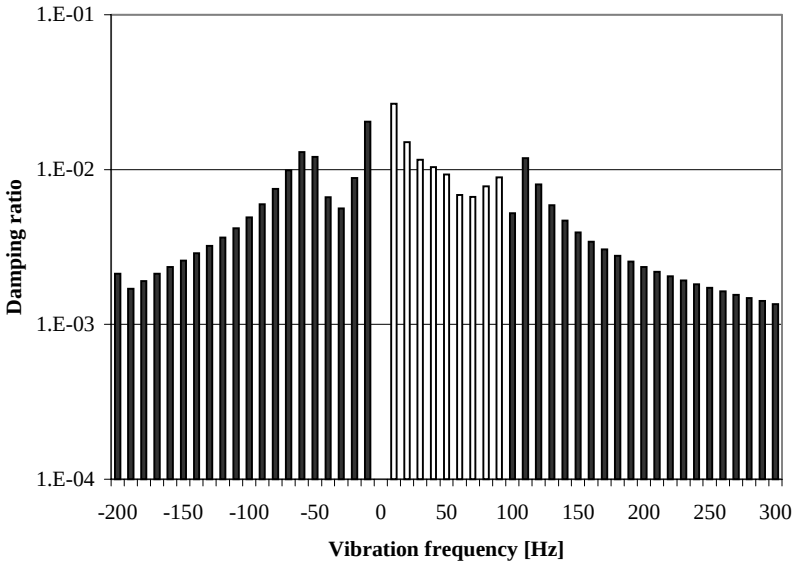

Figure 12. The magnitude of the damping ratio associated with the electromagnetic damping of the radial vibration modes with wave number 4. The damping ratio is negative within the frequency range 0–100 Hz.

A typical damping ratio associated with material damping of steel structures is 0.01. Within the frequency range –100 Hz … 100 Hz, the magnitude of the damping ratio computed for the electromagnetic interaction is of the same order of magnitude as the one for structural damping. When the frequency increases

and approaches the region of acoustic noise (> 500 Hz), the electromagnetic damping decreases and becomes smaller than typical structural damping.

One can draw the conclusion that the two-directional electromechanical interaction may affect the low frequency vibration characteristics of an electrical machine. However, the electromagnetic forces associated with vibration start to decrease with an increasing frequency. At the frequencies typically associated with acoustic noise, the electromagnetic damping is small compared with the damping caused by mechanical sources.

The results above have been computed using an electromagnetic model only. One would need a mechanical model of the system to study in detail, for instance, what is the meaning of the negative damping in the vibration control of electrical machines. The mechanical and electromagnetic models should be used together to study the electromechanical operation of an electrical machine.

4. Conclusions

The electromagnetic damping of mechanical stator vibration of a cage induction motor was studied. Such damping may occur if the vibration causes electrical losses in machine structures. The losses considered were the resistive losses in the stator and rotor windings. According to the qualitative analytical results, all the lower vibration modes may generate eddy-current losses in the rotor cage of a machine. The stator winding is more selective, and only that the vibration modes have proper wave numbers can induce resistive losses in the stator winding.

The quantitative results were obtained from time-stepping, finite-element simulations of a 15 kW cage induction motor. During the simulations, the stator of the machine was forced to vibrate, and the work done by the electromagnetic stress on the stator core was computed numerically. The results of the numerical analysis predict negative damping within a frequency range at low frequencies. The damping powers were measured for a rotor performing circular whirling motion. The measured and computed powers showed good agreement, and the measurements confirm the frequency range with negative damping.

The relative electromagnetic damping is largest at the low vibration frequencies, and it may affect the low frequency vibration characteristics of an electrical machine. At higher frequencies typical for noise emission, the electromechanical interaction decreases, and the electromagnetic damping is smaller than the damping of vibration caused by mechanical sources.

References

[1] Früchtenicht, J., Jordan, H. & Seinsch, H.O. Exzentrizitätsfelder als Ursache von Laufinstabillitäten bei Asynchronmachinen. Parts 1 and 2. Archiv für Electrotechnik 65 (1982), pp. 271–292.

[2] Arkkio, A. Analysis of induction motors based on the numerical solution of the magnetic field and circuit equations. Acta Polytechnica Scandinavica, Electrical Engineering Series No. 59. Helsinki 1987. ISBN 951-666-250-1, 97 p.

[3] Arkkio, A., Antila, M., Pokki, K., Simon, A. & Lantto, E. Electromagnetic force on a whirling cage rotor. IEE Proceedings – Electric Power Applications. Vol. 147 (2000) 5, pp. 353–360.

Sound radiation from vibrating cooling ribs

Martti Verho & Paul Klinge
VTT Manufacturing Technology
Espoo, Finland

Abstract

The role of the cooling ribs seems to be important for the noise created at the cover of an electric motor. Relatively high peak velocities at the top of the ribs, induced by simple mechanical amplification, can make the ribs quite effective sound radiators. Based on a simplified 2D-model, a cover with ribs radiates as effectively as a flexible plate without ribs, if the peak velocity at the top of the ribs is three times the velocity of the plate. If the ribs are considered non-flexible, the velocity magnification depends on the height of the ribs. In the studied case, the magnification factor was 3.7. If the dynamic effects of flexible ribs are taken into account, the magnification factor could be even higher. Measurements made on a running motor seem to indicate that this level of magnification is quite realistic.

1. Introduction

This paper is part of the TEKES research project SMART/MASI. The goal of the project is to evaluate and develop vibro-acoustic models and tools that could be used in practical industrial applications. The subject of this paper is the noise arising from an electric motor and especially the role of the cooling ribs in this noise. This paper is based on a more detailed report on the subject [5].

A running electric motor always creates some noise due to the mechanical vibrations in the cover of the motor. If the cooling of a motor are based on cooling ribs mounted on the cover, it is possible that the cooling ribs will reinforce the noise generated by the vibrating cover. This potential amplification effect is analysed in this paper using a simplified two dimensional model of the cover modelled as a plate with cooling ribs.

Because a motor is always a three-dimensional object working in an acoustically active environment, it is obvious that this simplified plainer model cannot model the actual sound field. However, some of the essential features of this potential amplification can be analysed using this simplified model.

2. Model

2.1 Wave equation and boundary conditions

In practical acoustic problems, sound waves can be described by the linearised flow equation for a compressible ideal gas (air). If the vibration is harmonic at the surface where the radiated sound is generated, this equation reduces to the Helmholtz equation [4]:

$$\nabla^2 p = -k^2 p \tag{1}$$

where
p is the sound pressure
c is the speed of sound in air,
$k = \frac{\omega}{c}$ is the wavenumber and
ω is the angular velocity of the vibration .

In addition to the load velocity related boundary condition at the vibrating boundary, boundary conditions are needed at the reflecting and non-reflecting boundaries. At the reflecting boundaries the normal component of the pressure gradient must be zero. The non-reflecting boundary condition is the so-called far field or Sommerfeld boundary condition. The acoustic impedance must be imaginary at this boundary. This condition describes a passive or absorbing boundary that does not affect the pressure field radiated at the vibrating boundary.

2.2 Model geometry

The model geometry for the plate with ribs is shown in Figure 1. It consists of a closed half circle. The radius of the circle is 0.5 m. Sound waves are generated by the vibrating ribs at the bottom edge (referred as the data edge in the following). The length of the data edge is 0.93 m. The height of the ribs is 6.0 cm and the bottom width of the ribs is 3.0 cm. This is also the distance between the adjacent ribs. Other parts of the bottom edge are fixed. The 'passive' environment is modelled using a non-reflective semi-circular boundary with the Sommerfeld boundary condition.

Figure 1. Model geometry and edges.

A harmonic load velocity was applied at the data edge and the resulting Helmholtz equation was solved using a FEM solver. The solver was implemented using the Matlab programming language [3]. The finite element mesh consisted of linear triangular elements.

In all simulations, the vibration frequency was set to 3335 Hz. This frequency was selected, because it is the first natural frequency of the studied cooling ribs [2]. This corresponds to the sound wavelength of 10.19 cm in air.

3. Results

3.1 Sound radiation from a flexible plate

To verify the model, a vibrating flexible infinite plane without ribs was modelled first. The velocity of the structural wave turns out to be quite critical for the amount of sound energy radiated from the plate. Sound is radiated to the far field only if the speed of the structural wave is larger than the speed of sound in the air.

The effective radiation can be analysed by the acoustic impedance at the boundary. If the plane is vibrating with an arbitrary angular frequency ω, the wave impedance at the boundary is as follows [1, p. 73]:

$$(\tilde{p}/\tilde{v})_{y=0} = \pm \frac{\omega \rho_0}{\sqrt{1-(\kappa/k)^2}} \tag{2}$$

where $\tilde{p}$ and $\tilde{v}$ are the complex-valued pressure and velocity fields at the surface, ρ_0 is the fluid density at rest. Variables κ and k are the wavenumbers (ω/c) for the structural wave and the sound wave.

When the phase velocity in the structure is larger than the speed of sound in the air $(\kappa > k)$, the wave impedance is real, and sound energy is radiated from the plane. The wave impedance becomes the larger the more equal the wave velocities are, but the maximum case $(\kappa = k)$ is not physically possible, because the radiated sound energy would be infinite.

The model was solved for different structural wavelengths (wave speeds) at a constant vibrating frequency. A structural wave was modelled by using a velocity distribution at the data edge with a proper phase along the edge. The following velocity distribution was applied at of the boundary elements in the data edge:

$$v_{el} = \mathrm{e}^{\imath 2\pi \frac{x_{el}}{\lambda_s}} v_{ref} \tag{3}$$

where x_{el} is the element's x-distance from the centre of the edge, λ_s is the wavelength of the structural wave (it is referred to as spatial wavelength or spatial lambda below) and v_{ref} is the maximum value of the normal component of the velocity at the data edge. Throughout the simulations, this peak velocity was set to 1 mm/s. Because of the complex exponential term, this velocity distribution describes a travelling wave along the data edge.

The average pressure along the data edge was calculated using structural wavelength values between 5 and 20 cm. The calculated average pressure distribution is shown in Figure 2. It should be noted that pressure values for spatial lambda values smaller than 10.19 cm do not represent sound energy radiating from the plate, because the wave impedance is imaginary for those values.

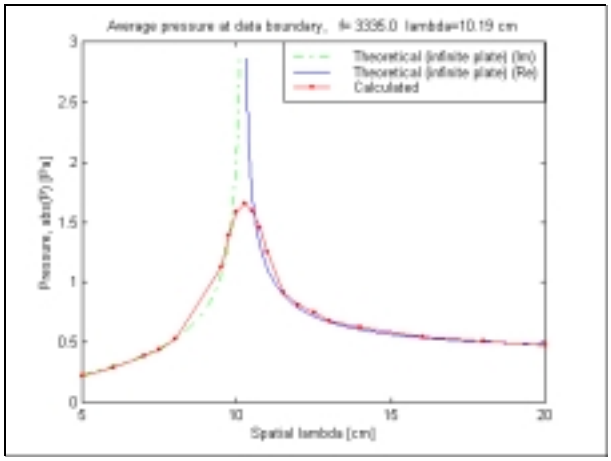

Figure 2. Flexible plate: average pressure at the data edge.

3.2 Sound radiation from a rigid plate with ribs

As the next step, the model with cooling ribs was analysed. In this case, the bottom plate is considered fixed, but the ribs are flexible and vibrating.

The initial velocity distribution at the rib boundary was estimated by solving a structural model for a single rib and by calculating the normal components of the modal velocities [2]. Initial rib velocities were again modified by a structural (spatial) wave along the positive x-direction. The peak velocity at the top of the rib was set to 1 mm/s.

The average intensity at the ribs for spatial wavelengths between 3.0 and 17.0 cm were calculated and the results are shown in Figure 3. As was expected, there is a strong correlation between the radiated sound intensity and the relation of the spatial wavelength to the wavelength of sound in air. The intensity increases when the spatial lambda approaches the wavelength of sound in air (10.19 cm for the frequency 3335 Hz used in the analysis) and drops in practice to zero for smaller spatial wavelengths.

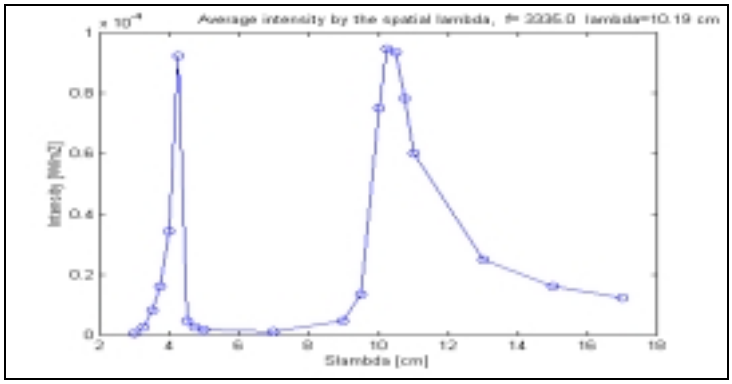

Figure 3. Plate with ribs: sound intensity at the ribs.

The calculated maximum sound intensity at the data boundary was about 0.1 mW/m^2 or 80 dB. This is nearly 10 dB lower than the corresponding intensity peak for the flexible plane. On the other hand, if the peak velocity at the top of the rib were just three times the velocity of the plate, the sound intensity levels would be similar in both models.

If the ribs were non-flexible, the velocity magnification factor at the top of the ribs would be $2\pi r / \lambda_s$, where λ_s is the wavelength of the structural wave in the cover and *r* is the height of the ribs. In the current case, the magnification factor

is 3.7. If the dynamic effects of flexible ribs are taken into account, the actual magnification factor could be even higher.

In contrast to the non-ribbed case, there was also another peak for the radiated sound. This peak occurs at a small spatial wavelength (around 4 cm in this case) and it represents a structural wave moving from right to left.

The calculated pressure field corresponding to the spatial lambda value 10.50 cm is shown in Figure 4. In this figure the theoretical wavefront angle for the infinite plate is also displayed. As can be seen, the wavefront direction for the rib geometry is very similar to the plate geometry.

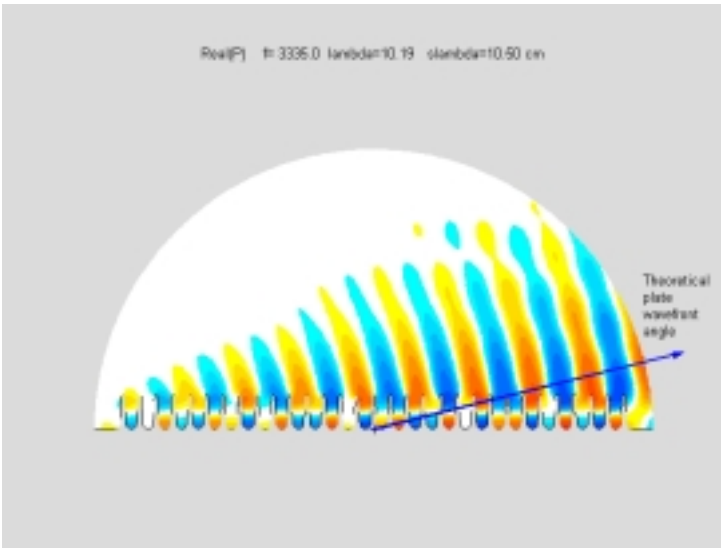

Figure 4. Plate with ribs: pressure field.

The sound intensity radiated by the ribs was analysed also using different values for the vibration frequency. The maximum sound intensity was estimated for each frequency. Most of these curves had multiple peaks. If only the 'real' peak (spatial lambda value not smaller than the wavelength of sound) is accepted, there seems to be a clear correlation between the frequency and the maximum radiated sound intensity.

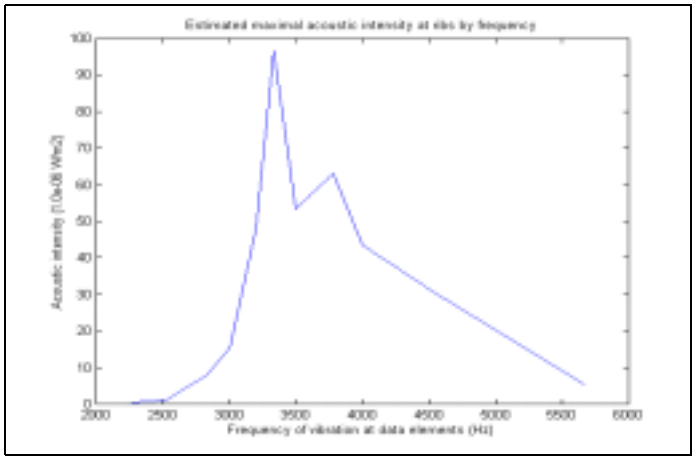

Figure 5. Plate with ribs: sound intensity by frequency.

Changing the frequency is equivalent to changing the relative size of the ribs in relation to wavelength of sound. Consequently, the results shown in Figure 5 seem to indicate that the noise level could be effectively controlled by the rib geometry. However, this conclusion cannot be taken for granted. One problem is the existence of the multiple peaks.

4. Conclusions

The role of the cooling ribs seems to be important for the noise created at the cover of an electric motor. Relatively high peak velocities at the top of the ribs, induced by simple mechanical amplification, can make the ribs quite effective sound radiators. Based on a simplified 2D-model, a cover with ribs radiates as effectively as a flexible plate without ribs, if the peak velocity at the top of the ribs is three times the velocity of the plate. If the ribs are considered non-flexible, the velocity magnification depends on the height of the ribs. In the studied case, the magnification factor was 3.7. If the dynamic effects of flexible ribs are taken into account, the magnification factor could be even higher. Measurements made on a running motor seem to indicate that this level of magnification is quite realistic.

It seems also possible to describe the sound radiation behaviour of a plate with ribs with an equivalent plate without ribs. However, the behaviour is not one to

one. Especially the existence of multiple intensity peaks corresponding to structural waves travelling in opposite directions, were unique for the ribbed geometry. It should be also noticed that the analysis was based on a simplified 2D model. In real motors, the ribs are three-dimensional structures and the characteristics of various resonance and coincidence phenomena are more complicated.

References

[1] Fahy, F. *Sound and Structural Vibration*. London: Academic Press, 1985. 309 p.

[2] Linjama, J., Himmi, M. & Klinge, P. *Sähkömoottorin jäähdytysrivan rakennemalli äänensäteilyn laskentaa varten.* Espoo: VTT, 1999. (Esitelmä SMART teknologiaohjelman tulosseminaarissa 29.11.1999.) (In Finnish.)

[3] Lyly, M. *Sähkömoottorin jäähdytysripojen äänensäteilyn mallinnus ja simulointi lineaarisilla kolmioelementeilla*. Espoo: VTT, 2000. 23 p. (Tutkimus-selostus VALB-444.) (In Finnish.)

[4] Pierce, A.D. Acoustics. *An Introduction to Its Physical Principles ans Applications*. 2nd. ed. New York: The Acoustical Society of America, 1991. 678 p.

[5] Verho, M. and Klinge P. Modelling of the sound radiation from cooling ribs. Espoo: VTT, 2000. 34 p. (Research Report VAL35B-001072)

Vibro-acoustic modelling and low noise design

Jukka Tanttari
VTT Automation
Tampere, Finland

Abstract

In this paper, the author considers vibro-acoustic modelling from point of view of the low noise design of products. The modelling must be integrated to the product development process. It must answer reasonable demands, which are relevant to the particular product development phase. This idea is realised using the design process of an acoustic enclosure as an example.

1. Introduction

There are many possible points of view of the modelling of sound radiation and other interactions between vibrating solid structures and acoustic disturbances.

From the modelling software developers' point of view, the idea would be, e.g., [1]: "Sysnoise predicts sound waves and the structural vibration induced by fluid loading effects onto a structure. The program calculates a wide variety of results such as sound pressure and radiated sound power, acoustic velocities and intensities, contributions of panel groups to the sound, energy densities, vibro-acoustic sensitivities, normal modes and structural deflections".

While the above is certainly true, it is useful to ask: "What is the key information to fulfil the needs of product development in different phases?"

From the point of view noise control in car industry it may be stated that [2]: "The details of components, materials and their properties are 'fuzzy' at the early stages of the design. The fuzziness is clarified as design is modified and matured slowly throughout the process until volume production is launched. The

engineers face the challenge of accurately representing and analysing the vibro-acoustic behaviour of a future product with insufficient data and in a design space that evolves every day. Therefore, at the early stages of the design, the accuracy of vibro-acoustic predictions for the final product are somewhat relaxed, and the attention is mainly focused on trend analysis (design A vs. B), narrowing design options and mean level responses."

In SEA-modelling of a car, the size of models of different hierarchy would be something like [2]

- "fuzzy" models, below 50 subsystems
- "large" models up to 200 subsystems
- "full detailed" models up to 1500 subsystems.

The aim of these models is of course to answer to design problems relevant to the particular design phase.

In [3, 4], results of FEM/BEM modelling of a cylindrical polyethylene test enclosure at some interesting frequencies were presented. The aim of this paper is to describe the design and modelling of the real enclosure in connection to its design.

2. Design and modelling of an acoustic enclosure

2.1 The objective

The objective was to construct a large (length approximately 8 m) effective acoustic enclosure for the frequency range 500–10000 Hz. The weight of the enclosure was quite restricted, so some effort was needed to optimise the acoustic characteristics.

It was also known, that the cross-section of the enclosure would be somewhat more cylindrical than rectangular and the preferred material was LDPE. Steel was considered as an alternative.

2.2 The gross design parameters

The basic parameters controlling the effectiveness of an acoustic enclosure are

- the contribution of leaks, %
- the average absorption coefficient inside the enclosure
- the transmission loss of the enclosure wall material

In many practical cases the contribution of the leaks dominates the acoustic transmission and determines the total effectiveness. In this case, the broad frequency range, cylindrical shape and restricted weight forced an examination of the sound transmission characteristics in more detail.

2.3 Airborne sound transmission through a cylindrical wall

The important frequency parameters controlling the sound transmission through a cylindrical wall are [5, 6] the critical frequency, f_c and the ring frequency f_r.

At the critical frequency the speed of the bending waves in the plate material and the speed of sound in fluid are the same. The ring frequency is the cut-off-frequency of purely axially propagating flexural "breathing mode" vibration in the cylinder cross section. The approximate relations giving these two important frequencies are

$$f_r = \frac{c_l'}{\pi D} \quad \text{and} \quad f_c \approx \frac{c^2}{1.8h\, c_l'} \tag{1}$$

where c is the speed of sound in the air, h is the material thickness, D is the cylinder diameter, and c_l' is the quasi-longitudinal wave phase speed in the plate material. It is related to the common solid material properties by

$$c_l' = \sqrt{\frac{E}{\rho(1-\nu^2)}} \tag{2}$$

In the vicinity of both the critical frequency and the ring frequency, a strong coupling of the acoustical and the flexural vibrations exist, thus yielding a poor transmission loss.

2.4 A simple SEA-model

A simple SEA-model consisting of an acoustic cavity with predefined sound pressure level, cylindrical enclosure wall with end caps and semi-infinite external sound field is presented in Figure 1. The mass-law coupling from the enclosure cavity and the coupling from the resonant modes of the enclosure wall are presented with separate blue lines.

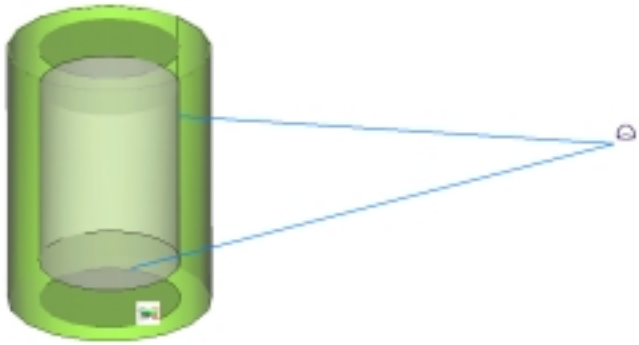

Figure 1. A simple SEA-model of cylindrical test enclosure.

Simulated sound pressure spectra in semi-free field for two enclosure materials, LDPE in its final rigidity and steel, are presented in Figure 2. The surface mass of the materials is about 10 kg/m^2 and the diameter of the cylinder 0.8 m.

The critical frequency is at the 8 to 10 kHz range for both. The ring frequency of the LDPE is at 300 Hz range and the ring frequency of the steel is at the 2 kHz range. The corresponding quasi-longitudinal wave speeds are about 880 m/s for LDPE and 5300 m/s for steel.

Clearly, the material properties of steel are not attractive in this case and the LDPE is fundamentally far better, almost the optimal choice. The results of these simulations were confirmed by laboratory measurement.

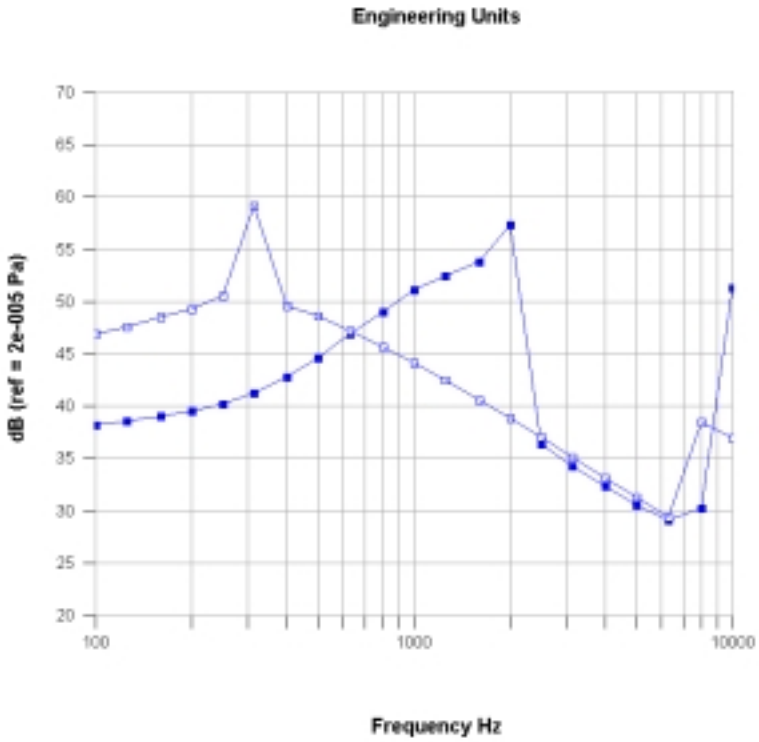

Figure 2. Sound pressure levels at the external field for two enclosure materials. Hollow marks=LDPE, solid marks = steel.

2.5 A more extensive SEA-model

After choosing the wall material as well as the absorption materials, it is worth examining the behaviour of the full enclosure in its presumed diameter and various lengths. It was possible to define the acoustical excitation inside the enclosure in terms of measured sound power.

To do “large model” simulations, the enclosure was broken down into one-meter long pieces, subsystems. By adding or removing the subsystems, many enclosure lengths were easy to construct.

An example of these models is in Figure 3. The acoustic excitation was located in three lowest parts of the enclosure. The “caps” between the parts were used to define couplings between the acoustical subsystems inside the enclosure.

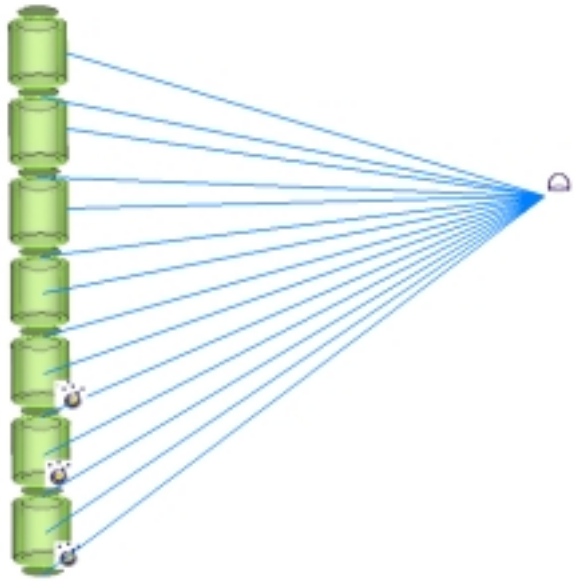

Figure 3. An extensive SEA-model of a cylindrical enclosure.

With models like in Figure 3, an optimum between the size, weight and effectiveness of the enclosure can be sought.

2.6 Detailed FEM/BEM-modelling

In order to examine the behaviour of the enclosure in the vicinity of 300 Hz, FEM/BEM-models were constructed. The results are reported in [3, 4]. The diagram 4 [4] reveals the long-wavelength axial behaviour characteristic of sound transmission around the ring frequency of a cylinder.

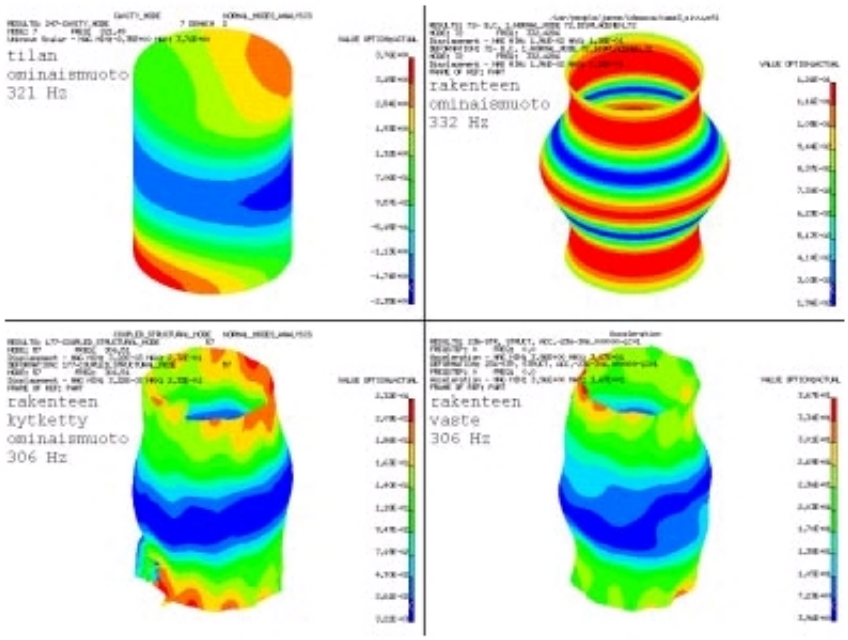

Figure 4. FEM/BEM-results at 306 Hz; acoustic mode shape at 321 Hz, structural mode shape at 332 Hz, coupled mode shape at 306 Hz and structural response at 306 Hz.

3. Conclusions

Vibro-acoustic modelling and simulation is a powerful tool. From the point of view of low noise design of products and structures, it may be used to find reasonable answers to questions relevant to the particular product development phase. The best method is the one that gives adequate answers with the least effort.

References

1. Sysnoise commercial; http://www.LMS.be/solutions/

2. Onsay, T. Implementation of SEA in the Automotive industry and its use in noise and vibration control. NOVEM 2000, Noise & Vibration: Pre-design and characterisation using energy methods. 31 August - 2 September 2000, Lyon – France. 12 p.

3. Haverinen, J., Linjama, J. & Tanttari, J. Kotelon äänieristyksen vibro-akustinen mallinnus elementtimenetelmällä. Akustiikkapäivät 1999. Tampere 4.–5.10.1999. Akustinen seura ry, Helsinki 1999. p. 53–58, ISSN 1236-8202. (In Finnish.)

4. Haverinen, J., Tanttari, J., Linjama, J. & Klinge, P. Sylinterimäisen kotelon vibroakustinen malli ja sen verifiointi. Espoo: Teknillinen korkeakoulu, Akustiikan ja äänenkäsittelytekniikan laboratorio. 40 s. Työraportti 31.6.1999. (In Finnish.)

5. Fahy, F. Sound and structural vibration. Radiation, transmission and response. Academic Press, 1985. 309 p.

6. Szechenyi, E. Sound transmission through cylinder walls using statistical considerations. Journal of Sound and Vibration, 19(1971)1, p. 83–94.

Modelling and condition monitoring of abrasive work machine parts

Johan Scholliers
VTT Automation, Machine Automation
Tampere, Finland

Abstract

In work machines with abrasive parts, wear affects the quality of the output material. In order to guarantee a constant quality output, the settings of the machine have to be adapted in regard to the value of the wear. Wear is however often difficult to measure directly. This article describes how wear has been modelled for a work machine, and how the wear is estimated, compensated for, and included in the condition-monitoring algorithm.

1. Introduction

A high degree of availability and reliability are important competitive factors for work machines, in addition to power efficiency and quality of the output. Machine downtimes should therefore be reduced to a minimum. On-line condition monitoring becomes therefore an important function for work machines. An efficient condition-monitoring system allows a more optimal use of the work machine, reduces machine downtimes through early detection of problems and will assist in planning machine maintenance.

Work machines often contain abrasive parts. Wear has a direct impact on the quality of the work machine output. The actual amount of wear is difficult to measure directly, often only through time consuming calibration procedures. Wear and machine condition are monitored on-line and on-board. "On-board" means that the algorithm is embedded into the machine controller; "on-line" indicates that the data is processed in the work machine and the results forwarded in real-time to the machine operator.

By analysis of the on-board sensor signals, the effect of the abrasion on the sensor signals can be analysed, and a method developed to adapt the machine settings automatically to compensate for the wear. Since the sensor signals are also analysed in the condition-monitoring system, wear monitoring and compensation are included in the condition-monitoring algorithm. The condition-monitoring system should also be able to detect abnormal wear patterns. Abnormal wear, such as localised wear or bursts, will have a negative effect on the quality of the output material, and will lead to early replacement of the abrasive part.

2. Wear compensation

In conventional machines, the machine settings are kept constant and changed when the quality of the output exceeds tolerance limits. To assure that the values of the machine settings are correct, the machine has to be calibrated (Figure 1).

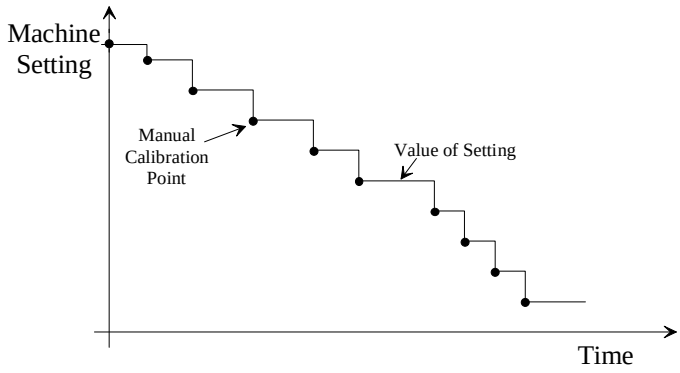

Figure 1. Classical method of wear compensation through calibration.

Machine calibrations are often performed manually, but are time and resource consuming. In some cases, the personnel who operates the machine can neglect the official procedures required for calibration of the machine, and use simpler procedures, which result in apparently acceptable machine behaviour. However, since the machine is not correctly calibrated, the machine's control algorithm lacks the information to guarantee optimal working performance.

By implementing a system, which monitors the machine wear and compensates the machine settings automatically, the number of calibrations can be reduced. There are different possibilities to determine wear:

- Wear can be measured directly, and then there is no need to model wear explicitly.

- The value of the wear can be derived on-line from the sensor signals. This effect can be modelled by analysing the sensor signals before and after calibration. This information can then directly be used by the condition-monitoring algorithm to determine on-line the value of the wear. In this case, manual calibrations could be avoided completely, depending on the accuracy of the wear model.

- Wear cannot be derived from sensor signals directly. If the influence of the wear on the sensor signals is not significant, wear cannot be determined on-line but is estimated from previous measurements. The relation between the machine settings and, e.g., the consumed energy for the previous part is analysed and used as reference. Not all the parameters which affect wear, can be measured, such as the abrasiveness of the input material, which affects the wear speed. Since these parameters can change during the lifecycle of the part, the wear model must have adaptive capabilities, so that it can adapt rapidly to the new material quality. A drawback of this wear modelling method is that manual calibrations still have to be performed, but at a much smaller frequency than with the classical method.

There are different possibilities to determine the moment to compensate wear:

- If the quality of the output can be measured directly, these limits can be used to directly determine the moment at which the setting has to be compensated. The new machine settings are determined from the wear estimation model.

- If the quality of the output cannot be measured directly, but the quality of the output can be modelled from the sensor signals, this information can be used to determine the moment of machine settings adaptation.

– If the influence of the machine output quality on the available sensor values is too small or unknown, the machine settings are changed if the machine wear exceeds a predetermined value. If the wear cannot be measured or determined directly, the machine settings are changed at a threshold for a sensor value, e.g., the consumed energy, which is calculated from the wear estimation model (Figure 2).

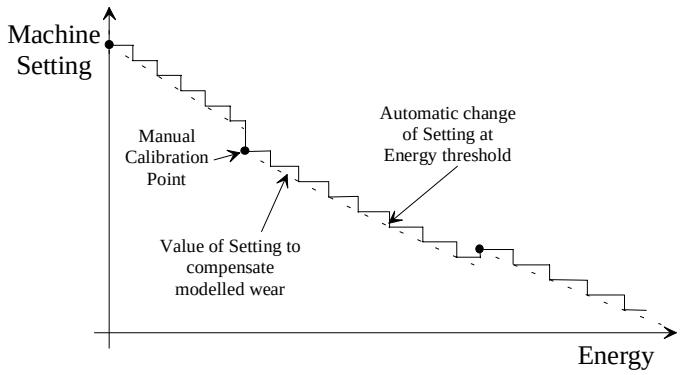

Figure 2. Wear compensation based on wear model.

3. Development of the wear estimation and condition-monitoring algorithm

The method, described in this article, starts from a behavioural black-box model for the operation of the machine, and not from a detailed machine model generated from system component models. Wear and machine condition are monitored on-line and on-board. Since on-line condition monitoring is generally not a high priority function of the machine, the use of additional sensors (and hence additional wiring) is not always acceptable. It may not be possible to affect to the quality of the sensor signals (e.g., sampling frequency). Work machines are delivered in different small series, dependent on the requirements of the customer. The condition-monitoring algorithm, including the wear estimation and compensation, should be comprehensible and easy to adapt to the different versions of the machine.

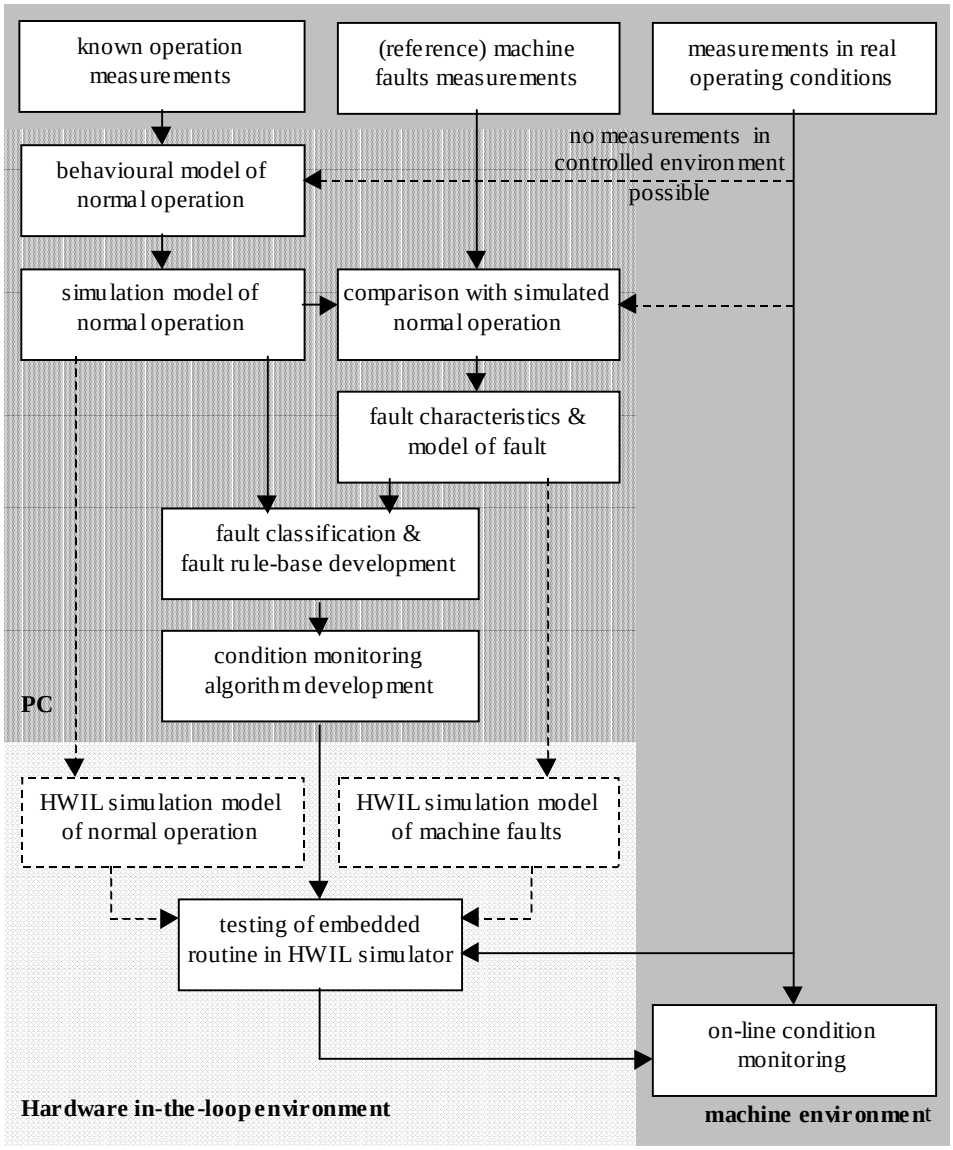

Figure 3. Method to develop on-line condition monitoring algorithm.

Figure 3 shows the proposed method for the development of the on-board condition monitoring system for the abrasive parts of a work machine. A behavioural model, which relates the different sensor signals to each other, is generated based on measurements. This model should also include the effect of wear. In the most ideal case, measurements can be performed under known and controlled operation conditions, over the whole range of input parameters,

including exceptional – but acceptable – situations. In this case, it is possible to develop a complete model of normal operation. However, due to the high cost of work machines and their high operational costs, such measurements are often not possible. The normal operation model has then to be extracted from real operating machine measurements. These do not however, always cover the complete set of input parameters, making it more difficult to identify whether a change in an analog sensor signal is due to a change in the process conditions or to a machine fault.

Faults are detected based on analysis of the normal operation and the behaviour of the diagnosed system. By modelling normal situations, faults can be detected and explained as exceptions (Kurki 1995). Information on machine faults is retrieved from measurements. The same comment as for the normal operation modelling applies: if measurements can be performed on a test machine, more complete and reliable data on the faults will be obtained. In case no quantitative information on the faults is available, qualitative information might be used, but this information is less reliable and has to be validated on pilot machines in operational conditions.

A rule-base is developed based on models of the normal operation of the machine and of the machine faults. The rule-base is developed in two steps: first the features, which identify the faults, are identified, and then the type and the severity of the fault are determined based on the fault feature values. The features can be derived from the time or frequency domain, like mean, variance, skewness, kurtosis, trend analysis, envelope analysis, FFT or Wavelet analysis. From this rule-base, an algorithm is derived, i.e., which determines the fault, and sends a message to the operator's display and/or – if required – an automatic corrective action to be performed (e.g., automatic change of machine settings). The algorithm is developed in a common programming language, which is suitable for embedding into the machine controller.

The embedded algorithm is then verified by means of a Hardware-in-the-Loop (HWIL) simulator. The HWIL simulator has a user-interface, which allows the user to generate the sensor values for the machine inputs, and to generate various fault scenarios. For testing the embedded condition-monitoring system, the models of the machine's normal behaviour and the machine faults should be

included in the HWIL simulator. This requires generally for modelling the time-behaviour of the normal operating machine, the wear and the machine faults.

4. Wear modelling for an abrasive work machine

The aim of the project MAMUR (Modeling of the abrasive parts of a work machine) was to determine which signals affect the normal abrasion of the machine and the faults in the abrasive parts of the work machine. The main target was to develop an on-line condition-monitoring algorithm, which is able to detect machine faults and to compensate for machine abrasion. The abrasion of the work machine is a long-term phenomenon, which depends on the quality of the input material and the settings of the machine. Analysis therefore required studying the long-term behaviour of the work machine. The work machine and its operation are expensive, and during the project, reference machines and processes could not be used, only a real operating machine.

4.1 Data acquisition system

Modern work machines use increasingly distributed architectures like CAN-networks. CAN (Controller Area Network) is a protocol for distributed control systems, which has gained widespread use in industrial automation as well as in automotive applications and mobile machines. The different on-board sensor signals are available on the CAN-network and can be used by the on-line condition monitoring system.

A data acquisition system has been developed, which consists of two parts (Scholliers 1998):

- a short-range system, which transmits the data from the machine to a data collection PC near the work site,

- a long-range system, which transmits the gathered data to an office, where the collected data is analysed and used for the development of the condition monitoring algorithm

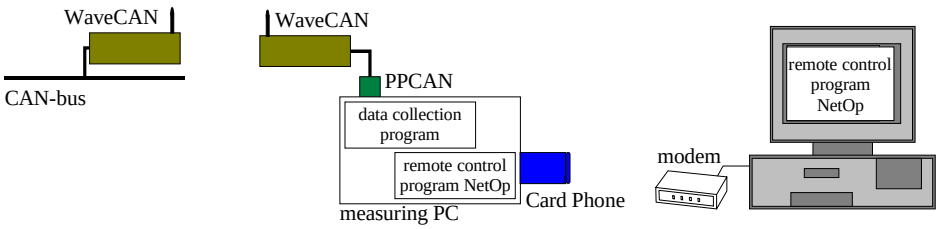

Figure 4. Overview of a data-acquisition system using WaveCAN (Scholliers 1998).

Figure 4 shows a system in which the main element of the short-range acquisition system is a WaveCAN radio link. WaveCAN is a two-way 2,45 GHz radio link from Kvaser Ab, which transmits the CAN-messages from the machine to the measuring PC, which is located in a sheltered place near the machine. A CAN-interface link interfaces with the PC, where the CAN-messages are stored in files. The files are transmitted over a GSM link to the office PC, where the data is analysed. A remote control program allows transferring files between the measuring PC and the office PC.

4.2 Behavioural model

4.2.1 Normal Operation Model

Measurements were performed during nine months on an operating machine. Starting from the measurements, relations are sought between the different on-board sensor signals. The available on-board sensors mostly do not provide complete information on the all the factors, which influence the process (e.g., outside temperature and humidity, parameters and amount of the input material, actual value of the wear). Digital inputs on the state of the machine, like devices on/off, are used to determine the operational mode of the machine (off, starting, idle, working, change of machine settings, calibration). One of the available on-board analog signals is selected as input. For each of the operation modes, a quasi-static model is derived for the behaviour of the other signals by the use of regression techniques.

Starting from this behavioural model, a model is generated for the Hardware-in-the-Loop simulator, which relates the output sensor variables to the input variables, using additional information on, e.g., the digital states of the machine.

In the pilot work machine, wear cannot be measured derived directly from the measurement results, only indirectly at the calibration moments by verifying the setting of the machine before and after calibration. However, the differences in the signals were too small to be useful for wear evaluation. These sensor signals can not therefore, be used for evaluating wear, and hence a method based on extrapolation of historical data is used.

4.2.2 Modelling of machine wear

Wear is modelled by a long-term analysis of the calibration data with respect to the on-board sensor signals. The wear relation is characterised by a curve, which should use a minimum of parameters, so that it can easily be maintained.

A simple regression curve is first evaluated, which relates the machine settings after calibration to a sensor value, or to the integral over time of a sensor value (e.g., consumed energy). If this approximation does not describe the real wear curve accurately enough, a polynomial or exponential curve is used. For polynomial approximations, attention must be paid to ensure that the shape of the polynomial always corresponds to the desired shape.

Changes in the operational conditions (e.g., quality of the input material if the machine is moved to a new site) may affect the wear rate severely, so that the algorithm to estimate wear should have some adaptive capabilities. The model of the wear is continuously reviewed during operation, both at a new calibration point and when changing the abrasive part (Figure 5). At a calibration point, the parameters of the estimation curve of the current part are reviewed, based on the difference between the curve with the existing parameters and the new calibration point data. At changing of a part, a curve is calculated which approximates the calibration data of the old part, and the new curve uses both the older parameter data and the new curve data.

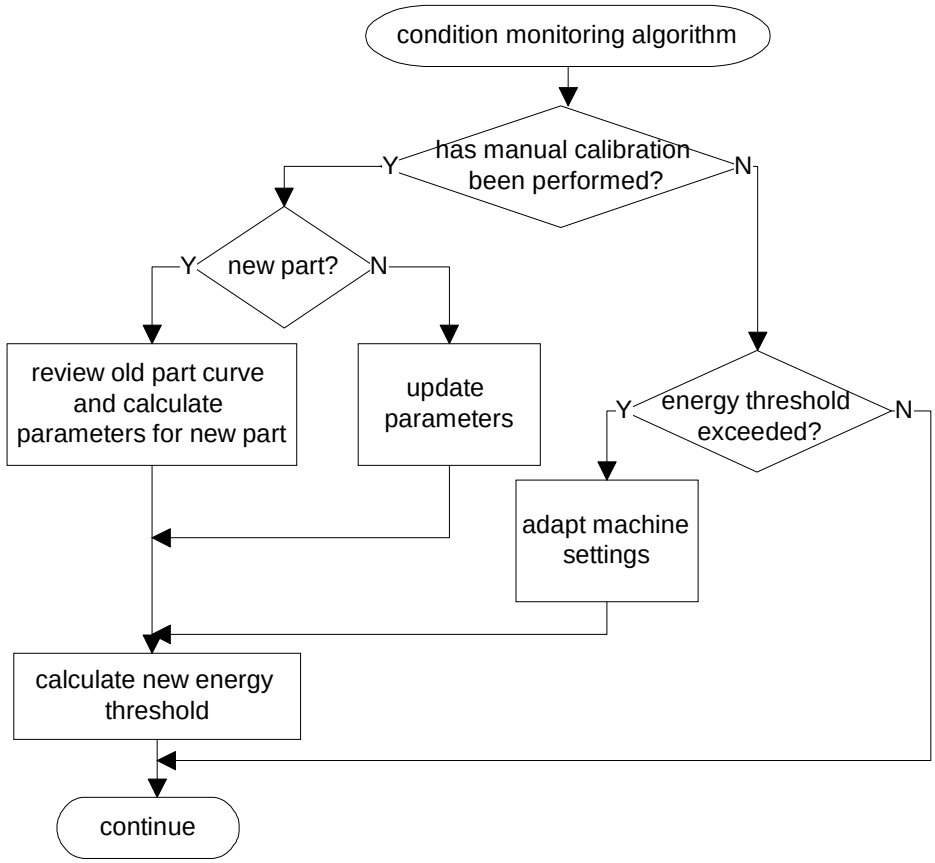

Figure 5. Algorithm for compensating wear and updating wear model.

Problems, which occurred during the project, are twofold:

– The development of the wear algorithm requires monitoring the machine over a long period. The data is stored and analysed off-site. If the data collection fails, data is missing, and, e.g., the total energy consumed for the current abrasive part, is erroneous. The data acquisition system, which is described in Section 4.1 is a prototype, which consists of components of different manufacturers. If a component fails or the power has been switched off during a longer time and consequently the data acquisition program is halted, this is only detected at the next attempt to download data to the office computer. For missing periods, data are extrapolated from previous measurements.

– Abrasion is a very slow process. In the project, one product cycle was about 3-4 months, so that only three parts were monitored. The method developed is, however very flexible, and should be able to handle different kinds of mantles.

4.2.3 Wear compensation

From the model, an algorithm for detecting the wear and hence for compensating wear automatically can be developed. In the pilot machine, the machine settings are altered if the consumed energy exceeds a threshold, which is calculated from the estimated wear curve (Figure 5).

5. Conclusions

This article describes the modelling and compensation of the wear for a work machine with abrasive parts. An algorithm has been developed for modelling and compensating wear. The algorithm is included in the condition-monitoring algorithm. In the next development phases, the algorithm has to be embedded in the machine and has to be further validated.

References

Kurki M. 1995. Model-based fault diagnosis for mechatronic systems. Espoo: VTT. 116 p. (VTT Publications 223), ISBN 951-38-4761-6.

Scholliers, J. 1998. Development of a data acquisition system for the condition monitoring of an off-road machine using WaveCAN. SMART technology programme, research projects MASI and HYSI. Workshop on Modelling and simulation of multitechnological machine systems – subsystems and their interaction. Spektri, Espoo, 28.10.1998.

Modelling of mechatronic device for condition monitoring purposes

Panu Kiviluoma
Helsinki University of Technology, Machine Design
Espoo, Finland

Abstract

A detailed Multi Body System model of a mechatronic device is applied to define measurements and signal the processing necessary for condition monitoring. The physics-based model combines the approximative dynamic characteristics of individual components, constraints and excitations both in normal and faulty conditions. The system dynamics depend highly on the flexibility, friction and damping of the joints and power transmission components, as well as on the mass and inertia properties of the system. Bodies with modes on the low frequencies are considered flexible and are therefore FE-modeled. Modelling of the faults is based on the analysis of the common faults detected in the device in its true operation environment. The models are verified by mobility and operation response measurements in laboratory and field conditions. The preliminary results indicate that response changes caused by faults can be detected in simulations. An applied procedure can be used in the design of condition monitoring instrumentation and signal analysis of systems with unstationary operation cycles.

1. Introduction

An increased demand on reliability and lower maintenance costs requires the development of condition monitoring and a fault diagnostics system that can operate in a multitechnical environment. Traditionally, the problem has been approached through prototyping and measurements. The approach used in this study is based on a detailed physics-based MBS-model (*Multi Body System*) of the system. Using this "Virtual Prototype" it is possible to find out which quantities of the system should be measured, where the measurements should be

taken and what kind of instrumentation is necessary. Measurements also provide a basis to outline what kind of signal processing would best describe the behaviour and condition of the system. This kind of a modelling approach has certain benefits in the product development process, in which MBS-models are normally used for the analysis and optimisation of the system construction and operation.

1.1 An automatic elevator door

An automatic elevator door is a typical mechatronic device containing complex and flexible multi degree-of-freedom mechanisms, a digitally controlled electric actuator and dynamic interaction between these subsystems. A door system that consists of landing and car doors is operated by a single actuator located in the car. The power transmission is implemented by a toothbelt and synchronisation wires. On a macro level the control of the operator tries always to repeat the same operation cycle (acceleration, constant velocity and deceleration phases). On a micro level much vibration is caused by contacts and faults. There is a great variety of door sizes, panels, etc. The door system model should be robust and easily modifiable to fulfill different needs.

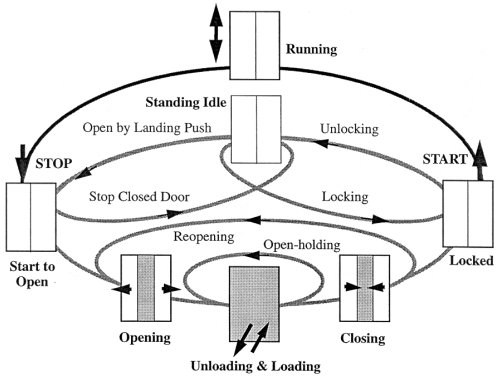

Figure 1. Operation cycle of elevator doors.

Some of the faults can be identified on the basis of the signals already available from the system but there is still need for additional instrumentation. Simulations using a physics-based virtual model offer an interesting and novel approach to instrumentation design. The research is focused mainly on

mechanical faults at certain phases of the operation cycle. Faults in electronics are left out because of their on/off-nature, which often makes them unpredictable.

1.2 Special features of modelling

When modelling for condition monitoring purposes we are mainly interested in changes in the system's state. The state can be, for example, structural (natural frequencies, modes), operational (cycle times, velocities, accelerations) or logical (operation sequence). Our approach focuses on the system dynamics. Usually the changes in system's natural frequencies, modes or dampings indicate error. Low frequency phenomena are related to the whole structure while local faults excite higher frequencies and are usually more difficult to determine. However, the faults in automatic doors appear mainly as excitation changes. though.

The dynamic behaviour of the automatic elevator doors is strongly dependent on the flexibility, friction and damping of the joints and power transmission components as well as on the mass and inertia properties of the moving parts. The most difficult properties to define are damping, friction and stiffness; the definition of mass and inertia properties is quite straightforward, but time consuming procedure if 3D-models are not available. Damping is generated both by friction and viscous damping in the contacts and by the mode-dependent proportional damping coefficients of the flexible bodies.

The door is designed to operate in plane, but gaps, tolerances and out-of-plane forces can excite motions in an out-of-plane direction too. Each point has six degrees of freedom and constraining is always an approximation.

The flexible door panels are important in this case since they are very sensitive to the excitation changes at low frequencies. The door panels are thus potential locations for the real condition monitoring instrumentation. On the other hand, the model consists of many contacts producing sudden force changes and thus exciting the wide frequency band.

2. Methods

2.1 Modelling tools

ADAMS 10.0 (by *Mechanical Dynamics Inc.*) which is used for MBS modelling is able to handle large mechatronic models including kinetics, flexible bodies (separate FE-models), contacts, friction, damping and run-time control. The FE-models were created by using IDEAS 6.0 (by *Structural Dynamics Research Corporation*).

2.2 Modelling sequence

Structurally, the door system is modeled as a set of modular sub-assemblies as given in Figure 2.

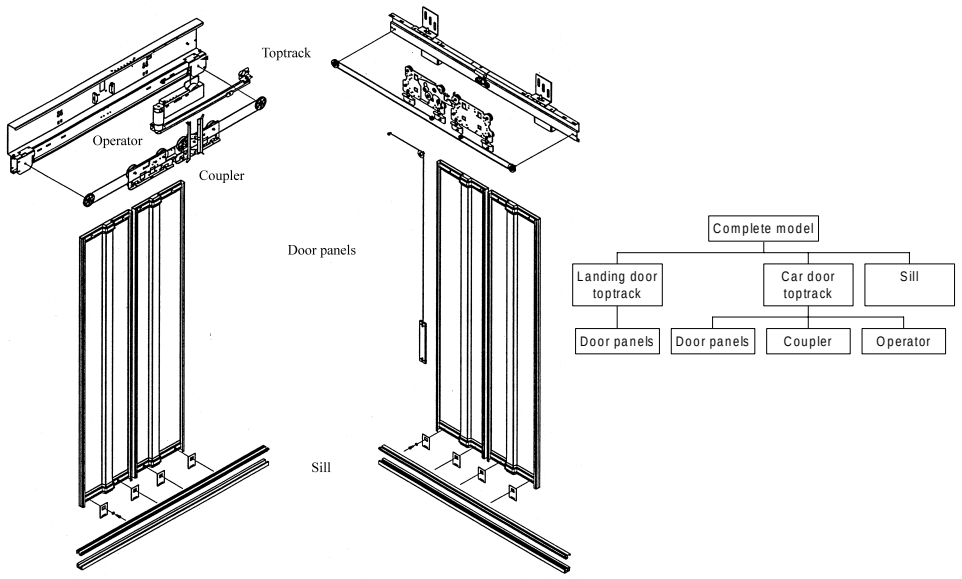

Figure 2. Sub-assemblies of a typical automatic elevator door and their modelling sequence.

Technically, modelling is carried out stepwise and develops more complex models for more sophisticated phenomena (Table 1).

Table 1. Modeling sequence of an automatic elevator door. Each step includes the model of the preceding step until the model is completed.

Modeling step	Input	Output
Geometry	Geometry and locations of parts	Static visualisation
Kinematics	Geometry of assembly and joints	Rigid, main motions
Kinetics	Mass and inertia properties, friction	Energy, finite motions
Flexible joints	Joint flexibilities and dampings	Finite forces, vibrations
Flexible parts	Internal flexibility of parts $\Rightarrow$ FEM	Response of mechanics
Control	Mathematical model of control	Door in normal conditions
Car, shaft, hoist	Car and its suspension	Final model
Faults	Physical models of faults	Fault effects

2.3 Model components

The physics-based virtual model is a combination of the approximative characteristics of individual model components: parts, constraints and force features, and control loop. As modelling is always an approximation, the complete model may include cumulative inaccuracies.

The only external forces applied to the model are gravity and the driving torque. Other forces are supporting forces caused by the motions and external forces.

2.3.1 Rigid parts

Rigid static and moving parts are modeled directly in ADAMS. Their modelling is associated with the visualisation, the definition of the joint locations and the definition of inertia properties. The structural parameters of the static parts are neither used nor needed.

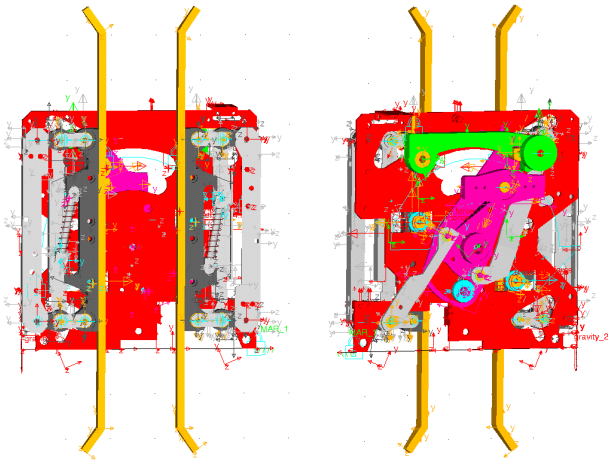

Figure 3. Two views of the model of the coupler.

2.3.2 Flexible parts

Moving and static parts containing internal flexibility on the interested frequency range, i.e., the door panels, are FE-modeled and used in ADAMS as flexible bodies with experimentally defined proportional damping coefficients. FE-modelling of the door panels introduced familiar problems into the locally loaded sheet metal structures.

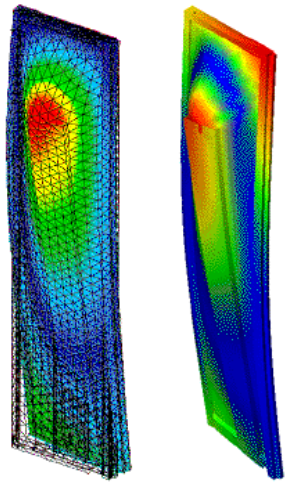

Figure 4. Mode shape of a door panel: FEM (left), ADAMS-Linear (right).

2.3.3 Flexible joints

Rigid moving parts containing flexible connections are also modeled directly in ADAMS. These parts may vibrate relative to the connected parts and/or vice versa. Their flexibility is taken into account by using deflection and velocity dependent forces, e.g. springs-dampers and contacts. The flexible connections related to these parts have a great effect on the dynamic behaviour of the whole system.

Flexible transmission components are modeled in ADAMS as deflection dependent spring forces. The non-linear stiffness properties of belts and wires are taken into account as well as the effective inertias of the transmission components. Constraints and force features are modeled using basic joints and forces of ADAMS which provide a wide variety of space or part-fixed force definition methods. Elastic properties of the elastometric buffers have been determined in part by geometry and material parameters and/or measurements.

Belt and wire transmissions have notable flexibility in the direction of the load. They also act as flexible couplings thus damping high frequency vibrations. Elastic behaviour of these transmission components is also highly non-linear. In principle they carry only traction loads.

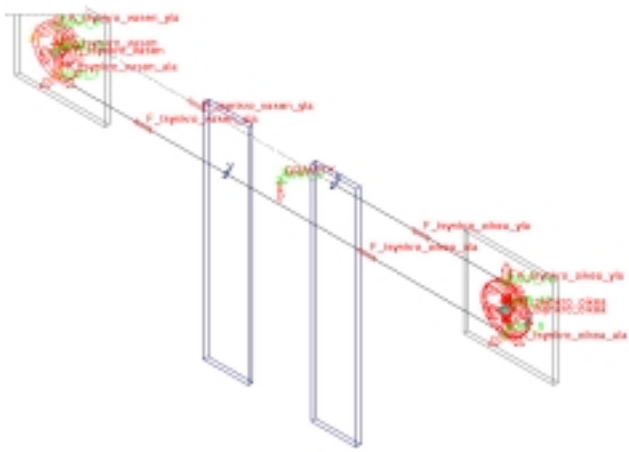

Figure 5. Simplified test model of the door synchronisation.

2.3.4 Contacts

Remarkable clearances are modeled as ADAMS predefined contact types, which cover most ideal frictional contact types. Contacts produce transient excitation and increase the number of degrees of freedom simultaneously. New circle-to-curve and curve-to-curve type of contacts in ADAMS 10.0 made it possible to model with ease the operation of locking mechanisms that earlier would have had to be done using complex force-functions.

Figure 6. Locking mechanism is modeled using curve-to-curve-contact.

2.3.5 Operator and control

Automatic door actuator is permanently magnet synchronous AC-motor, whose control is realised by DSP (Digital Signal Processing). As the motor itself is one possible source of excitation, the model should describe its dynamic behaviour with sufficient accuracy. In this project the control loop is modeled as simply as possible but may contain some differences to the real control system as the operation of the actual control is not know in detail. However, simplification is justified as the power transmission is very flexible and thus filters the effects of high control frequencies. The control loop is modeled using a FORTRAN user-subroutine supported by ADAMS. Other ways for modelling the control would be to use the control module of ADAMS or to run Matlab simultaneously with ADAMS. Using Fortran-subroutine for motor control makes is the possibility to carry out necessary calculations easier during simulation and it would also enable the adjustment of the control loop timing.

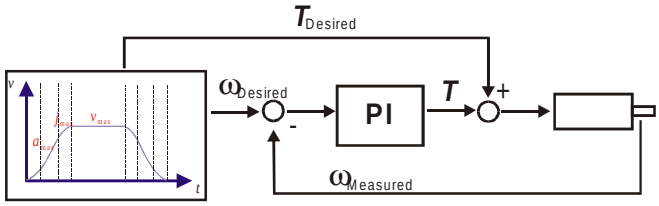

Figure 7. Model of the control system.

The model is driven by applying controlled torque to the output shaft of the motor, from which the power is transmitted through a stiff planetary gear to the elastic belt/wire transmission. Torque is restricted by the maximum allowed static closing force between the door panels.

The velocity reference is constrained by maximum jerk, acceleration and velocity in different phases of the cycle. The velocity curve is optimised for fixed opening distance.

2.4 Modelling of faults

The modelling is preceded by an extensive fault analysis, which is based on the common faults detected from the doors in their true operation environment. The main objective in the fault analysis is to find out the physical phenomena (deformation, increase of friction or clearance, etc.) causing the fault and the corresponding fault frequency. Related physical phenomena are needed for modelling purposes. Most mechanical faults can be modeled by changing model parameters like friction, clearances and disturbances associated with the sliding and rotating motions. For condition monitoring it is essential to know if the faults can be detected using measurements.

Certain typical faults such as increased friction or obstacles in joints and contacts were selected for the model verification and simulations. The most probable fault types for future investigation produce transient excitation during the operation cycle. In addition, faults producing increased friction slow down the operation cycle since the maximum torque of the motor is restricted by the maximum closing force.

2.5 Model specifications

The modelling was done in *Silicon Graphics Octane* workstation with 512 MB of memory installed. Analysis of open-close-cycle (9 s in real time) with 3 ms step takes about 2 hours. This analysis is practically the best one that can be run on present workstation due to memory constraints.

Table 2. Model specifications (number of different modelling elements).

Moving parts	141
Flexible bodies	4
Cylindrical joints	4
Revolute joints	43
Spherical joints	16
Translational joints	3
Fixed joints	87
Inline Primitive_Joints	6
Inline Primitive_Joints	6
Coupler	1
Contacts	69
Degrees of freedom	132

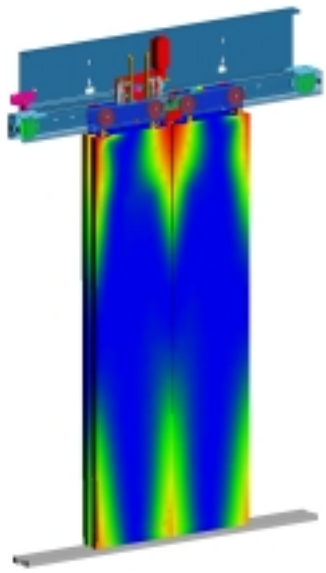

Figure 8. The model of automatic elevator doors.

3. Results and experiences

The verification of the model is still unfinished. The open-close cycle simulations in normal condition were performed and the velocity of the door panels is very consistent with the measurements.

ADAMS is not at its best in modelling of 3D geometry so either a specialised 3D software should be used for geometric modelling or model geometry should be simplified (without losing the mass or inertia properties of the parts). There are still some problems in ADAMS related to basic geometry construction and modification. Furthermore, requirements for modelling hardware increase rapidly as the model gets more complicated. Mechanisms with dozens of parts and joints may cause instability in the whole system.

The model was build exactly according to design drawings, which proved to be wrong approach. This kind of complex and detailed model is hard to parameterise and manage. It would have been better first to test and verify selected modelling techniques using simplified models. Then, if necessary, more accurate modelling and analysis could been made on the phenomena that needed further investigation. The most challenging elements in the model were:

- flexible joints and contacts
- belt and wire transmission
- control
- complex mechanisms (especially in coupler).

However, ADAMS proved to be very capable in handling the problem under investigation. Its predefined modelling tools are easy to use and the forces, constraints and flexibility definition possibilities cover the needs of modelling mechatronic devices. Although the model was not parameterised because of the amount of extra work needed, the developed modelling principles can be applied as they are or adapted for the modelling of different door configurations or the whole elevator system.

4. Discussion

The development of the 3D-CAD software provide better data transfer between different types of modelling software, releasing the modeler to concentrate on the building of the model. The MBS-modeler should be a part of the product development team. That would help designers to understand the needs of MBS-modelling. No matter what the current state of the applications of this kind of technology is in the industry, it will be seen that MBS-modelling will be a solid part of design process. It depends highly on the application, how complex the model should be and which phenomena should be taken into account. In the future we will see single modelling tools capable of doing both basic product modelling and specialised modelling and simulation (FEM, kinematics, kinetics and dynamics) for different purposes.

This research indicates that modelling and simulation are appropriate tools for the design of condition monitoring systems. Modelling for condition monitoring purposes requires, however, deep understanding of the physical phenomena of the structure and operation and their relation to the faulty behaviour. Fast and accurate modelling requires that the necessary information of the system is available from the beginning. Deep understanding of the system is also the only way to simplify the model.

4.1 Input requirements

The applicability of the modelling and simulation in the product development process of a mechatronic device depends on the data available. The product information needed to modelling a mechatronic device for condition monitoring purposes differs to some extend from basic modelling needs. The following data is a minimum requirement for successful modelling:

- geometry (parts and connections)
- material, mass and inertia properties
- stiffness and damping
- control algorithms and principles
- operational parameters.

3D-CAD-software tools used for basic product modelling can provide the geometric data of the structure, which in most cases can be imported directly to ADAMS. 3D-models are in practice essential for correct assembly of the model. If the parts are modeled in their actual dimensions, ADAMS can calculate the necessary mass and inertia properties for them. Otherwise the data must be available from the product documentation. The dynamic behaviour of the system is highly dependent on the elastic properties of the structures and joints. Therefore the values for stiffness and damping for relevant components should be accurately defined. Especially in mechatronic devices where the operation is actively feedback controlled, full documentation of the control system is necessary for successful modelling. Using C++ or Fortran subroutines, almost any control algorithm can be adapted to ADAMS-model. Detailed specifications of the actuators are naturally needed for proper description of their operation.

4.2 Model simplification

Models must simplified in order for modelling to be a flexible tool, which can keep pace with product development processes. Building and modification of the model must be easy and fast. To fulfil these conditions complex structures must be simplified a great deal. The simplification of the model must begin already before modelling by examining how the structure can be reduced to the components that are necessary for desired operation. So understanding of the structure and phenomena related to it forms a basis for this procedure. The purpose of modelling must be kept in mind during this process. Simplification also serves the versatility, robustness and parameterisation of the model.

Some guidelines to easier and simpler modelling are:

- model the parts in 3D-CAD-tool and import them in ADAMS
- keep modelling to 2D (if possible)
- simplify parts and mechanisms
- reduce number of parts and joints
- reduce number of degrees of freedom
- brake the model down into sub-models.

In dynamic modelling most part features like fillets, chamfers and holes have no effect on the results unless mass or inertia properties are changed. That also applies on the purely esthetic forms in parts. In fact, adding them in ADAMS-model, increases the instability of the model. In addition, parts that are fixed in relation to each other should be combined.

Mechanisms can be simplified first by simplifying parts and then combining them if possible. Reduction of parts and joints reduces also the number of degrees of freedom of the model, which leads to a faster and more stabile model.

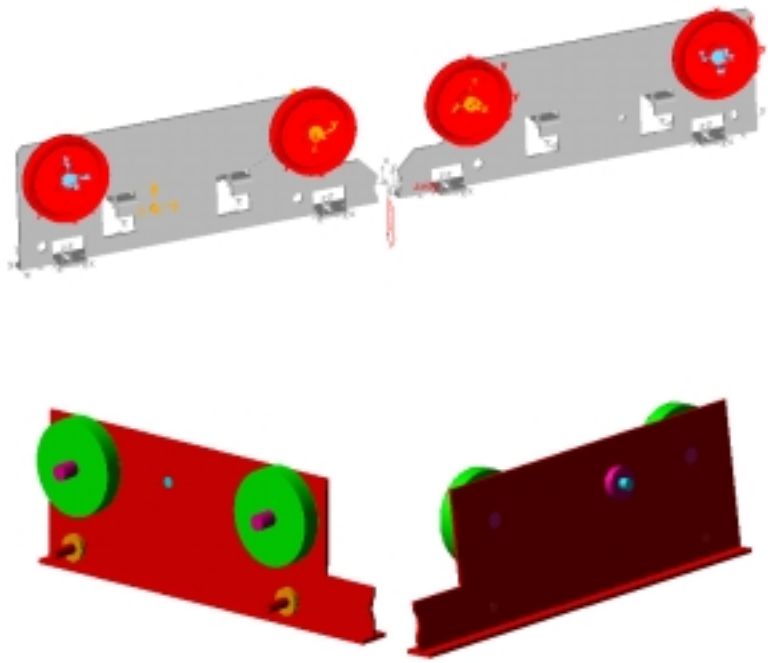

Figure 9. Only the necessary elements (contact surfaces, joint locations) of parts need to be modelled; detailed model of hanger plate (above) and simplified model (below).

In some cases it is acceptable to divide the model into several submodels. Then, for example, the problematic sub-systems can be analysed in more detail than the whole system. Output results of one submodel can then be used as input for other models.

MBS-model of a mechatronic device for the design of a condition monitoring system

Esa Porkka
Helsinki University of Technology, Machine Design
Espoo, Finland

Abstract

A detailed MBS-model (*Multi Body System*) of a mechatronic device is applied to define measurements and signal processing necessary for condition monitoring. The model is verified by mobility and operation response measurements in laboratory and field conditions. The preliminary results received from simulations of an automatic elevator door indicate that response changes caused by faults can be detected by the simulations. In addition to the ordinary mechanism design and analysis associated with the product development, the applied procedure can be used in the design of condition monitoring instrumentation and signal analysis of mechatronic systems with unstationary operation cycles.

1. Introduction

The design of the condition monitoring system is normally based on prototyping and measurements. In this study we use physics-based MBS-modelling and simulation (*Multi Body System*) for the operational simulations in both normal and faulty conditions. Using this "Virtual Prototype" we try to find out which quantities of the system should be measured, where the measurements should be taken and what kind of instrumentation and signal processing are necessary. This kind of modelling approach has certain benefits in the product development process, in which MBS-models are normally used for the analysis and optimisation of the system construction and operation. The case device is an automatic elevator door, which was measured for the model verification and updating. The research was done in the SMART-MAHIS-project, which is a co-operative project co-ordinated by TEKES (the National Technology Agency).

1.1 An automatic elevator door

An automatic elevator door is a complex mechatronic device, which has a long life-cycle and intensive maintenance program. A typical automatic elevator doors consist of landing and car doors, operator and the parts binding these to the car and hoist. In this study we concentrate on the door operation cycle (lock opening – door opening – door keeping at open position – door closing – door locking) in both normal and faulty conditions.

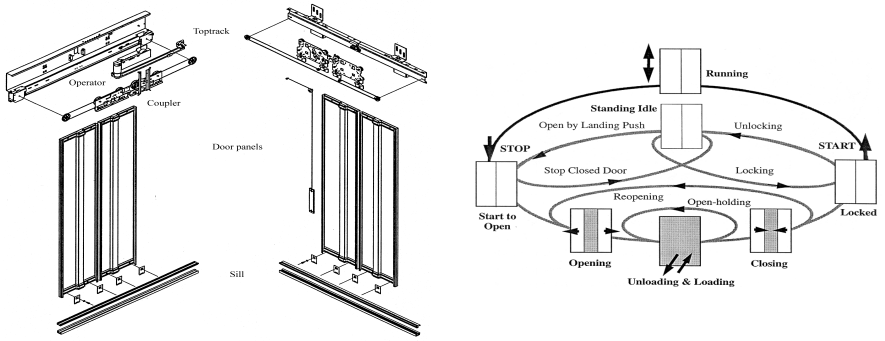

Figure 1. An automatic elevator door and the flowchart of its operation.

2. Methods

2.1 Modelling

ADAMS 10.0 (by *Mechanical Dynamics Inc.*) was used for MBS modelling including the definition of bodies, constraints, contacts, force features, friction, damping and control. The PI-control model was realised by Fortran user-subroutine supported by ADAMS Solver. The FE-models of flexible bodies were created in IDEAS 6.0 (by *Structural Dynamics Research Corporation*). The verification measurements and analysis were performed with HP3566A (by *Hewlett Packard*) - Star System 5.22 (by *Spectral Dynamics Inc.*) measurement and analysis system.

Structurally, the door system was modelled as a set of modular sub-assemblies: landing door – car door – coupler – operator. Technically, modelling steps were geometry – kinematics – dynamics – control – faults.

An extensive fault analysis was performed in order to find out the physical phenomena (deformation, increase of friction or clearance, etc.) causing the fault. The most mechanical faults produced transient excitation and vibrations during the operation cycle or slowed down the operation cycle.

2.2 Measurements

The verification measurements of the system were made in two phases. The first phase was performed in the laboratory environment with idealised boundary conditions. In the second phase the elevator doors were installed into their actual operation conditions (shaft, hoist, car and car suspension).

The measurements in both normal and faulty conditions were performed by measuring accelerations (and motor current) at different locations of the door assembly during the door cycle. Operation response measurements were excited by the normal driving forces. The mobility measurements and the modal analysis were carried out for door panels and door assemblies in a static state.

In the hoist measurements the effects of boundary condition changes and car/hoist dynamics were under investigation. A typical measured operation response (acceleration) is given in the Figure 2.

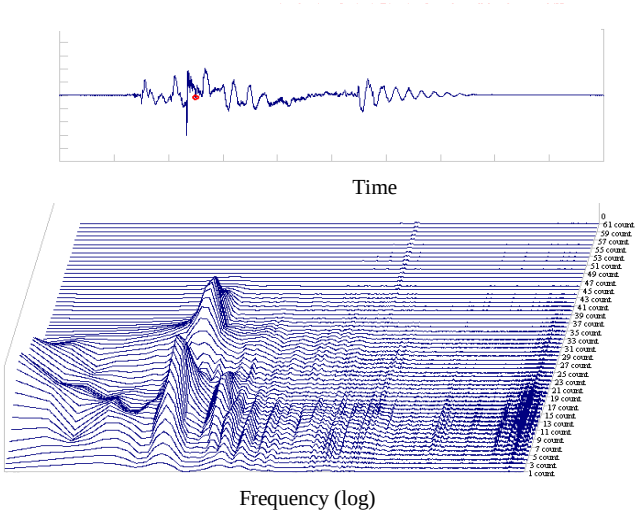

Figure 2. Measured acceleration and its waterfall plot.

2.3 Simulations

The first simulations using the complete model are related to the model verification and updating. The model without faults (normal conditions) is a subset of the model containing faults, i.e., only the faults are added to the basic model. Each simulation starts with static equilibrium.

During the dynamic simulations we take care that the joint and contact forces do not have sudden changes compared to the time step used. Usage of flexible parts notably increase the number of degrees of freedom and only the most remarkable modes must be used in order to achieve reasonable simulation times.

The nature of ADAMS dynamic analysis approach requires that the time step must be reduced until the output does not change (complete response is achieved, i.e., aliasing is avoided). As a model consists of many contacts producing sudden force changes and thus exciting a wide frequency band, it is hard to define an adequate time step size for simulation. Normally the step size must be set short to get stabilised results. This is not very effective, as we are not normally interested in the high frequencies excited by the transients. In the measurements analogue anti-alias (lowpass) filters are applied to the analogue signal in order to avoid the aliasing phenomena in the AD-conversion.

Eigenfrequencies and associated mode shapes and proportional damping coefficients calculated by ADAMS Linear are used in the verification process.

2.4 Verification and updating

The model is verified by mobility and operation response measurements, taking into account that the normal condition results must not be affected by the fault modelling. The quantities that are used in the verification process are natural frequencies and normal modes of the door panels and assemblies, door cycle duration, maximum acceleration and velocity, frequency content and vibration levels at certain frequency ranges.

Constraints and force features are a more probable source of modelling errors than the mass and inertia properties, which are results from 3D-modelling and thus normally out of updating interest. Mainly the stiffness, friction and damping

parameters of contacts and joints are updated within certain tolerances. The overall damping, which is mostly generated by friction in the joints can be verified on the free vibration response and on the total energy loss during the whole operation cycle. The updating process is a “trial-and-error”-procedure requiring engineering judgement.

The measured response signals are accelerations, which also give high amplitudes on the high frequencies. Integration into velocity or even displacement weighs the lower frequencies. In the measurements the lowest frequencies (main motions of the door) are filtered automatically by the accelerometer/amplifier characteristics. In ADAMS such filtering requires definition of similar filters in order to achieve similar results in the time domain. In the frequency domain these problems are not so clearly seen as are the main motions on the lower frequencies.

Lateral velocity and acceleration (measured and simulated) of a hanger plate is given in Figure 3. It can be seen that it is easier to reach good agreement for the velocity than for its time derivative.

The model can not handle high frequency vibrations correctly. It is obvious that the damping is over-estimated especially in the contacts.

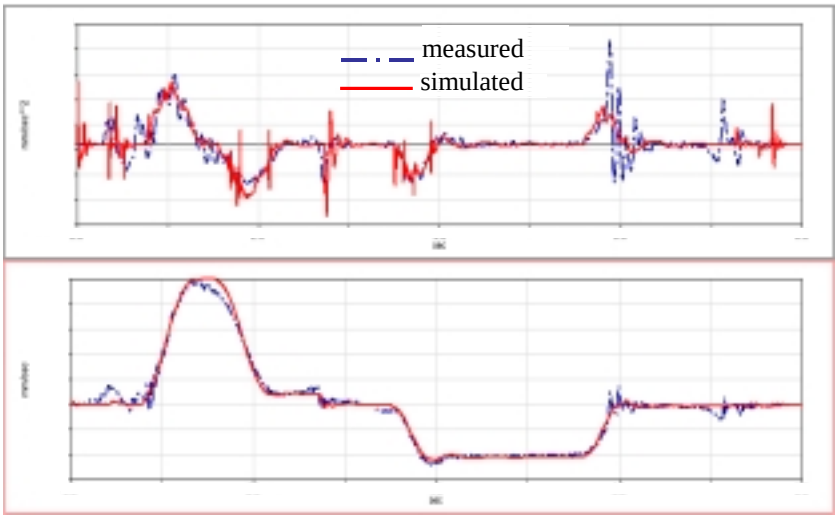

Figure 3. Lateral acceleration and velocity of a hanger plate during the door cycle.

The model is roughly updated and final simulations are not completed. The model sensitivity on the friction parameters, clearances and damping values could give additional information of the model's robustness.

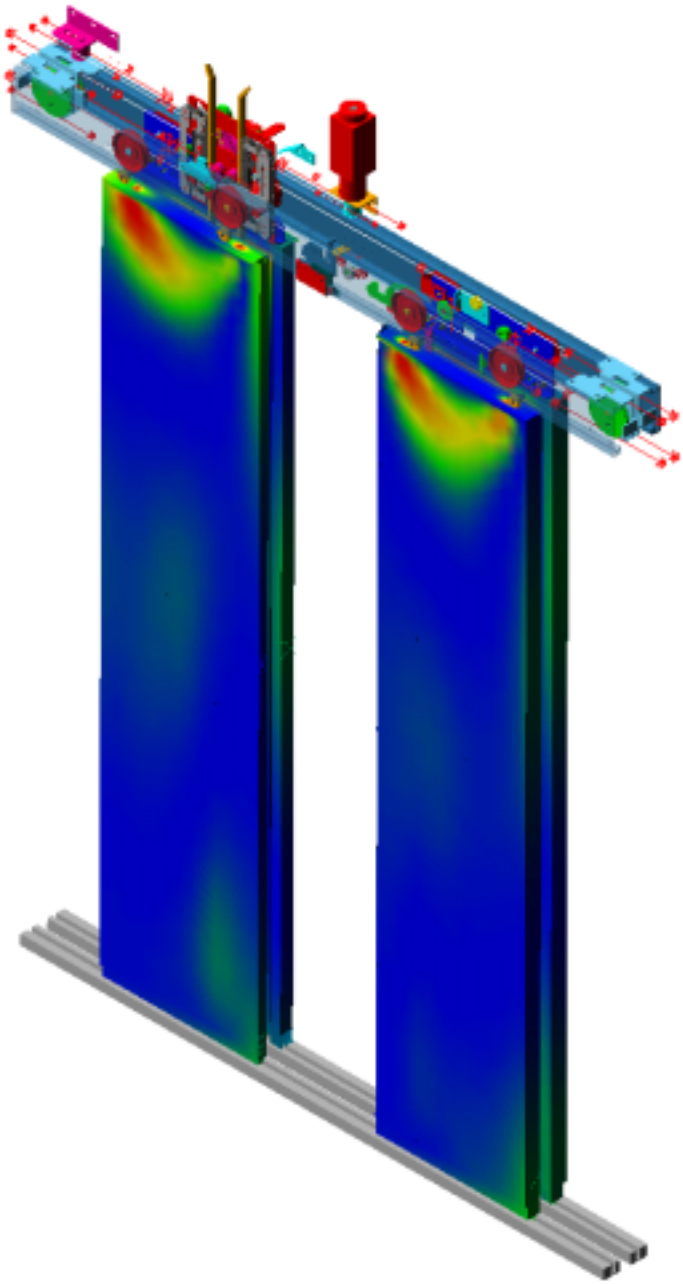

Figure 4. An automatic elevator door at simulated position.

3. Development of machine diagnostic system

The condition monitoring and fault diagnosis are normally based on the measurement of vibratory signals and their signal processing. In rotating machinery a lot of techniques use vibration signal analysis such as spectrum, order and cepstrum analysis. The door system has rotating components with time, or actually position, dependent rotating velocities connected to parts with linear movement. The diagnosis of the linear movement is associated with the non-stationary dynamic excitation, simultaneous transient effects and an unknown type of excitation.

Basically, the condition monitoring and fault diagnostic methods can be divided into continuously measuring methods and on methods which require occasional health tests. The signal analysis in both methods can be done using the same methods. Continuous fault diagnosis can be done only by using continuous monitoring or by automating frequent health tests in the operation environment.

Machine diagnosis can be divided into the following categories, depending how accurate the fault detection is:

1. identification of fault existence
2. identification of the fault type and location
3. identification of the quantity of the fault
4. prediction of the residual lifetime.

In most applications the first level is accessible and adequate. Applications associated to levels two to four are normally well known and they have large economical or safety aspects. In the case under study the first level is realistic and objective; in some cases the fault location can be detected. In the real world the reference based condition monitoring may recognise how the fault is developing but simultaneous faults may disturb the response complicating the fault identification.

3.1 Identification of faults from responses

The natural frequencies of an elevator door are installation dependent and structural changes can be normally seen on high frequencies, where mode density is intensive. The faults in automatic elevator doors seem to change mainly the excitation not the structural parameters. This leads to a diagnosis system, which should identify the fault by analysing the response. Some faults generate friction changes, which does not necessarily excite vibration unless stick-slip phenomenon is present. These kind of faults may be detected by increased operation time or by increased motor moment with a clear relation to motor current, which is measurable and thus one potential signal to be monitored in most mechatronic devices.

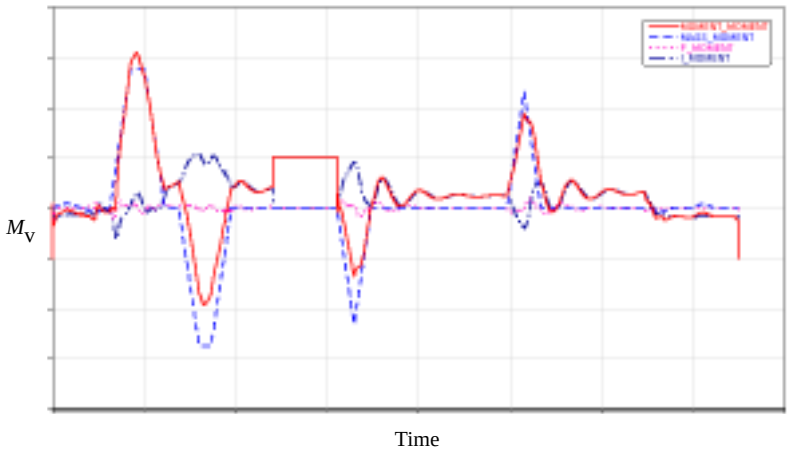

Figure 5. Driving moment and its base moment (mass) with P- and I-portions.

Identification of faults leads to state, time, frequency and/or amplitude domain approaches. The operation cycle can be divided into several subtasks by an external trigger signal from the motor control pulse or state sensors, for example. Distance- or angle-based external sampling which is a widely used technique in rotating machines compensates the effects of unstable velocities.

The state type method is based on the on/off signal from state sensors added into the system. This could be an applicable method for rough fault diagnosis, but it needs numerous sensors for adequate definition of the door's state in each set of

operation conditions. Fault prediction is still a problem in this kind of monitoring.

Time domain analysis can be used to define the duration of the operation subtasks. This could help the identification of the transient arrival times and, on the other hand, this could be used in the operation cycle partitioning. The time domain signal can be compared to the predefined envelope, which can not be exceeded without warning. This kind of method requires accurate time synchronisation between the envelope and the measured signal, especially in transients. Time domain data contains the whole measured information and makes it possible to proceed with the analysis in other domains also.

Fast Fourier transform (FFT) of the signal defines the frequency content and the corresponding vibration level at each frequency. The measurements should be done on a quite wide frequency range, i.e., wider than used in simulations (333 Hz sampling frequency). Frequency resolution limits the interpretation of the low frequency vibrations as the cycle duration is limited.

Operational transfer function can be formed between two measures (for example accelerations) and it gives information about the frequency content and the local response phases. This can also be valuable information in the machine diagnosis of automatic elevator doors although its applications are mainly related to the rotor dynamics.

Spectral maps (waterfall plots) give a fast description of the frequency and amplitude distribution on each operation phase. Changes between the reference spectral maps would indicate fault or at least some kind of changes in the operation. Excitation of a wide frequency range would give information about the transients.

Amplitude domain methods (histograms) can take into account the amplitude distribution, frequency ranges and the operation subtasks also. This is more accurate indicator than the pure average vibration level. The development of the door vibrations can be easily visualised and conclusions can be made of the fault appearance.

3.2 Implementation

A true condition monitoring system should be quite robust so as to clearly identify if faults are present and give the information on which signal changes the identification is based. As a conclusion the operation cycle should be divided into sections, which describe certain phase of the operation. The sections can be analysed by using time, frequency or amplitude domain methods. The data transfer in the time or frequency domain make it possible to use case dependent signal analysis for each section. The amplitude domain is perhaps the most robust method making further analysis unnecessary and impossible. Time domain data contains the whole measured information and makes it possible to proceed with the analysis in other domains also.

Some developed faults can be detected directly from the control signals. As long as the control can compensate for the effects of the faults, the fault can not be necessarily seen but the control has already detected the changed conditions. If we want to know if there are any faults, this approach could be adequate for robust predictive condition monitoring. These signal are already available, which is desirable when a universal condition monitoring system is under development.

Elevators have quite intensive dynamic response during the ride and under moving loads (persons in the car). It is recommended that the monitored signals should be measured during special health tests or each time the car is unloaded, i.e., when the excitation from the environment is smallest. During the health tests the car must be stopped at landing and occasionally between the landings. These measurements give information not only from the car door but also from the individual landing doors, if each landing is separately monitored. Periodic health tests minimise the data transfer and give case-independent data. This kind of approach is a reasonable basis for the robust condition monitoring, which utilises the measured signals in association with the control and actuator signals. The reference state is the true signal of an elevator without faults and the changes in these signals indicate faults.

4. Conclusions

In this research we MBS-modelled an automatic elevator door for operation simulations. The verification of the model is based on the operational vibration measurements and mobility measurements. The model was mainly constructed in ADAMS using manufacturing diagrams of the door components. The selected approach is quite laborious but very informative.

The dynamics of a mechatronic device are strongly dependent on the flexibility, friction and damping of the joints and power transmission components, as well as on the mass and inertia properties of the system. Bodies which have modes on the low frequencies must be considered flexible. The approximative dynamic characteristics of individual model components may lead to cumulative inaccuracies that sets high verification demands for this kind of application.

Simulations which use a reliable physics-based model can replace measurements typically needed for design of condition monitoring instrumentation and diagnosis methods. The applied procedure has certain advantages in systems, which have unstationary operation cycles, because response changes caused by faults can be detected and predicted already in the product development stage. However, MBS-modelling is a better tool for selecting different design proposals than for modelling large detailed assemblies.

A true condition monitoring system should be quite robust so as to identify clearly any faults present and show which signal changes the identification is based on. For modelling of a condition monitoring system it is essential to find out the physical phenomena related to the faulty behaviour. The utilisation of the control and actuator signals is highly recommended.

Literature

Collacot, R. Vibration Monitoring and Diagnosis. George Goodwin Ltd, London 1979.

Dalpiaz, G. & Rivola, A. Condition Monitoring and Diagnostics In Automatic Machines: Comparison of Vibration Analysis Techniques. Mechanical Systems and Signal Processing, Volume 11, No. 1., Academic Press Ltd 1997, p. 53–73.

Doebling, S. W, Farrar, C. R. & Prime, M. B. A summary review of vibration-based damage identification methods. The Shock and Vibration Digest, Volume 30, No. 2., Sage Publications, Inc. 1998, p. 91–105.

Simulation of the hydromechanical roll system

Tommi Hammarberg
Lappeenranta University of Technology
Lappeenranta, Finland

Abstract

This paper shows the development of the simulation model of the hydromechanical roll system. The roll system model consists of a rotating flexible shell supported by hybrid pad bearings, which locates inside of the flexible shell. The hybrid pad bearing is controlled with single-acting hydraulic cylinder.

All components, control system and interactions (such as bearing, sliding contact, hydraulics) between these components and subsystems are modelled with in ADAMS® mechanical analysis software.

The rotating flexible shell is modelled by using assumed modes method which means, that mass matrix, stiffness matrix, mode shapes and corresponding frequencies are transferred to ADAMS from ANSYS®.

1. Introduction

A deflection compensated roll is widely used in the paper making industry. The deflection compensation will potentiate the adjustment and control the nip pressure along the line of the nip. However, the deflection compensated roll is a quite complicated, especially when the flexibility of parts is taken into account.

Figure 1 shows the software environment which was use to develop the simulation model of the hydromechanical roll system. Flexible parts (assumed modes) are created with ANSYS, every interaction is created within ADAMS such as: bearing, hydraulics, sliding force effect, etc.

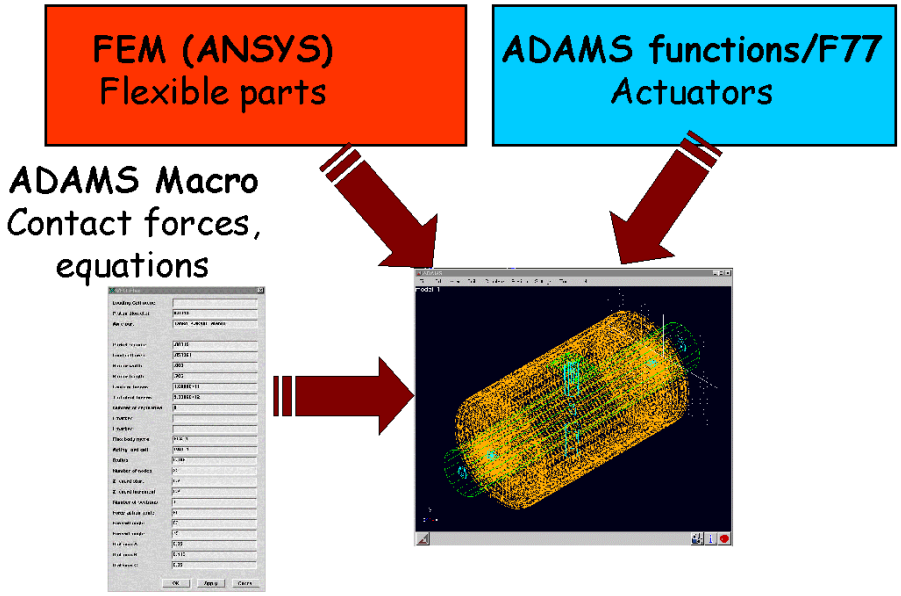

Figure 1. Software environment in Lappeenranta University of Technology.

2. Simulation model

Figure 2 shows that the constructed simulation model consists of several interactions. The hydraulic system and the pad bearing model are modelled by using the theory of lumped fluid together with semi-empirical method (hydraulic components). Figure 3 is a simplified model of a deflection compensated paper roll. The simulation model consists of one pad bearing and cylinder combination.

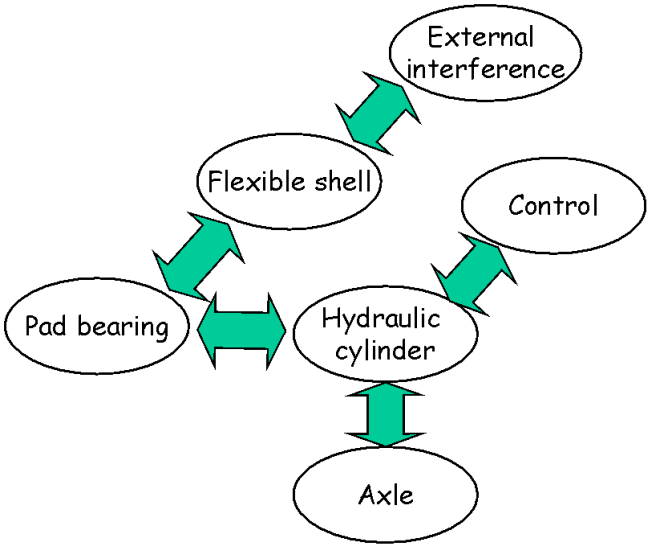

Figure 2. Interactions.

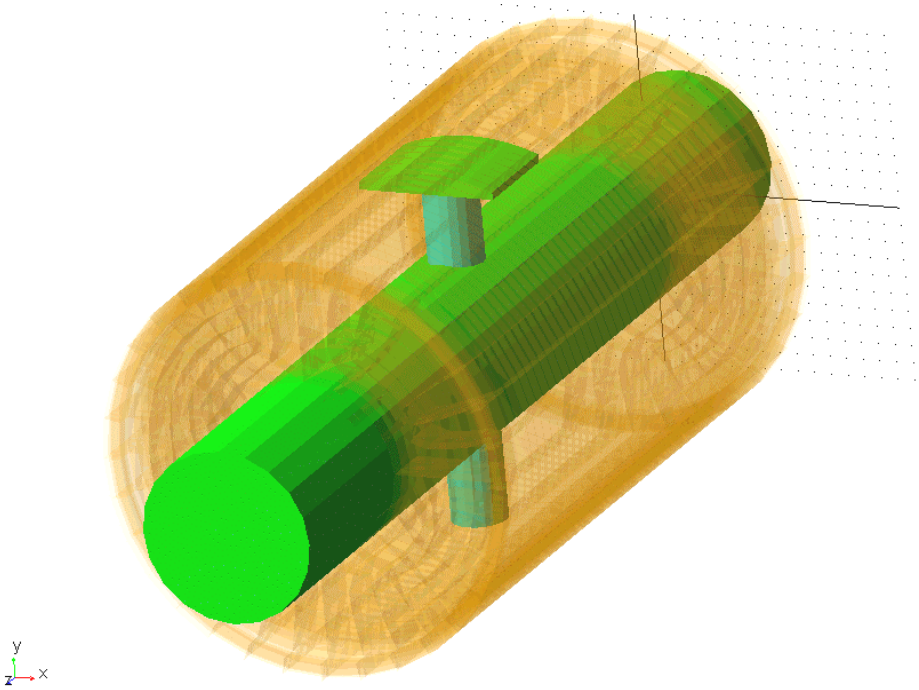

Figure 3. Simulation model.

The sliding contact and measurement of the distance between the pad bearing and the flexible shell needs special procedures. The biggest problem using so-called ADAMS/Flex-parts is that the forces or joints, etc. can only be located in the nodal points (Figure 4). The engagement of each force depends on the rotational angle of the shell and distance between the bearing and the shell.

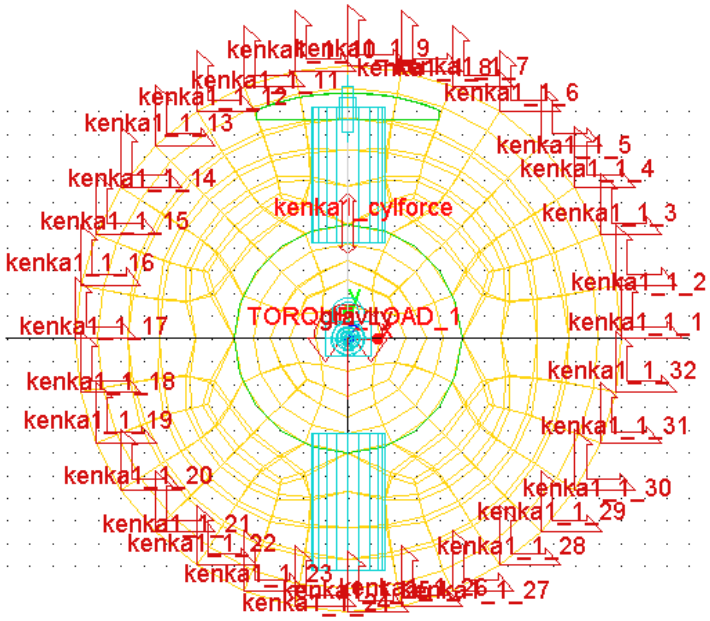

Figure 4. Placement of forces.

3. Results

Simulation model is completely faultless unless the model allows for faults. Faults may come from manufacturing tolerances, assembly or material faults. Simulation of the faulty shell is possible. Imbalance is relatively easy to model while the geometric fault needs more effort. Figures (Figure 5, Figure 6 and Figure 7) show how the ellipticity of the shell affects the operation of the simulation model when accelerating the rotating shell. Figure 5 shows the amplitude of the ellipticity, Figure 6 shows the alternation of the oil cap between the pad bearing and the shell. Ellipticity is too much for the simulation model and the pad bearing hit the wall of the shell. Figure 7 shows the movement of the pad bearing.

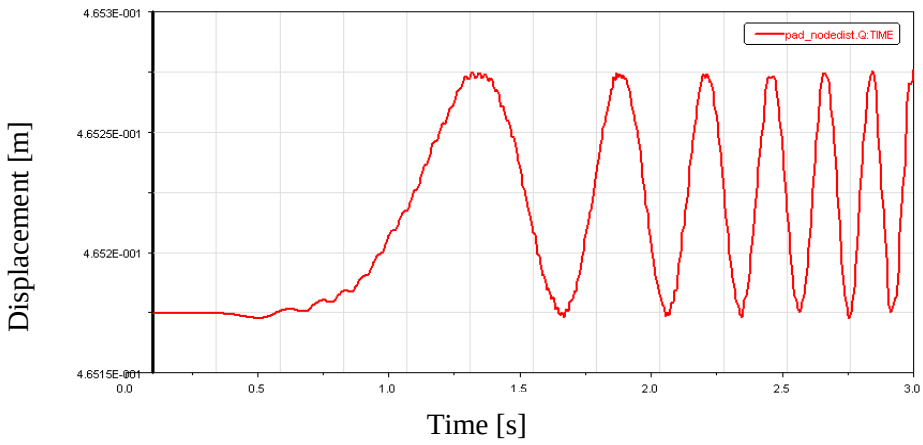

Figure 5. Alternation of the radius of the shell.

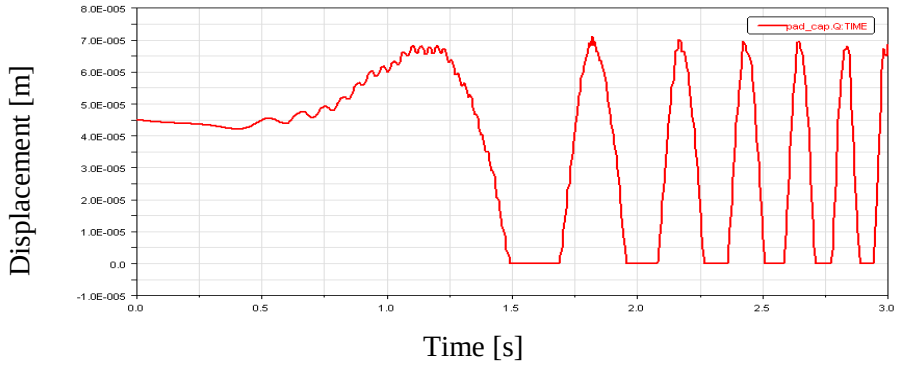

Figure 6. Oil cap between the shell and pad bearing.

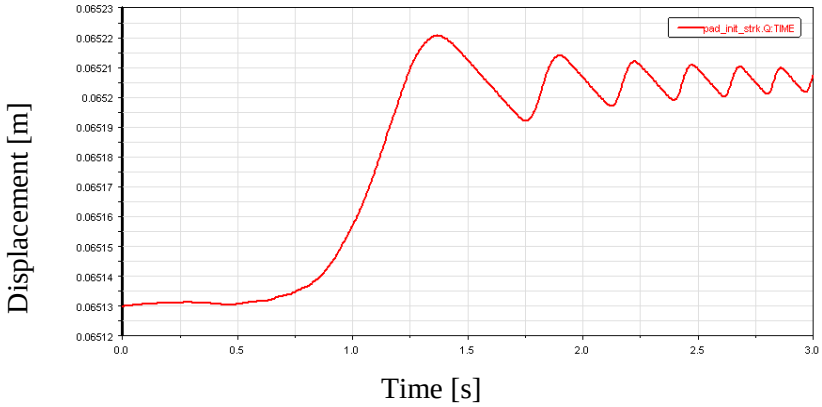

Figure 7. Movement of the pad bearing in radial direction.

A one noteworthy feature of present method is, that the user has the possibility to animate and scale the eigenmodes (Figure 8) of the model. Scaling of the eigenmodes makes possible to “actually see” the shape of the eigenmode of the simulation model.

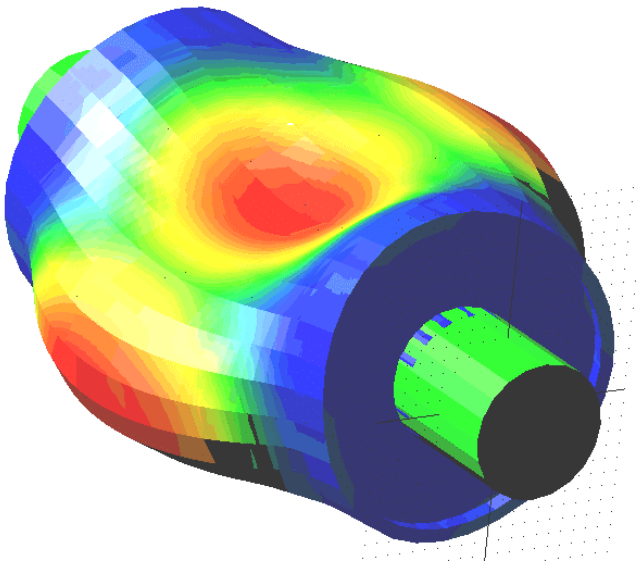

Figure 8. One eigenmode.

Flows, pressures, accelerations from different places are easily available.

4. Discussion

It was observed that modelling of the rotating flexible shell supported by pad bearings is possible. Results were quite good and promising, although substantial simplifications were done. Numerical results are based on simulations only, insofar all verification measurements were not performed for the present model. However, earlier experience from similar systems shows that results are accurate and promising.

Nowadays, the use of available simulation programs is quite effortless and modelling of the simple mechanisms is comparatively easy. However, successful modelling of the complex systems requires a lot of knowledge about both the system to be modelled and the simulation program.

It is very important to notice that the phenomenon or function to be modelled should always be represented mathematically. If the phenomenon is very complex and not well known, it is practically impossible to model and simulate reliably. Virtual prototyping will force to us to think about the “basics” of every single function. Design of a hydromechanical system requires knowledge of the hydraulic systems, control systems and construction of a flexible mechanism. Virtual prototype, which include all these subsystems is a great tool for designers, it helps to understand how a single change affects to the operation of the whole system. It also helps to understand better the interactions between all subsystems and their functions.

The constructed model provided a good tool for engineers to investigate the operation of the whole system. The biggest problem was a limited computer capacity, which restricted the accuracy of the model (number of the nodes and selected modes in the flexible parts). For example, sliding contact with flexible parts needs much force, which may cause problems with computer capacity.

Although presented model is quite crude and contains many simplifications, it will create a good basis for follow-up research. The follow-up research could embrace, for example, the possibility of adding the backing roll, more bearings and more flexible parts.

A simple 2D-model for vibration analysis of hydromechanical roll systems

Tero Kiviniemi, Timo Holopainen & Kai Katajamäki
VTT Manufacturing Technology
Espoo, Finland

Abstract

In this paper a two-dimensional hydro-mechanical simulation model for a deflection compensated roll system is presented. This model includes several details, which call for special modelling techniques. The simulation model consists of several submodels such as the hydraulic system, the rotating flexible shell, the hybrid pad bearings, the rolling contact, the sliding contact, and the paper web with a defect. Between these subsystems appear various interactions, e.g., in the form of forces. The obtained results indicate that the model can describe the basic dynamic behaviour of the system.

1. Introduction

A deflection compensated roll is a complicated multitechnological machine system, which functions as a part of an even more complex papermaking machine. A deflection compensated roll consists of a stationary shaft, a rotating cylindrical shell, and a set of hydrostatic bearing elements supporting the shell (Figure 1). A deflection compensated and an opposing roll compose a roll system, which compresses the paper web in the nip between the rolls. The optimal nip pressure depends on the properties of the paper web and the required treatment.

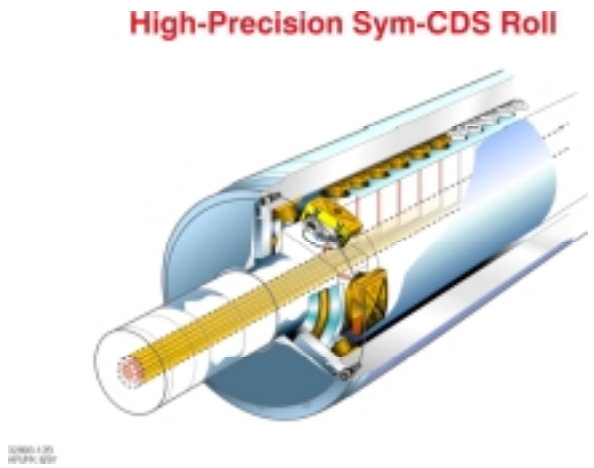

Figure 1. A deflection compensated roll (Valmet Oy).

A deflection compensated roll enables the adjustment and control of the nip pressure along the line of the nip. The required distribution of the nip pressure between the rolls can be enforced by adjusting the transmitted forces of separate bearing elements. Furthermore, the transmitted force of each bearing element can be controlled by the hydraulic pressure under the element. Finally, the controllability of the system is achieved by the separate piping and adjustable valves of individual bearing elements or zones of elements. A more detailed description of the operating principles of a deflection compensated roll is given in the reference [Niskanen 1988].

The numerical modelling of a deflection compensated roll is a demanding task. Even more challenging though, is to simulate realistically the dynamic behaviour of a roll system in operating situations. The modelling of the whole system requires advanced models for mechanics, hydraulics, fluid flow, material behaviour, and heat transfer of all the relevant sub-systems. In addition, the subsystems interact with each other's, and thus, the sub-models have to be integrated into a system model.

A three dimensional realistic model of a roll system is hard to build and to simulate with it requires many numerical resources. A two dimensional model of a roll system is relatively easy to build and the simulation is computationally light. Furthermore, some of the essential phenomena are better suited to be studied with a two dimensional model. In addition, the numerical behaviour of

the model components can be studied more effectively using a smaller simulation model. Thus, a two-dimensional roll model has several application areas and it can be very useful even with its restrictions.

The purpose of this paper is to present a two-dimensional simulation model for a deflection compensated roll system. The main aspect of the model is its multitechnological character. It includes the models for the hydraulic system, rotating flexible ring, hybrid pad bearings, rolling contact, sliding contact, rigid bodies, and paper web with a defect. Between these subsystems appear various interactions, e.g., in the form of forces. As an application example, we will study the effects of velocity on the behaviour of the hybrid pad bearings.

2. Methods

The main features of the model are presented in Figure 2. The original model of the hydraulic system was developed in Lappeenranta University of Technology (LUT) by Hammarberg [2001] and it was imported to the current model. Similarly, the basic model of the hybrid pad bearing is developed by Hammarberg. The latter developments carried out by the authors are described in this paper. Here we address the modelling of a flexible ring, hybrid pad bearings, and the squeeze damping of pad bearings.

2.1 Flexible ring

The flexible ring represents the mechanical behaviour of the cylindrical shell in two dimensions. The flexibility of the ring is modelled by the Finite Element Method (FEM). The analysis program employed was I-Deas ms 7.2 by SDRC (Structural Dynamics Research Corporation). The ring consists of two material layers. The material of the inner layer is cast iron and of the outer layer soft coating.

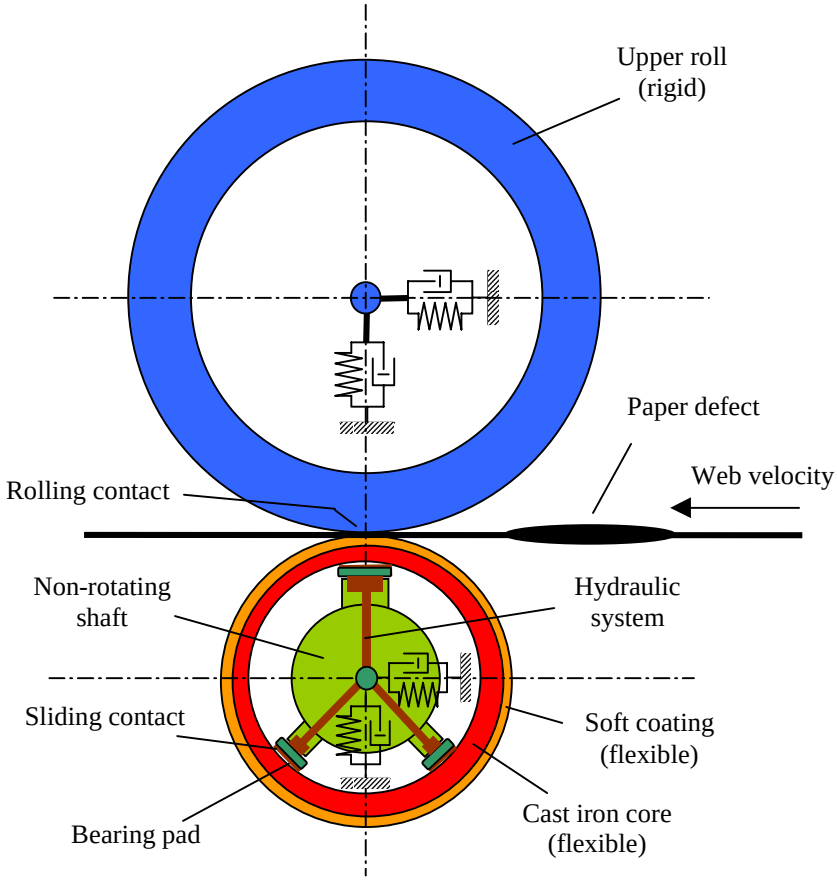

Figure 2. The main features of the model.

In the structural analysis, the boundary conditions were defined in the cross-section planes. In these planes, the translations in the normal direction were constrained. The natural modes and frequencies were calculated. In this case, three rigid body modes were obtained. The natural modes were transferred into the simulation program ADAMS using component modes method. The approach is a modification of Craig-Bampton Method [Craig & Bampton 1968]. In this special case, no constrained modes were used, because there were not any fixed contact point during the simulation. The essential natural modes used in the simulation model were (a) rigid body modes; (b) the lowest flexural modes; and (c) the lowest radial mode. The last mode is important because the deformations caused by the centrifugal forces resemble the deformations of this mode. Altogether, the stiffness and inertial properties of the ring were described in the

simulation model by six generalised co-ordinates [Katajamäki & Holopainen 2000].

2.2 Hybrid pad bearings

The hydrostatic bearings used to support the shell and produce the required nip pressure are designed to operate at relatively high rotational speeds. The applied nip force on the pad will then be reacted to by the combined effect of hydrodynamic and hydrostatic bearing film pressures. Bearings of this kind are specified as hybrid bearings. In this paper, the original bearing model is expanded so that the hydrodynamic effects will be taken into account.

There are two characteristic equations for a hydrostatic bearing. Firstly, the static bearing film force is defined as [Rowe 1983]

$$W = p_r A\overline{A} \tag{1}$$

where p_r is the recess pressure, A is the total projected bearing area, and $\overline{A}$ is the area shape factor. The dimensionless area shape factor can be thought of as the ratio of the effective area, which carries the load, to the total area. Secondly, the flow rate from the recess is defined as [Rowe 1983]

$$q = \frac{p_r h^3}{\eta} \cdot \overline{B} \tag{2}$$

where h is the film thickness, η is the dynamic viscosity, and $\overline{B}$ is the flow shape factor. The flow shape factor is dimensionless and, like the area shape factor, depends only on the shape of the bearing.

The estimates for the area and flow shape factors are required in the development of a simulation model. Diagrams for common bearing types are available and simple formulas can be used to approximate the parameters of other bearing shapes. However, the effects of relative velocity between the surfaces call for a more detailed study.

In a typical deflection compensated roll the hybrid bearings are self-aligning. This means that the bearing sets up in a position and tilts, which fulfils the equilibrium equations. The position and tilt depends on the transmitted loads and the velocity of the shell. In order to determine the position the Reynolds Equation of oil pressure coupled with appropriate equilibrium equations were calculated [Lyly 1999]. Figure 3 shows the effect of the velocity in one case.

The calculation of Reynolds Equation as a part of a simulation model is computationally a very laborious task. Thus, a simplified approach was employed. In this approach the modified area shape factor and flow shape factor were calculated as functions of bearing force and surface velocity. Firstly, the numerical values for these factors were calculated for a grid of force and velocity values. The calculated numerical data demonstrated the form of the unknown function. Secondly, two approximate functions, obtained by a simple curve fitting process, were employed for the modified area and flow shape functions. These parametric functions are:

$$\overline{A} = \overline{A}_0 + \alpha_A \cdot \left(\frac{U}{p_r} \right)^{\beta_A} \quad \text{and} \quad \overline{B} = \overline{B}_0 + \alpha_B \cdot \left(\frac{U}{p_r} \right)^{\beta_B} \tag{3}$$

where A_0 and B_0 are the numerically calculated area and flow shape factors at zero velocity, U is the relative velocity between the surfaces, p_r is the recess pressure, and α_A, α_B, β_A, and β_B are the parameters obtained by a curve fitting process. Thus, the data calculated by a relatively large numerical model can be compressed and transferred into the simulation model in the form of four additional parameters.

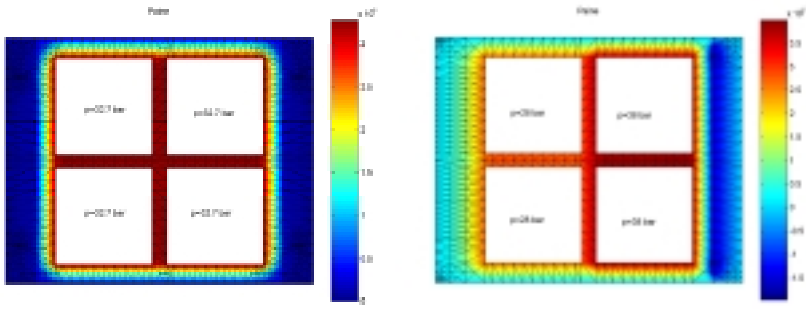

Figure 3. The oil pressure distribution of a hybrid bearing. On the left the velocity is zero. On the right the velocity is 20 m/s. The total transmitted forces are equal. The constant pressure in the pockets is given by the numbers. The pressure distribution on the right shows that the pad is tilting. [Lyly & Holopainen 1999.]

2.3 Squeeze damping of pad bearings

In addition, the model of the hybrid pad bearing was developed by adding the effect of damping force caused by the parabolic distribution of pressure on the bearing lands. The formula for this effect on thin lands is [Rowe 1983, Bassani & Piccigallo 1992]

$$C_2 = \frac{\eta A_L a^2}{h^3} \tag{4}$$

where η is the dynamic viscosity, A_L is the land area of the pad, a is the land thickness, and h is the oil film thickness. The viscous damping force due to this pressure distribution effect is obtained by the formula

$$F_D = -C_2 \dot{h} \tag{5}$$

where $\dot{h}$ is the time derivative of the film thickness.

3. Results

A simulation model was generated using the data of a roll system. The parameters of the mechanical and hydraulic system, as well as the hybrid pad bearings, were used as the input data. The spring coefficients of the upper roll were adjusted to describe the lowest bending natural frequency of the roll in vertical and transversal directions. The damping coefficients were adjusted for each rigid component to represent the damping factors of similar structural components. The operating situation was chosen describing the reference pressures of the cylinders and the speed of the paper web (2400 m/min). The paper defect was modelled by modifying the thickness of the paper with the formula [Keskinen et al. 1997]

$$\Delta(x) = h \sin^2 \frac{\pi x}{L} \tag{6}$$

where h is the maximum height of the defect, L is the length of the defect, and x is the local co-ordinate in the direction of the web motion. The defect is in the nip during the time interval 0.2000–0.2026 s. The parameters of the defect are shown in Figure 4.

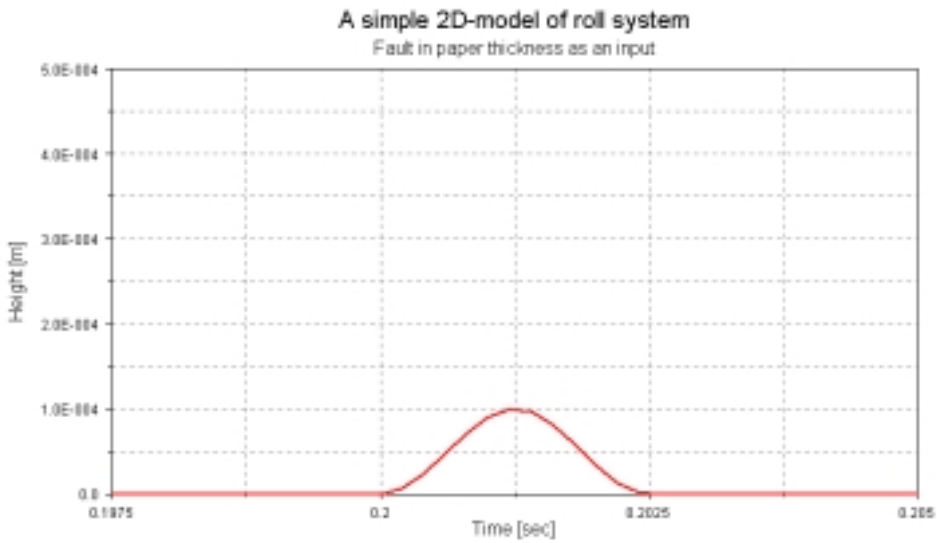

Figure 4. The defect in the paper web is given as a modified thickness.

The paper defect causes an impulsive excitation force between the rolls. Figure 5 shows the time history of the nip contact force as an example of the transient response. Figure 6 shows the deformations of the lower roll and the bearing forces shortly after the defect has passed (t = 0.2034 s).

Figure 7 shows the spectrum of the contact force between the bearing pad and the roll shell. The spectrum is made for the transient part of the signal. The spectrum shows some resonance frequencies. A simple linear mechanical model was developed including the upper roll, the flexible lower roll, and the spring elements. This model yielded the following natural modes and frequencies: 42 Hz in which the rolls move in the same phase, 87 Hz in which the rolls move in opposite phases and the lower roll deforms, 235 Hz & 260 Hz which are the two lowest flexural modes of the roll, and 645 & 655 Hz which are the second pair of flexural modes. It can be concluded that these natural frequencies are not contradictory by the results obtained by the simulation model (see Figure 5 and Figure 7).

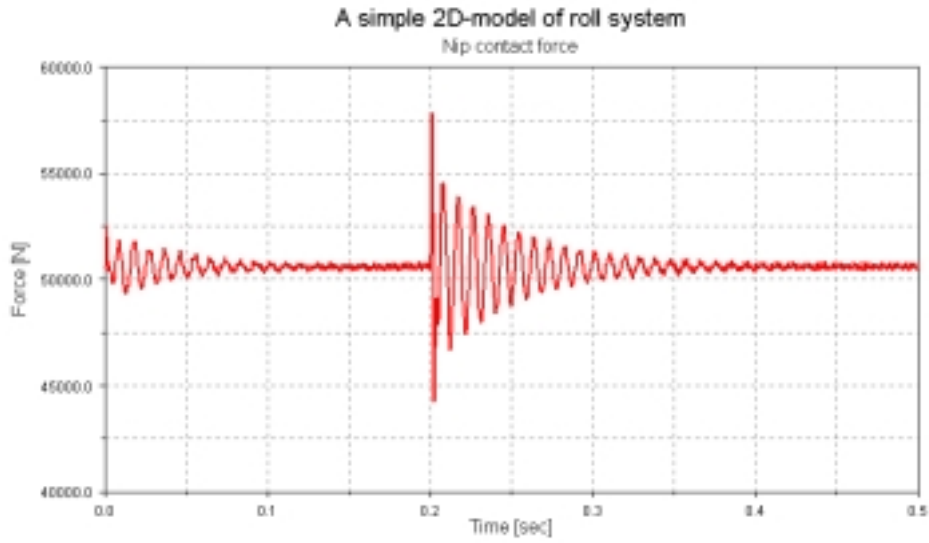

Figure 5. The transient contact force in the nip after the paper defect. The defect enters the nip at time 0.2 s. On the left the system approaches the steady state condition before the blow. The prevailing frequency component after impact is 84 Hz.

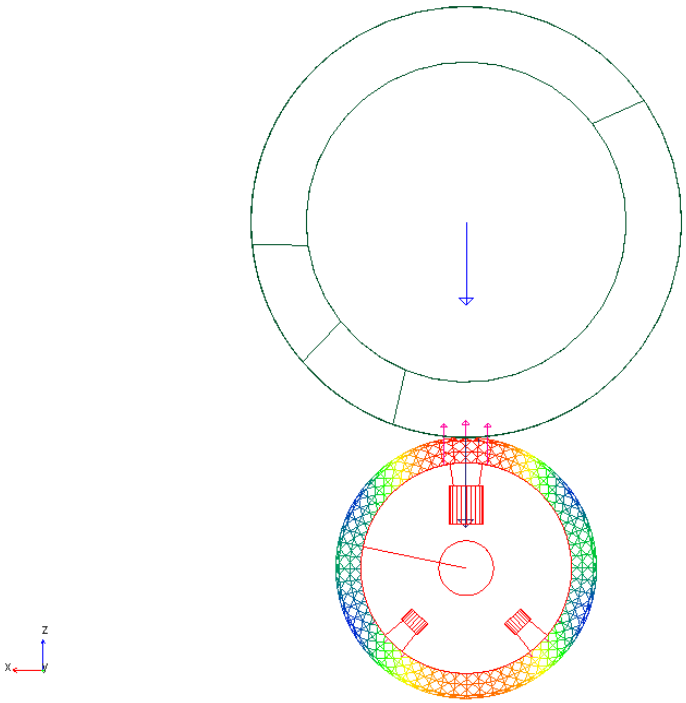

Figure 6. The deformations and the forces of the ring when the paper defect is in the nip.

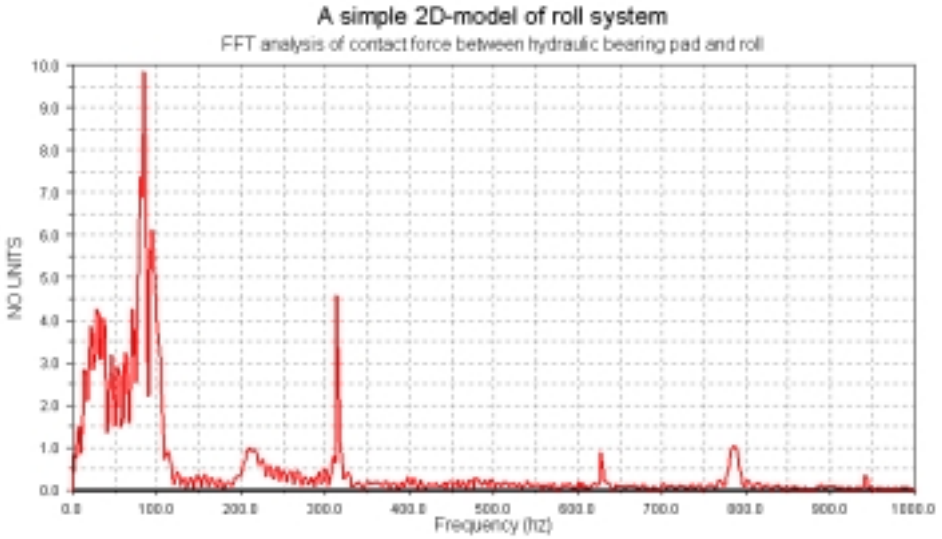

Figure 7. Spectrum of the contact force between the upper bearing pad and the shell.

4. Discussion

In this paper, a two-dimensional hydro-mechanical simulation model for a deflection compensated roll system was presented. This model included several details, which call for special modelling techniques. The obtained results indicate that the model can describe the basic dynamical behaviour of the system. The obtained numerical results are preliminary and they are not compared to any experimental results. This means that some of the important features may be discarded. Some potential weak points of the model are the constant temperature of the oil, the material model of the soft coating, and the acoustical waves in the hydraulic system. All of these have an effect on the dynamics of a roll system.

References

Bassani, R. & Piccigallo, B. 1992. Hydrostatic lubrication. Amsterdam: Elsevier. 542 p. ISBN 0-444-88498-x

Craig, R.R. & Bampton, M.C.C. 1968. Coupling of substructures for dynamic analysis. AIAA Journal, Vol. 6, No. 7. Pp. 1313–1319.

Hammarberg, T. 2001. Modeling of the interaction between the hydraulic pad bearing and rotating flexible tube. Proceedings of the NAFEMS World Congress 2001: The Evolution of Product Simulation, Lake Como, Italy, 24–28 April 2001. (submitted)

Katajamäki, K. & Holopainen, T. 2000. Finite element models of a deflection compensated roll for the simulation model. Espoo: VTT Manufacturing Technology. Research Report VAL35-001835. 5 p. + app. 35 p. (in Finnish)

Keskinen, E., Keskiniva, M. & Laasonen, P. 1997. Simulation of machine systems. Lecture notes. Tampere: Tampere University of Technology. 243 p. (in Finnish).

Lyly, M. 1999. On the Equilibrium of Self-Aligning Hybrid Bearings. Proceedings of the Twelfth Nordic Seminar on Computational Mechanics (NSCM-12), October 22–23 1999, Espoo. Eds. Kouhia, R. and Mikkola, M. Pp. 116–119. ISBN 1456-6311.

Lyly, M. & Holopainen, T. 1999. Kallistuvan liukukengän hydrostaattis-dynaamisen painekentän määritys yksinkertaisella 2D-mallilla. Espoo: VTT Valmistustekniikka. (Raportti VALC-603.) 25 p. (in Finnish)

Niskanen, J. 1988. SYM-ROLL Z. In: 1988 Papermakers Conference. Proceedings of the Technical Association of the Pulp and Paper Industry, Chicago, 11–13 April, 1988. Atlanta: Tappi Press. Pp. 305–311.

Rowe, W.B. 1983. Hydrostatic and hybrid bearing design. London: Butterworths. 240 p. ISBN 0-408-01324-9

Simulation based design of mobile machine vibration control and active cabin suspension prototype

Ismo Vessonen
VTT Manufacturing Technology
Espoo, Finland

Markku Järviluoma
VTT Automation
Oulu, Finland

Abstract

This paper gives a summary of the results of development work aimed at studying means to control low frequency vibration of rubber wheeled mobile machines. An experimentally verified virtual prototype of an agricultural wheeled tractor is prepared and this simulation model is used to study and evaluate different vibration control alternatives. The virtual prototype is found to be a powerful tool in the design of dynamic properties of mobile machines. A physical prototype of an active cabin suspension system, aimed at increasing driving comfort and at maintaining the “working ergonomics”, is designed, implemented and tested in a laboratory. This prototype system, comprised of inexpensive hydraulic components, shows measurable vibration suppression effect in typical tractor driving conditions and thus is a realistic basis for further testing and development work.

1. Introduction

Drivers of agricultural wheeled tractors are exposed to low frequency (< 10 Hz) vibration, mainly caused by unevenness of the terrain, driving speed, loading, and driving style. This "whole body" vibration affects firstly, the comfort, working ability and health of the driver and secondly, in some driving conditions also the handling characteristics and safety of the machine.

The characteristic feature for the low frequency vibration of a rubber wheeled mobile machine is that the body of the tractor vibrates as a rigid body supported by the sprig-damper systems formed by the tyres. In many conventional mobile machine designs no suspension system is used between the wheel and the body. One very basic problem is that the damping capacity of the tyres is one order too low to control the vibration.

From vibration point of view, one of the worst driving conditions is found to be the driving on an ordinary road at a speed of about 30–50 km/h. In this case the phenomenon is such that the eccentricity, out of roundness and mass imbalance forces from the wheels, as well as the road, irregularities excite the pitching vibration of the machine. In the worst case the vibration amplitude can reach the limit where the front wheels loose their contact to the ground and this may cause loss of steerability of the vehicle. Figure 1 illustrates this phenomenon, which is quite common with several other rubber wheeled mobile machines also.

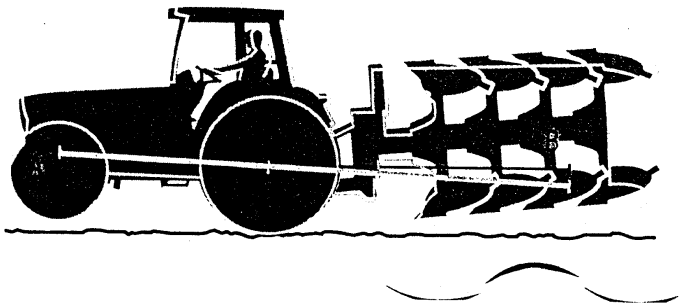

Figure 1. Pitching vibration of an agricultural wheeled tractor.

The research work described in this paper has two main goals. The first goal is to build an experimentally verified simulation model of an agricultural wheeled tractor and to use this model to study and evaluate different vibration control alternatives. The second goal is to develop an active vibration damping system for the tractor cabin to increase driving comfort and to maintain the “working ergonomics” at a high level despite the swinging of the machine.

This study was done in research project AKSUS – Control of low frequency vibration of a mobile machine (1998–2000) which was part of the TEKES

technology programme Smart machines and systems 2010 (1997–2000). The partners of the project were TEKES, Nokian Tyres Plc., Valtra Inc., VTT Automation and VTT Manufacturing Technology.

2. Simulation-based design of mobile machine vibration control

2.1 Simulation of vehicle dynamics in product development

To be able to design and produce high-quality and well-performing products, vehicle design engineers have to gain knowledge of the dynamic properties of the components and the entire vehicle. One traditional way to achieve this goal is to do testing on physical prototypes. In modern vehicle design process engineers build computer models, using mechanical system simulation (MSS) software, of the entire vehicle and run them under various load conditions to predict handling, vibration and performance characteristics as well as to check the safety properties. The growing utilisation of numerical simulation in the vehicle design process is due to the fact that with the efficient use of this technology it is possible to simultaneously shorten product development time and design better performing products. The time saving is mainly due to avoidance of building many successive physical prototypes and of doing extensive hardware testing. The performance and quality improvement comes from the ability to easily vary the dynamic properties of the vehicle in the numerical model, and in this way to test various design alternatives to achieve the design requirements.

Mechanical system simulation tools are widely used especially in the international automotive industry, where the pressure of global competition and customer demands have drastically shortened marketing time, brought new technical requirements (safety, noise & vibration, etc.) and lowered the product prices.

2.2 Simulation model of an agricultural tractor

The tractor chosen for modelling was the Valtra Valmet Mega 8050. The main modeling tool was Mechanical System Simulation (MSS) software ADAMS by Mechanical Dynamics Inc. (MDI). Mechanical engineering and data management software I-DEAS was also utilised.

The simulation model was built based on information delivered mainly by Valtra Inc. Modeling the geometry of all necessary parts in I-DEAS software started the process. The parts were input to ADAMS, where proper mass and inertia properties as well as center of mass locations were given for the parts. Parts included in the model are:

- Tractor body
- Front axle as a rigid body
- Swinging subframe supporting the front axle as a rigid body
- Front and rear tires as ADAMS 3Dtyre models
- Cabin as a rigid body
- Cabin seat + driver as mass objects

The parts were connected to each other by idealised joints and forces, which model the elastic interactions between the parts. To hold the link to the physical reality, the modeling of the component properties was done as precisely as possible, according to component data delivered by the manufacturers.

To simulate the vibration excitation coming from the ground irregularities, two different tracks were modeled. The first track is the rougher track of International Standard ISO 5008. This track is 35 m long and contains two parallel strips, the profile of which is formed by defining ordinates of elevation with equal spacing (80 mm). The profiles of the both strips were input to I-DEAS software, where the surface model of the track was created. Finally the track surface was transferred to ADAMS to be used in conjunction with the 3Dtyre model. Another modeled track was a specially designed bump track that was used in actual tractor tests. The surface of the first two bumps of this track was modeled using the same procedure as with the ISO-track.

Full scale vibration measurements of one Valtra 8050 tractor were arranged in order to gather data to be used in the design process of the active cabin suspension system, as well as to be utilised in verification of the simulation model. Test conditions included driving on a ploughed field, on a forest road, on a country road and on an artificial bump track. All this was done with different driving speeds and by varying some selected structural parameters of the tractor (front suspension ON/OFF, tire pressures, front weight ON/OFF, rear load ON/OFF).

In addition to driving tests some mobility measurements for stationary tractor were done in order to verify the dynamic properties of some subassemblies like driver's seat, cabin floor, front axle and the cabin.

For model verification purposes only the results of the bump track vibration measurements were valid, because this was the only driving condition from which a well-defined track profile for numerical modeling purposes was available. The fit between measured and simulated time domain vertical vibration, even in the cabin area, was fairly good and thus the model was accepted for numerical studies of the tractor dynamics.

2.2.1 Design simulations

The simulation model of the tractor was used to study, among other things, the effect of rubber wheel properties, selected construction parameters, cabin and front axle suspension and separate vibration dampers on the vibration properties of the vehicle. The main purpose was to find out the relative significance of various means of vibration control rather than to produce absolutely consistent simulation results with the measured real responses.

The vibration behavior of the tractor was simulated on three different numerical tracks to cover the different vibration excitation conditions encountered by a tractor. The first track is the ISO rough track defined in International Standard ISO5008. The purpose of this track is to study vibration characteristics of the machine in conditions where rather high ground irregularities are present (fields, forest terrain, etc.) and the tractor is operated at quite low speed. The second track is the artificial bump track including several sets of bumps with varying

bump heights and bump phasing for the front and rear axle tires. The aim of this track is to test vibration behavior in case of a single rather heavy swing caused by a bump or a pothole. The last test track is flat surface on which the speed of the tractor is slowly accelerated from 0 to 50 km/h and vibration excitation is coming from the modeled wheel eccentricity. Figure 2 shows the tractor model on these three numerical tracks and gives examples of typical simulated vibration signals.

The means of vibration control were evaluated from two different viewpoints, the first of which was the ability to reduce cabin vibration and the second was the performance in controlling vibration of the front axle (pitching motion). As an example of this latter analysis viewpoint, in Figure 2 there are some comparison results simulated on the flat test track. In this figure the colored bars indicate the relative maximum vibration amplitude of the center of the front axle with different vibration control methods. The reference value is front axle vibration amplitude in the case where the cabin of the tractor is mounted with rubber isolators. The driving speed of the tractor for each simulation case is the speed, located from driving speed sweep from 0 km/h to 50 km/h, at which the vibration amplitude of the front axle reaches its maximum value. From Figure 3 can be observed that passive cabin suspension combined with front counter weights reduce fore axle vibration amplitude by 16 %. Most of this effect is due to passive cabin suspension, which changes the dynamic properties of the whole system so that the vibration amplitude of the front axle is also affected. Lowering the tire inflation pressure from normal 1.6 bar to 0.8 bar seems to be a quite efficient way to reduce front axle vibration, especially in the case where inflation pressure of all tires are reduced. Despite good vibration reduction results, tire inflation pressure reduction is probably not a very practical vibration control solution for high speed road driving conditions, because the inflation pressure also affects, for example, steering properties of the tractor. A front axle suspension system and a properly designed and positioned auxiliary mass damper are the most effective ones of studied vibration control methods to reduce front axle vibration. Especially interesting is the effectiveness of the quite simple mass damper assembly.

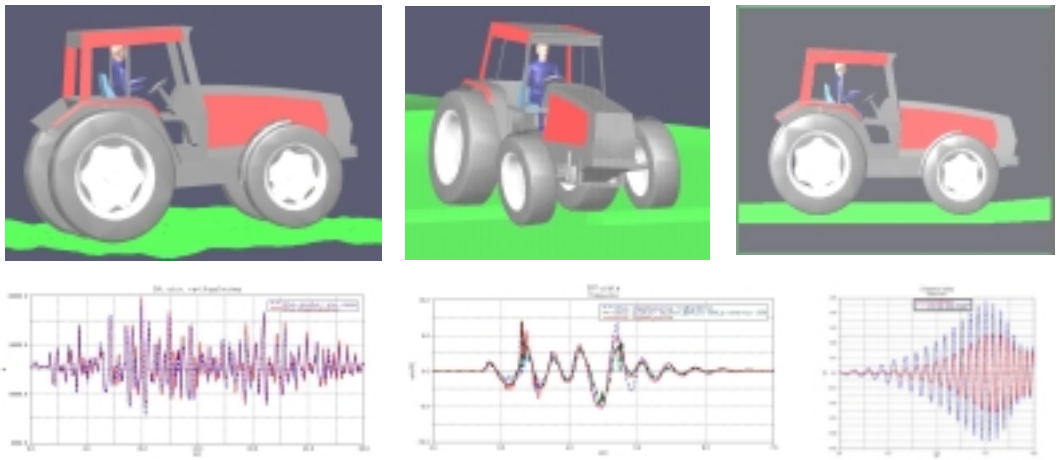

Figure 2. Tractor simulation model on three numerical test tracks and examples of typical simulated vibration signals.

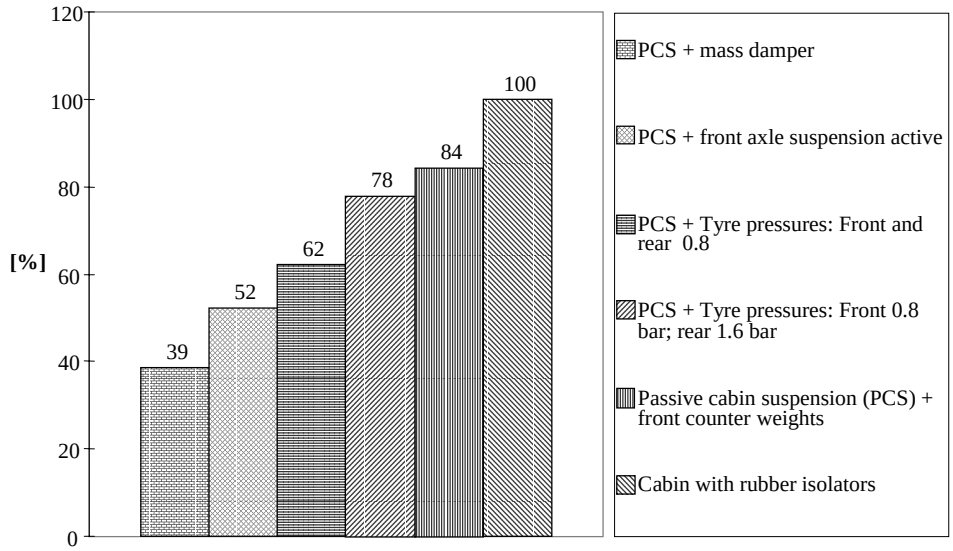

Figure 3. Relative performance of some vibration control methods in controlling pitching vibration of the modelled tractor while driving on a flat road within speed range 0–50 km/h. Vibration excited by wheel eccentricity at the left front wheel. Relative maximum acceleration of the centre of the front axle in vertical direction. Tractor with cabin suspended with rubber isolators as reference.

3. Development of active cabin suspension

3.1 System configuration

The same tractor model Valtra 8050 that was modeled for numerical simulations was also chosen as a development platform for the active cabin suspension. In this tractor model the cabin is attached to the tractor body at four corners. Passive vibration isolators are used for the two front corners and various damping elements are used for the two rear corners. The study of the active damping methods is carried out in the same context and the active suspension mechanism consists simply of two computer controlled electro-hydraulic valve-cylinder actuators, which are mounted in the same way as the passive elements, i.e., at the two rear corners. At the front the cabin can be attached to the tractor frame with a joint enabling, in addition to vertical motion, also sideward rotation control of the cabin.

In addition to the electro-hydraulic actuators the control system of the active suspension consists of motion sensors (acceleration sensors and gyros), cylinder position sensors, measurement and control electronics and mobile PC with DOS operating system. The hydraulic power is taken from the tool hydraulics of the tractor.

3.2 Control design

3.2.1 Goal definition

Test runs with a real tractor (Valtra 8050) determined the requirements for active damping. Test runs were performed on a special testing track and on different natural terrain (forest, field). The accelerations of the tractor body, the cabin and the driver's seat were measured and analysed. In the analysis the measured accelerations of the seat were compared to the frequency dependent exposure limits given in the standard ISO2631(1985). The worst case in the test runs was found to be driving on a ploughed field, from which the horizontal and vertical acceleration spectra are shown in Figure 4. These results can be considered to represent extreme vibration loading condition for an agricultural tractor, because

the driving took place during winter on a frozen field while driving perpendicular to the furrows at a rather high speed of about 12 km/h.

Figure 4 indicates that there is need for damping especially in the range 0–3 Hz, where, if the absolute exposure limit is taken as the goal upper limit of the accelerations, the degree of damping should be at least 30% in both directions. However, from the point of view of ride comfort and especially in the horizontal direction, it is desirable that frequencies up to 10 Hz are damped as much as possible.

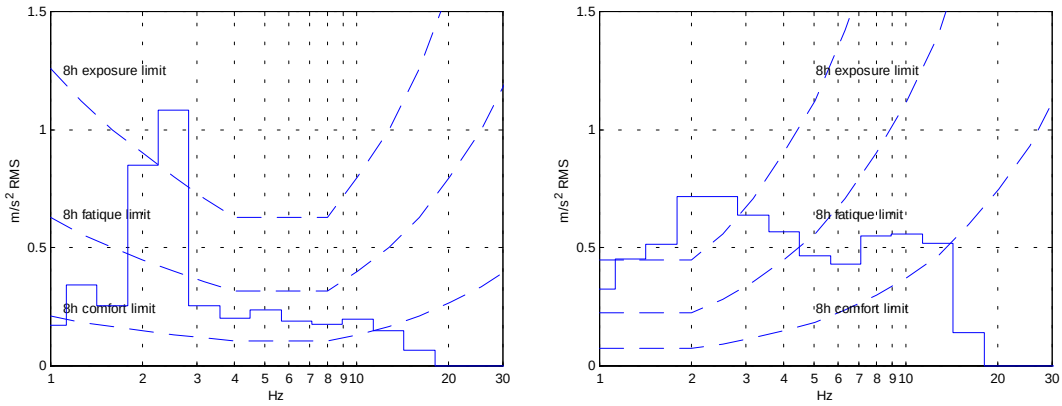

Figure 4. Vertical (left) and horizontal (right) acceleration 1/3 octave spectrums from a test run on a frozen ploughed field with speed 11.8 km/h and ISO2631 8-hour limits.

3.2.2 Kinematics

If several degrees of freedom are damped simultaneously, the kinematic model is needed for determination of the state of movement of the driver, based on the sensor readings, and for the determination of how the active suspension system should react in that state. The latter includes definition of the set values for the speeds of the actuators in the suspension system and leads, in the case of multiple degrees of freedom, to, e.g., minimisation of some criteria for the movements of the driver.

If only one direction is damped, the situation is much simpler, e.g., if in this case example only the vertical motion of the driver is damped, the control of the suspension actuators can be done by simple feedback regulation from vertical speed or acceleration sensor. Since the actuators produce nearly vertical movement for the cabin, the kinematics of the suspension mechanism can be neglected.

3.2.3 Dynamics and compensator design

Depending on the case, especially the relative masses of the vehicle-cabin system, the control of the suspension system can be very difficult. The problems arise from the flexibilities in the vehicle body and tyres and other parts and interactions between the various components. Simple PID-type algorithms were found to be very laborious or impossible to tune manually and, hence, model-based control algorithms were needed.

The case of active damping of the tractor cabin can be compared to the situation where we have a mass on a non-rigid base (ground and tyres) and another mass is manipulated on it. In addition to this, the system also contains other oscillating modes and delays. The structure of the used dynamic model for the system was a transfer function, which consists of the two-mass-system model, one additional second order component, a first order delay component and a gain component. Values for the parameters of these components were defined by manually fitting the frequency response to a measured response.

The obtained linear model was used for the design of model based predictive control algorithms (GPC) [Clarke *et al.*, 1987]. These designs tend to lead to phase lead controllers with very high gains in high frequencies and thus make them sensitive to measurement noises. For better performance also so called H_∞-control design [Francis, 1987, Chiang & Safonov, 1988] was tried. The so called mixed sensitivity problem [Kwakernaak, 1985] approach was used, where the designer gives bounds both for system sensitivity to noise and modeling errors and for disturbance attenuation, directly in frequency domain. The disturbance attenuation bound gives the bandwidth in which the damping system is to operate and the sensitivity bound is used for avoiding high gains in higher

frequencies. SciLab software [http://www-rocq.inria.fr/scilab/scilab.html] was used for solving the H_∞ design problem.

3.3 Laboratory tests

The laboratory test bench is shown in Figure 5. This bench contains two steel beams, on which the tractor cabin is attached with the same suspension mechanism as is used in a real tractor. The beams can be swung in two directions to mimic the vertical movement and roll rotation of the tractor body. These motions are controlled according to signals, which are measured from the real tractor during test runs.

Figure 5. The test bench.

Laboratory tests were carried out only in the case of damping one degree of freedom at the time. The damped directions were vertical motion, with feedback from vertical acceleration sensor, and the sideward roll rotation, with feedback from rotation speed sensor (gyro). The dynamic models are obtained by measuring the frequency responses of these two cases using PRB (Pseudo Random Binary) test signals. In the vertical motion case the two damping

cylinders are controlled with the same test signal, and in the roll rotation case they are controlled with test signals with opposite signs. The frequency responses calculated from these tests are shown in Figures 6 and 7. Shown also the responses of the transfer function models, which are fitted to the measured responses. It can be noted that there are poorly damped flexibilities in the system, caused by the deflections in the steel beams. Also the phase lags are quite large at the 10 Hz operating limit.

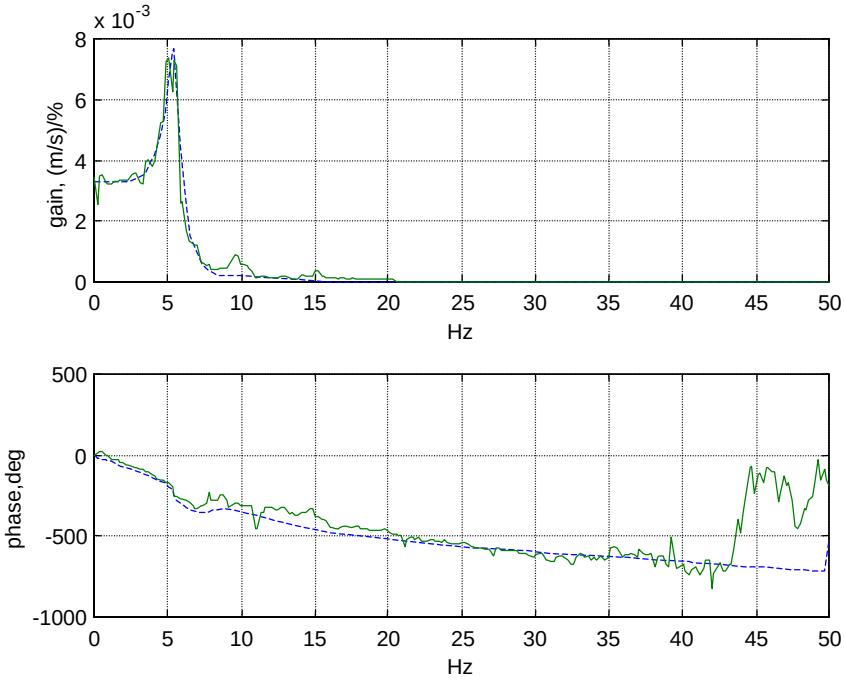

Figure 6. Frequency response of the vertical motion. Solid line = measured, dashed line = modeled frequency response.

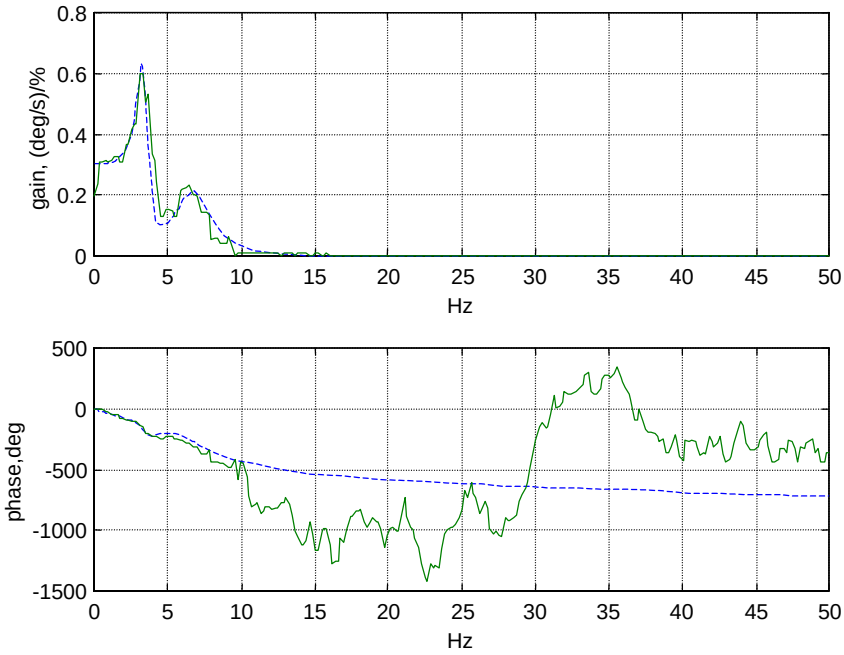

Figure 7. Frequency response of the roll rotation. Solid line = measured, dashed line = modeled frequency response.

The dynamic models were used for the design of the feedback controllers. For the vertical movement damping the predictive GPC design [Clarke *et. al.*, 1987] gave reasonable results, an example of which is shown in Figure 8. The resulting controller had a very high gain in higher than 10 Hz frequencies and, hence, was a bit sensitive to measurement noise.

In the case of roll rotation damping the high gain at high frequencies property was much worse and the GPC control could not be used at all. That is why the H_∞ controller design was used for roll rotation damping. The method involves the selection of weighting filters for the disturbance attenuation (sensitivity) and sensitivity to noise (complementary sensitivity) of the system. A result from one test is shown in Figure 9.

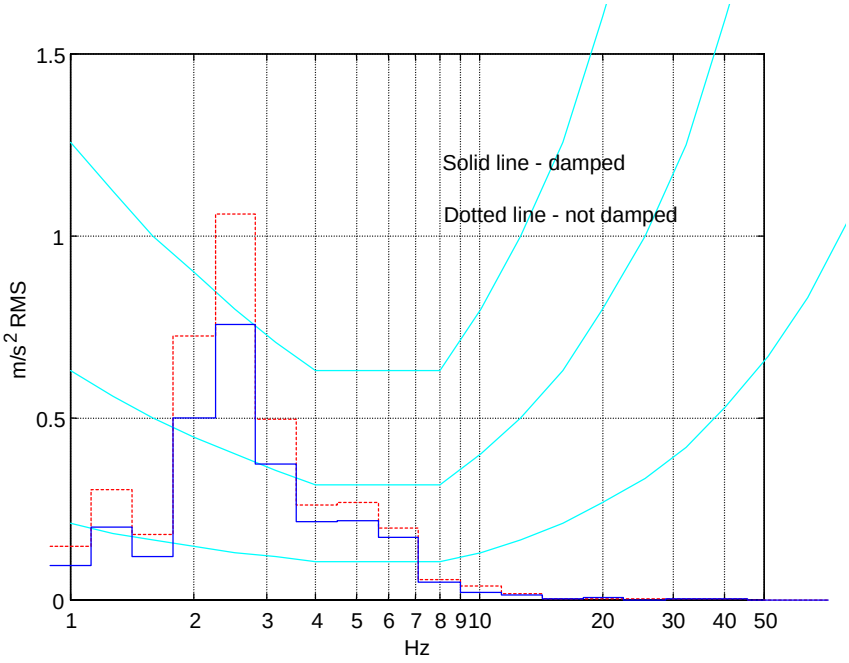

Figure 8. Vertical motion damping with GPC control.

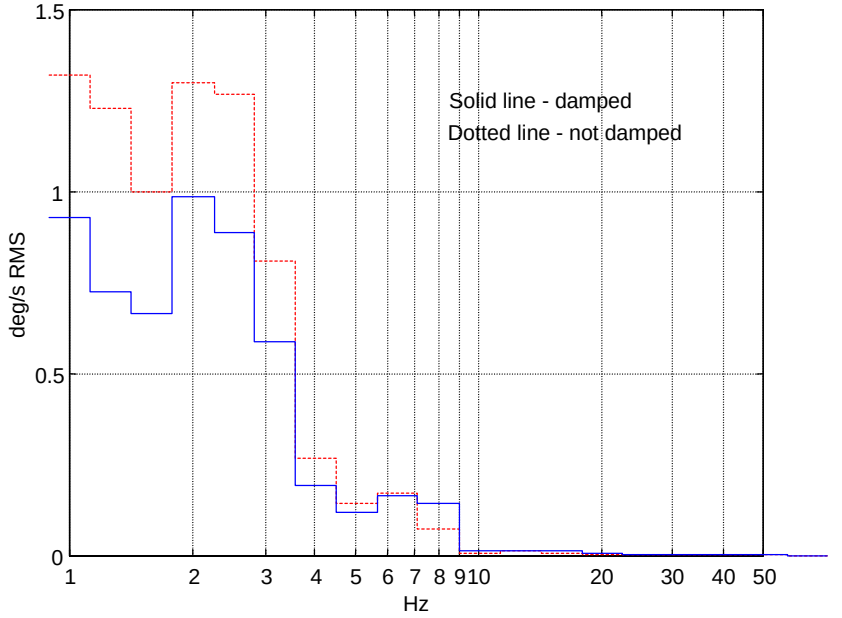

Figure 9. Roll rotation damping with H_∞ controller design.

The laboratory tests show, that in the case of active cabin suspension the flexibilities of the base structure (beams in the test bench, tractor body and tires in real tractor) makes the design of the feedback controllers rather difficult. Simple solutions like PID control are not applicable but instead model based design methods, preferably with possibility to weight the design in frequency domain, are needed. The tested methods, GPC and H_∞ did give reasonable results and the goal of the damping efficiency was reached at least at the most critical frequencies up to 3 Hz. The sensitivity to high frequency noise still remains a problem and needs further development.

4. Conclusions

The research work done on simulation based design of vibration properties indicated that it is possible, based on component data and by using engineering judgement, to create a simulation model which describes dynamic characteristics of a mobile machine realistically enough to study different design alternatives. Vibration measurements made on a real tractor also show that the indications that the numerical simulations gave about the relative performance of different vibration control methods also hold true in reality. Altogether the mechanical simulation model is found to be a very useful tool in designing the dynamic properties of a mobile machine.

However, despite of good results there is still room for improvement in modeling technique. At their present state the simulation tools do not model properly all vibration phenomena of a rubber wheeled mobile machine. For example the tyre model should, in addition to vertical stiffness, include also models for longitudinal and transverse stiffness of the tyre. Moreover, the dynamic behavior of the human driver should be modeled more precisely.

The result of the development work of the active cabin suspension is a system prototype, with which measurable vibration suppression effect is achieved both in off-road and in the road use of the tractor. The components chosen for the system are relatively cheap in order to form an economically reasonable base for possible commercialiation. In this respect the prototype can be considered to be a realistic starting point for further testing and development work. One matter of interest is that do the dynamic properties of, e.g., the hydraulic valves, selected

for the prototype, limit the performance of the system. Another obvious subject for further studies is the control system sensitivity to high frequency noise. Moreover, control system adaptability to changes in operating conditions as well as automatic tuning of the control algorithm should be considered in future development work.

The number of design parameters in active systems, trying to control external loading as well as complicated internal dynamics, is often so large that it is impossible to achieve the optimum design with simple dynamic models. Computer simulation of mechanisms and vehicle dynamics offer a powerful tool to improve design procedure. In virtual prototyping it is possible to link a mechanical model of the vehicle with a mathematical model of the control system. Design study of different design parameters can be done to achieve the optimum design of mechanical structure and control system. The control system for active suspension will be modeled with –control design software (e.g., Matlab/Simulink, MatrixX). In the final stage the whole vehicle – actuator – control system should be one model of a real vehicle. The vehicle model in mechanical system simulation software (e.g., ADAMS, DADS) and the control system model in control design software are linked to achieve calculation and simulation simultaneously. Then the control system can be optimised for a specific suspension system.

One industrial partner of the project, Valtra Inc., is utilising the findings of the project in designing passive cabin suspension systems for their tractors. In addition they will run a thorough test programme for the active cabin suspension prototype installed on a real tractor. Evidently, the results of both the simulation and active control activities of the project are most directly applicable in the vibration control of tractors and other rubber wheeled mobile machines. But a good deal of the general principles and practical experiences can be generalised to be of use in other applications as well.

References

Chiang, R.Y. & Safonov, M.G. 1988. Robust-Control Toolbox for Use With MATLAB, User's Guide. The MathWorks Inc., USA.

Clarke, D.W., Mohtadi, C. & Tuffs, P.S. 1987. Generalized Predictive Control – Part I & Part II. Automatica, 23, 2, pp. 137–160.

Francis, B.A. 1987. A Course in H^{∞} Theory. Springer-Verlag, Berlin.

Kwakernaak, H. 1985. Minimax Frequency Domain Performance and Robustness Optimization of Linear Feedback Systems. IEEE Transactions on Automatic Control, Vol. AC-30, No. 10, pp. 994–1004.

Simulation oriented R & D of hydraulically driven machines

Asko Ellman & Timo Käppi
Institute of Hydraulics and Automation
Tampere University of Technology

Heikki Kauranne, Jyrki Kajaste, Klaus Heiskanen & Matti Pietola
Laboratory of Machine Design
Helsinki University of Technology

Contents

1. Introduction

Virtual testing means that a system is tested by a computer model instead of testing the real physical system. The test is carried out by a simulation model of the system. Rapid development in computer power and software development has turned trend into virtual testing covering complete machine systems. Computer aided virtual prototyping is to replace physical prototype phases in product development. The machine system can thus be tested in a normal work cycle as well as in extreme load and operation situations. The information received is highly dependent on scope of the model:

- Essential physical phenomena of the model
- Knowledge of parameter data

A fluid power system usually generates high forces and can move high inertial loads. These systems are typically under damped and they have potential to vibration problems. Design of steady state behaviour of the system is easy but designing of dynamic properties is more difficult, especially if the system contains closed loop controls.

Fluid power is traditionally devided into mobile hydraulics and stationary industrial hydraulics. In industrial hydraulics the primary power source is an electric motor and the number of pumps in the system is not restricted. In practice the pump supply is always sufficient considering both flow and pressure requirements. Volume or weight limitations hardly ever cause difficulties. Mobile applications are more integrated due to space and weight limitations. The primary power source is typically one diesel engine. One or several pumps are placed to the engine shaft. The pump system must also be able to handle the limited power and therefore prevent exceeding the diesel power available.

The fluid power industry in Finland has shown increasing interest towards simulation work. Co-operative projects with industrial partners and academic institutes make possible to put the research results into practice in an optimal way. One of the main benefits in co-operative projects is the two-way knowledge transmission between participants. The theoretical knowledge and

understanding of the product performance is improved among the company people while applications and their specific features become familiar among researchers and universities. This is important because virtual testing requires knowledge of application, software and hardware as well as of theory as shown in Figure 1.

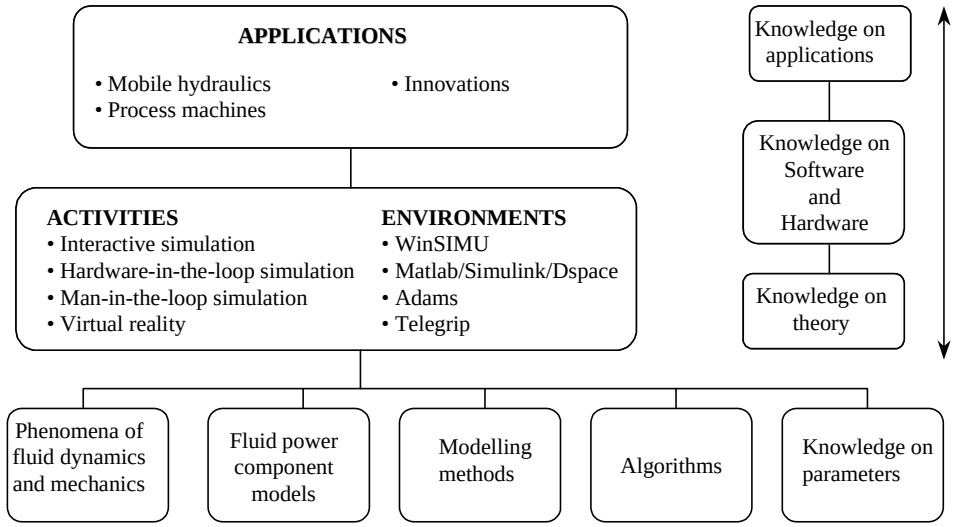

Figure 1. Elements in virtual testing.

2. Virtual testing as a R&D-tool

2.1 Virtual design environment

One virtual prototype is hardly sufficient in the design process of a mechatronic device. In a concept design phase the model can be simple and it gives qualitative results. Later on the accuracy and complexity of the model has to be increased. The best benefit is achieved when virtual testing is applied already in a concept design phase.

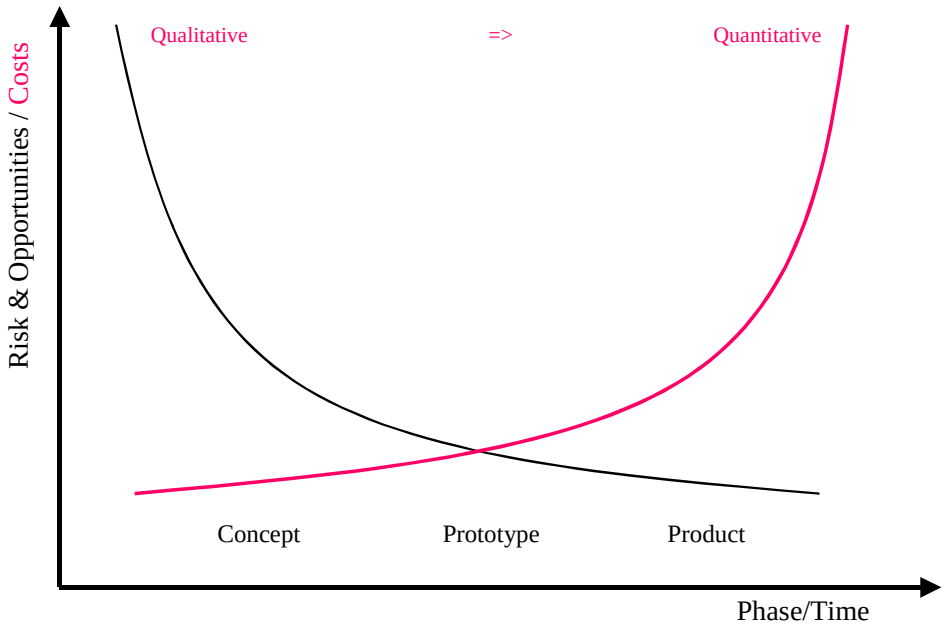

Figure 2. Product life time versus simulation opportunities & costs.

The most important design step is taken in steady state system design. This is done by using traditional design rules by using either conventional paper-and-pen-method or some spreadsheet program. Steady state system design reduces parameter space significantly and dynamic dimensioning can be completed in the simulation model.

The task of the simulation model is to calculate the dynamic response of the system under given loading and control effort. Two kinds of simulations exist: off-line simulation has no exact requirement for the calculation speed while in real-time simulation it is required that simulation model is capable to calculate the system response in real time.

One example of a real-time simulation is a so called hardware-in-the-loop simulation where only a part of the real system is replaced with a model. Typically they are used for testing some hardware such as testing of a real electronic control unit against a real-time simulation model. Another example of real-time simulation is a so called man-in-the-loop simulation where a human operator is part of the simulator. Typically this is used for training a human operator in a safe simulated environment such as an aeroplane training

simulator. There the pilot drives a real-time simulation model instead of a real aeroplane.

The design of a mechatronic product is an iterative process. This can take place in a virtual testing environment including both offline and hardware-in-the-loop simulation as shown in Figure 3.

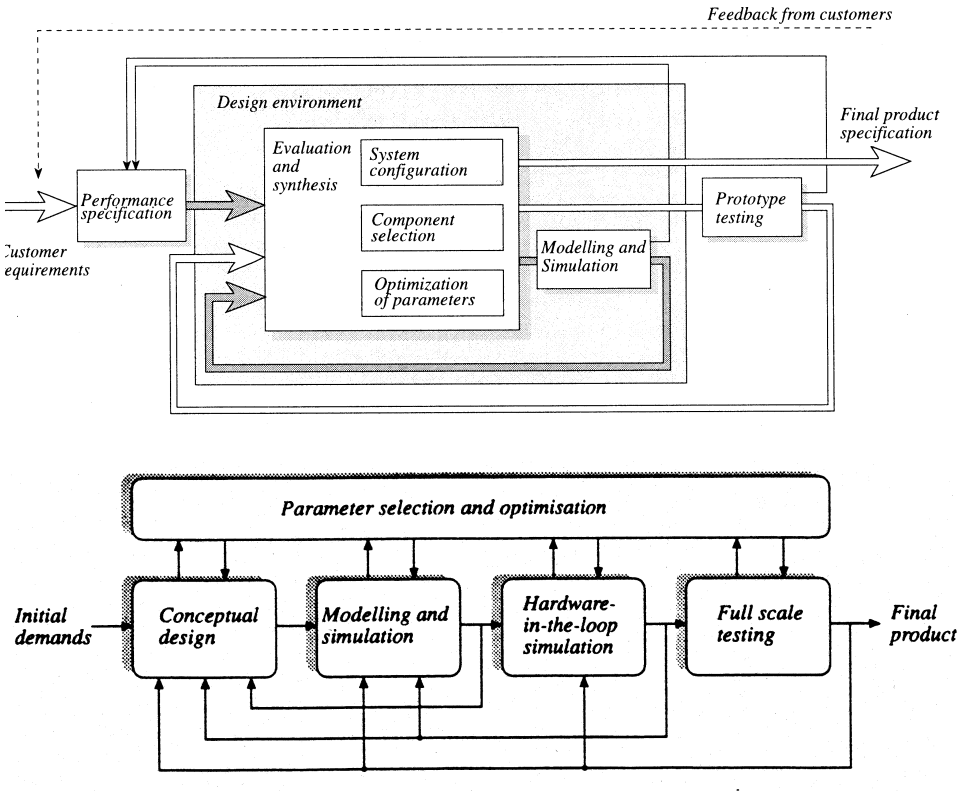

Figure 3. Virtual design environment. [1]

2.2 Needs for virtual testing

Needs for virtual testing come from recent industrial needs:

- Decreased R&D-time. Profitability of a new product depends more and more on the Time-to-Market period. Decreasing of R&D period requires an efficient design environment and minimizing number of prototype stages.

- Improving the quality of design. Customers specify the features of the product more and more precisely. Control of reclamation costs is essential.

- Supporting the marketing. Customers want to ensure the functionality and properties of the product while making decision of purchase. The created documents and software can be used for marketing support.

- Improved product knowledge. Designers need to know how their product can be used in different environments and with different process conditions.

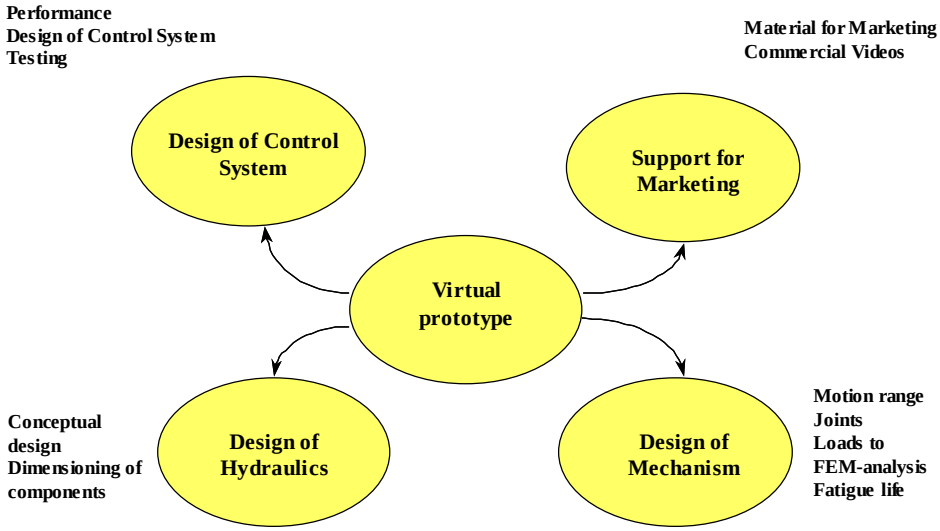

Figure 4. Advantage coming from virtual prototyping.

2.3 Project milestones

A simulation project can be divided into the following milestones:

- Problem definition. In this stage purpose of the model is defined. All physical phenomena affecting the system are considered. A plan for the model is created including names for variables of the simulation model. A plan for simulation tests is done.

- Creating the simulation model of the system. The simulation model is programmed by using selected software.

- Definition of parameter values. This is a major task.

- Performing simulation tests.

- Analyzing results and documentation

2.4 Special problems of fluid power simulation

- Systems include several nonlinearities such as turbulent flow mechanism, finite displacement of valve spools and devices, friction, play and saturation. For this reason efficient linear solvers can’t be used.

- Mathematical rigidity of simulation models, in other word, time constants of systems differ several decades. Numerical solving of a model can be time consuming and a special stiff solver might be needed.

- Availability of parameter data. Manufacturers of hydraulic components usually give only little parameter data of their products. Also some system parameters such as bulk modulus are not precisely known.

- There exists two-way interaction between hydraulic and mechanical systems as well as the work process. Due to this fact the complete model easily becomes large.

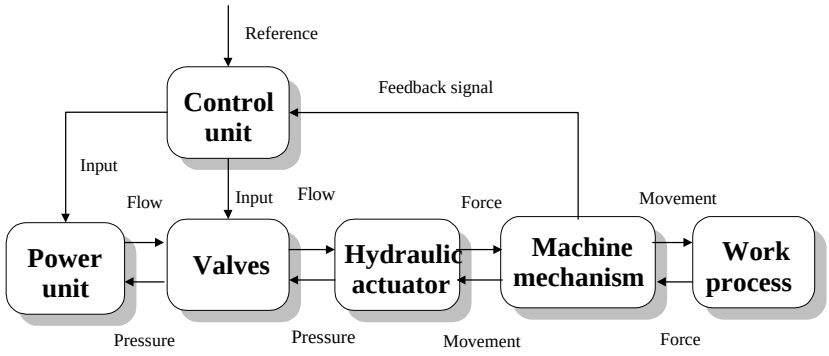

Figure 5. Interactions in a hydraulically driven machine system.

2.5 Usability of a simulation model

A simulation model is useless unless some extra value for the product is gained from the modelling. Usability of the model is dependent on the following properties:

- Quantitative accuracy. How well numerical values of simulated results correlate with measured ones.
- Working range. How wide is the working range where the model can be used.
- Identification. How easily the required parameter information can be found.
- Parameter sensitivity. If the model is very sensitive to some parameter values it may indicate a modelling error.
- Computational speed. How many simulation tests can be done during e.g. one day.

3. R&D example a of forest machine

3.1 Introduction

The purpose of using mobile machines differs but their basic construction is more or less similar. The machines normally include a base machine with transmission system and swing of the cabin, a crane and an attachment with work hydraulics. Typical examples of mobile hydraulics are forest machines, excavators, access platforms, drilling machines and agricultural machinery. Typically each machine does a work cycle although the process and working environment can change considerably. Mechanically mobile machines have typically 3–9 degrees of freedom when mechanism parts are considered as rigid bodies.

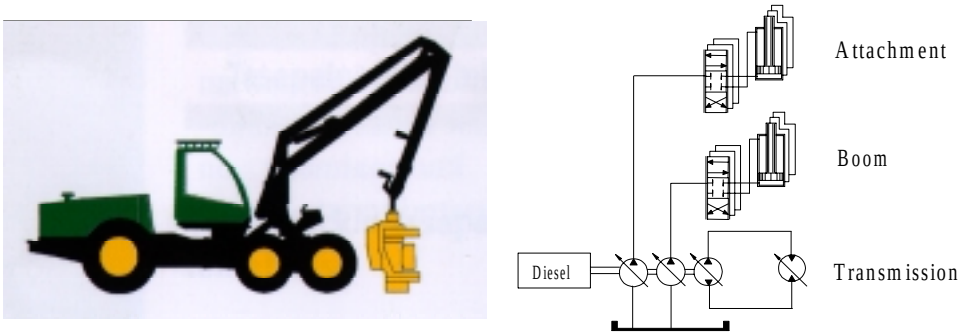

Figure 6. Typical hydraulic layout of a mobile machine.

Production series of heavy machinery are relatively small and unit prices are high. Due to this physical prototypes are rarely available for product development. There are also a lot of quantities to be measured from the prototype machine. Comprehensive study of a fluid power system of a mobile machine may require 50 flow and pressure measurements. Therefore measurement equipment with same amount of sensors must be installed. Sensors and connections also tend to be sensitive to environmental circumstances such as moisture and dirt. These reasons make field measurements difficult to arrange and very costly. It typically takes weeks or even months to arrange conditions for field measurements to test new ideas.

It gets even more time consuming if several machine configurations, mechanic or hydraulic, are to be tested. Changes in mechanical structures require a lot of manufacturing and installation work and a very limited number of variations can be tested in practice. The amount of possible hydraulic configurations depends on the number of hydraulic actuators and pumps in the system. For a mobile machine typically tens or even hundreds of possible combinations can be found.

An analysis of measurement results is difficult since equal conditions for separate measurements are in practice impossible to arrange. The results are affected by the variations in work process and performance of the machine operator as well as varying environmental circumstances. A simulation model offers equivalent and repetitive conditions for qualitative analysis and thus easy comparison between different systems.

The basic construction of the mobile machines can be assumed to be quite constant over a long period of time. In this case a carefully done and verified simulation model can be used as a design tool for years. All design modifications and R&D ideas can be examined by the model. Previously large modifications have been avoided but in the future the simulation approach will make it possible to take larger steps in R&D work. The simulation concept can be exploited best in the beginning of the product lifespan when the basic selections can be made utilizing simulation with relatively small costs comparing to empirical testing.

3.2 Mobile valve

A mobile valve is normally of proportional type. Main spools are either electrically (proportional solenoid) or hydraulically pilot operated. They can be open center or closed center type with load sensing ability. Hence the valve can be used with LS-pumps. Several directional valves (1–9) are placed into one common valve block. The compact design is achieved and the need of hosing is decreased.

There are also several valve functions integrated into the single valve blocks. The most common are:

- Pressure compensation
- Load drop check
- Pump flow sharing (anti-saturation)
- Pressure relief
- Anti-cavitation.

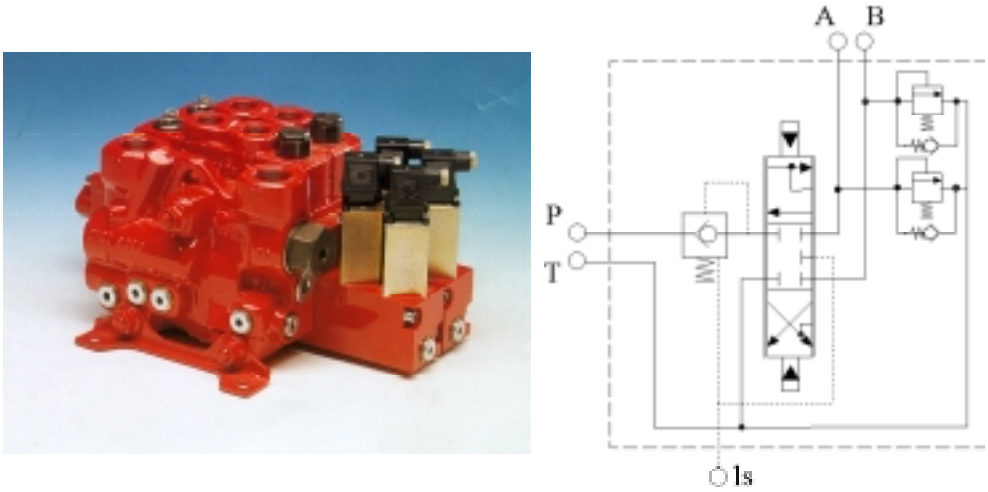

Figure 7. Mobile valve.

3.3 Simulation environment

Commercial software is almost exceptionally implemented in a certain way, which limits its suitability. It either lacks of readily available component models or the software itself is not flexible enough for required modifications. In house software equipped with comprehensive component library forms an effective engineering tool.

WinSIMU is a fluid power simulation package developed at Tampere University of Technology during the last ten years. It has a component library including all the basic fluid power components. The user is allowed to make his own extensions based on already existing model classes such as orifices and fluid fields or more complex models. The source code of WinSIMU is implemented

with 90 standard FORTRAN. Then the fluid power system model itself consists of simple FORTRAN subroutine calls to the library or user-written subroutine models. In that case even a very complex system entity becomes easy to control and modify.

Due to the nature of mobile hydraulics, a special model library for mobile hydraulics components is also created. The following sub-models referring to the theory are in the component library:

- Variable displacement pump with LS-regulator and power limiter
- Mobile valve including integrated functions
- Models for passive and active oil cooling
- Non-linear mechanism model
- Models for load conditions and working process

The software implementation is based on object-oriented programming while each component forms an object of its own. By employing indexed structures supplied by FORTRAN programming language the number of fluid power components in a simulation model can vary. The major benefit of this implementation is that a single simulation model can cover a large number of possible hydraulic configurations. Commercial software packages require that the fluid power circuit is constant i.e. the number of hydraulic components and connections (pipes/hoses) between components are fixed. This means that separate simulation models for each configuration of the fluid power circuit has to be created. In the presented software concept the number of pumps is given as a parameter and each hydraulic actuator is parameterized by giving a number corresponding to the pump system it belongs. In the initialization phase of numerical simulation the hydraulic circuit equivalent to the current parameterization is formed.

Number of pumps
1

Cylinder 1
1

Cylinder 2
1

Cylinder 3
1

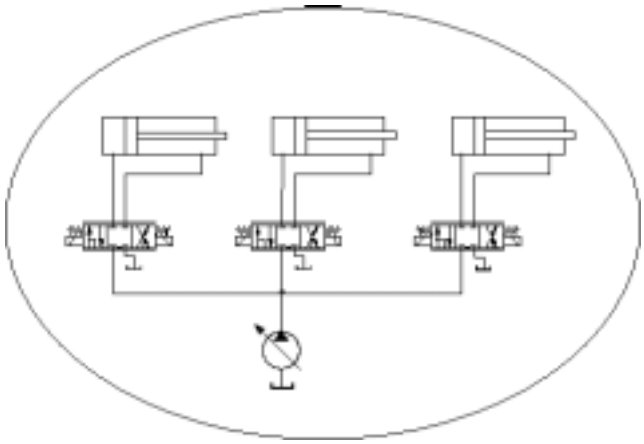

Number of pumps
3

Cylinder 1
1

Cylinder 2
2

Cylinder 3
3

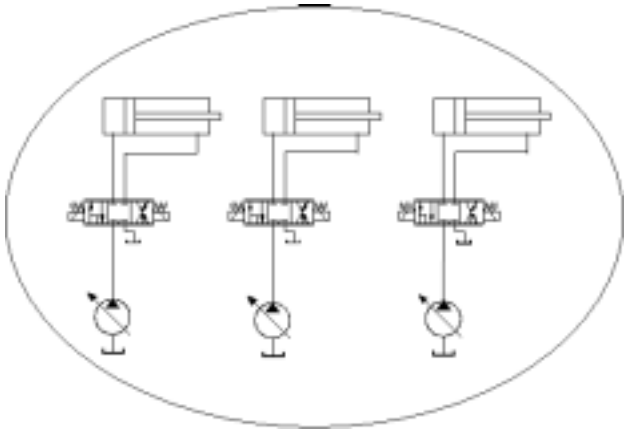

Figure 8. Example of two systems generated by different model parameterization.

In the example illustrated in Figure 8 two simple hydraulic circuits are generated based on the four parameters given. Considering the number of components and possible different connections in the real machine systems the presented implementation saves a great deal of programming work while the performance of different configurations is studied.

The model parameterization, simulation with on-line plotting and post-processing of simulation results are carried out using WinSIMU user interface. Because of three-dimensional movement of the mechanism a special software tool is created for animating the displacement and orientation of the machine.

3.4 Model utilization

The complete simulation model covers a complex mechanic hydraulic entity. It can be used as a virtual prototype to predict the real machine performance under any dynamic conditions. Several industrial R&D cases were carried out utilizing the model. Three kinds of typical applications were dealt with which can be assorted as

- Testing of functionality of novel R&D ideas
- Research of various dynamic phenomena
- Studies of long term behavior of the system such as energy efficiency.

3.5 Energy efficiency in mobile hydraulics

Energy efficiency is one of the main topics while considering the product development of mobile hydraulics. This can be motivated by several reasons. Naturally, since the primary power source of the machine is usually a diesel engine, fuel economy is one of them. Even more important is the system temperature balance. The power losses in the systems are converted into heat. The oil tanks of the machines are relatively small and the system temperature rises fast while hydraulic power is produced inefficiently. This has many unwanted effects. The oil cooler must be dimensioned larger which increases

price of the machine and may cause problems in machine layout. In the worst case the primary motor must also be larger than needed in a well designed and energy efficient system. This creates a chain reaction where heavier structures must also be used.

The pressure and flow requirements vary considerably during mobile machine operation. This sets demands for the system design in order to minimize the losses and thus maximize the efficiency. The traditional practice in mobile hydraulics is to use fixed displacement pumps with open-center valves. Constant pressure systems are also used. However, the current trend is towards load sensing (LS) systems with variable displacement pumps. The basic reason for this is the supposition for improved energy efficiency. Nevertheless, this is not unambiguous in case of mobile machines.

In load sensing systems the supply pressure is determined based on the highest load pressure in the system. The best system efficiency is achieved when only one function is carried out at one time or when two or more simultaneous functions have the same pressure requirements. However, typically the pressure levels of simultaneous functions vary. In order to prevent load dependence and load interactions between simultaneous functions pressure compensation is utilized in modern machines. Pressure compensator maintains nearly constant pressure loss across the main spool so the speed of an actuator remains constant and is a function of main spool opening only. This makes the machine control easier for operator and productivity is increased. Nevertheless, it usually means remarkable pressure losses i.e. heat generated into the system due to pressure losses occurring in pressure compensators.

Different systems are compared below with respect to energy efficiency. In Figure 9 a typical situation is presented while three simultaneous functions are carried out.

Figure 10 presents the worst situation with respect to energy efficiency. It can be seen that load sensing system itself does not necessarily offer remarkable improvement in energy efficiency though careful system design must still accomplished.

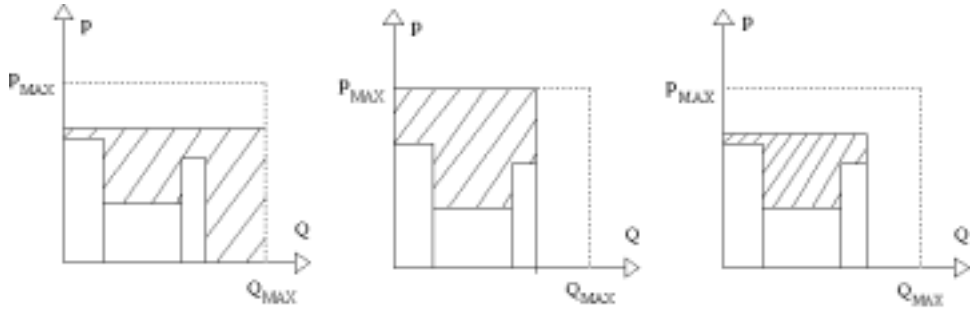

Figure 9. Energy efficiencies of open center, constant pressure and load sensing systems, respectively, in typical case.

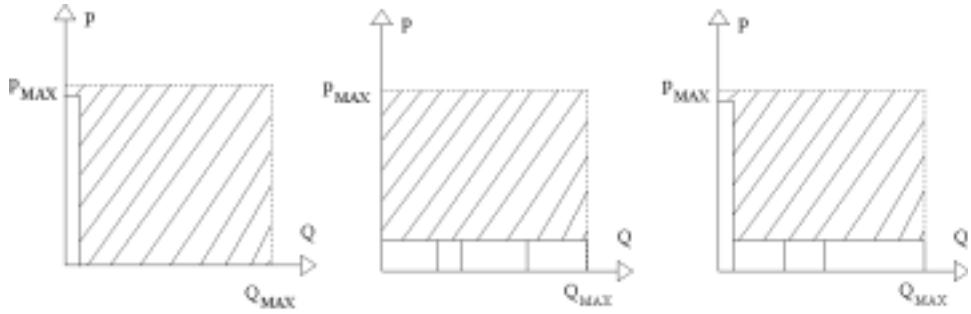

Figure 10. Energy efficiencies of open center, constant pressure and load sensing systems, respectively, in the worst case.

3.6 Simulation example

One of the main questions for the machine designer is how many pumps the machine should have and what functions should be grouped together for each pump systems. Considering pressure compensated load sensing systems the most advantageous design is achieved when the actuators with the approximately equal average pressure level are placed in the same pump system.

The research procedure can be carried out in the following way

1. Mobile machines typically undergo certain work cycles. The first task is to determine the average test cycle, which is utilized to compare the alternative system designs.

2. The work cycle is programmed to the simulation model of the machine.

3. The loss work done per work cycle for each alternative system is determined by means of the simulation model.

4. The temperature gradient of the system as a function of time can be solved when the loss work and active (oil cooling) and passive (heat transmission) cooling power is taken into account. The temperature rise in the system during consecutive work cycles is determined using some numerical mathematics software available such as Matlab.

5. The physical prototype tests are carried out with the most promising alternatives.

Different systems can now be rated by means of qualitative analysis. The accuracy of the results depends on how exactly the 'average' work cycle can be determined. Several work cycles should be investigated in order to get reliable results for decision making.

In the following an example considering energy efficiency study is presented. The simulation model utilized covers a forest machine having 7 degrees of freedom, 9 hydraulic actuators and variable number of LS-pumps.

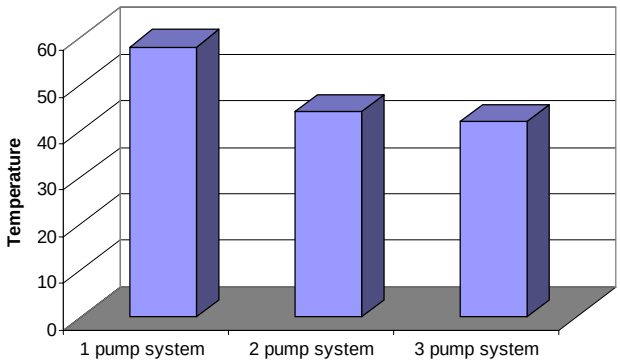

Figure 11. Temperature balances of three different systems.

The simulation model is employed to compare systems having different number of pumps. As seen in Fig. 11 the change from 1 pump system to 2 pump system is advantageous and considerable difference between temperature balances can be seen. However, the improvement from 2 pump system to 3 pump system is only marginal and considering financial aspects hardly worthwhile.

4. R&D example of paper machine hydraulic system

4.1 Introduction

In modern papermaking process several technologies are needed to produce high quality paper with high production speed. The hydraulic driven devices of a paper machine have an essential role in achieving this goal.

Figure 12 presents the oil volumes of hydraulic and lubrication systems of a modern paper machine. The total amount of oil can be up to 150 000 liters and the nominal power of electro motors in hydraulic units can have a total value of 2.2 MW.

A paper machine contains a great amount of rolls, as shown in Figure 12. Two against each other pressed rolls form a nip, a basic machine element in paper making environment. In the papermaking line the paper web is led through several nips. The most important function realized by hydraulics is to control the linear load and the load distribution exerted on the paper web through the nip length. The rolls where the deflection of the roll shell and the form of the shell can be compensated and controlled by hydraulics are called deflection compensated rolls, Figure 13.

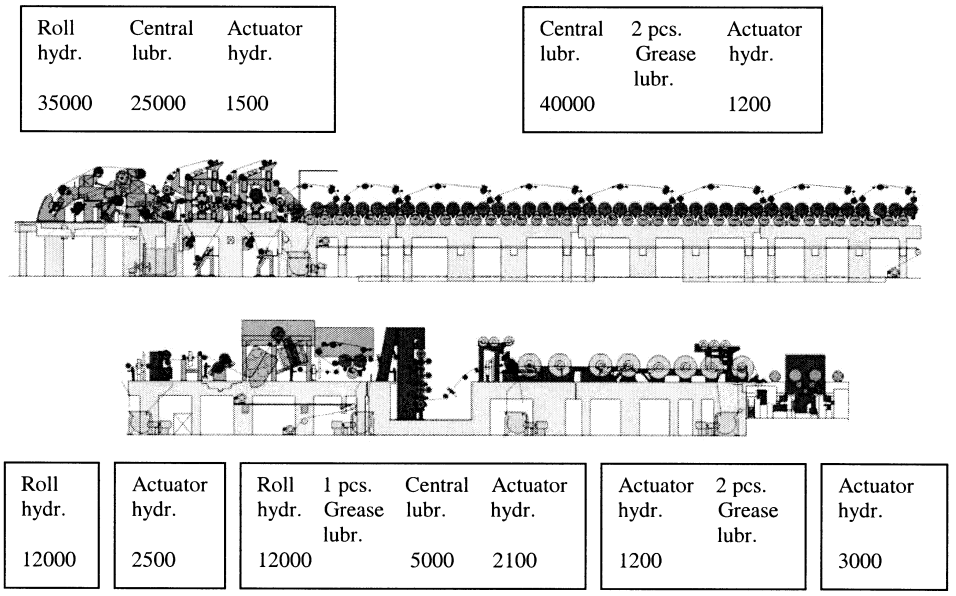

Figure 12. Hydraulic and central lubrication systems of a modern paper machine, oil volumes are in liters.

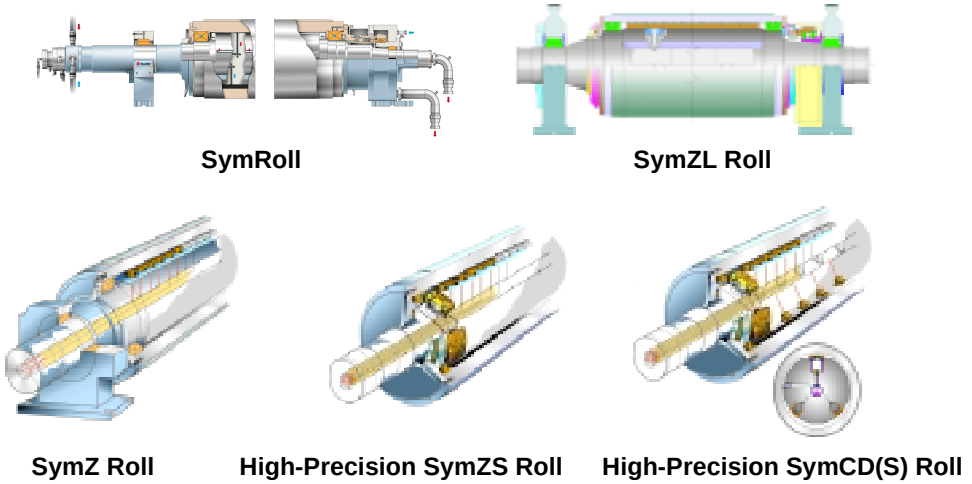

Figure 13. Deflection compensated rolls.

The characteristic features of roll hydraulics are: high oil volumes, high viscosity oils with low pumping temperature, high pumping power, considerably high power requirement (although not high compared with the total power consumption in the papermaking process), long and large-diameter pipelines, high air content of return oil and several pressure control loops (max. 80 pcs./roll) with a requirement of high pressure control accuracy.

As a consequence of the long pipelines the nominal frequencies of the pipelines become low which makes the system dynamics very complex thus causing the danger of resonance and complicating the control of the system.

The main objective of this research was to study the methods that could be utilized to achieve better efficiency in a roll hydraulic system. The task of the system studied is to control the linear load exerted on the paper web in a nip. The force between rolls is actualized by the pressure of a hydraulic system, which in turn necessitates a pressure control system.

Comparison of different pressure control methods in a real paper machine is in practice impossible, because during the tests the machine is non-productive which causes very high expenses. On the other hand applying a totally new, yet not tested control method to a massive installation like paper machine is very risky and it may lead to a costly shut-down. Therefore, in order to achieve a reliable system, the characteristics of the pressure control and its interactions with other system components have to be known beforehand. This is possible by using simulations, which in turn causes the need for accurate and reliable component models.

4.2 Pressure controls

A pressure control system can be accomplished either as a valve control or a pump control system, Figure 14. Both of these have their advantages and disadvantages.

In a valve control system (Figure 14A) the system pump is usually a fixed displacement pump rotating with constant speed. The pump delivers thus a constant flow. The system pressure is regulated with a pressure relief valve,

which can be either mechanically or electrically controlled. The advantages of valve control are the low price and easiness of system realization, but the disadvantages are the high power losses and operation costs. The power losses are the greater when the pressure need of the load differs from the setting value of the pressure relief valve or the flow need of the load differs from the pump flow because the flow has to be throttled in order to achieve the desired pressure and/or flow values. If a proportional pressure relief valve is used, the power losses can be reduced partly by adjusting the pressure level to load needs.

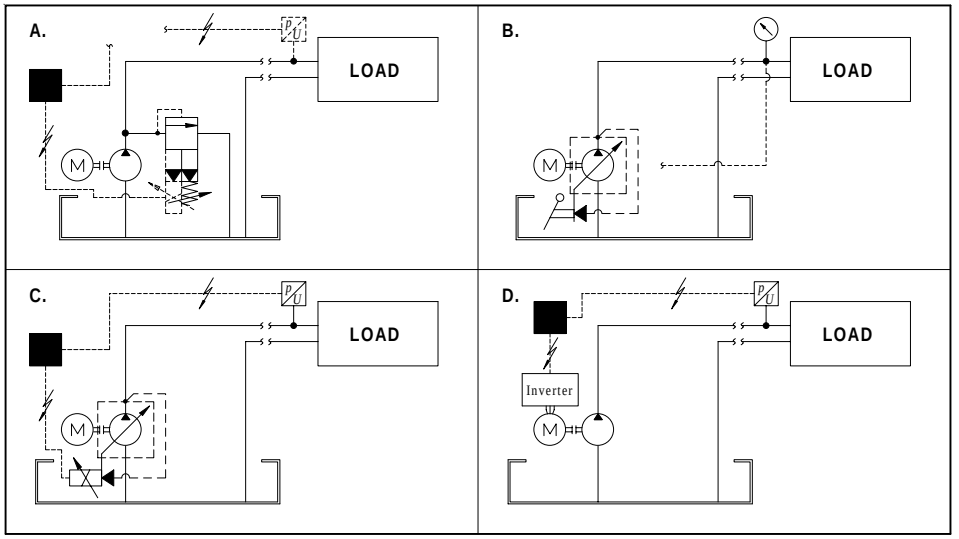

Figure 14. Pressure control methods.

When using pump control the amount of flow is adjusted to the load needs. This can be achieved either by using a constant speed motor and a variable displacement pump or by fixed displacement pump with variable speed motor. The main advantage of pump control over valve control is the better efficiency but the disadvantage is the higher price.

In pressure control systems based on variable displacement pump, the pump is equipped with pressure controller that monitors the system pressure and adjusts the displacement of the pump according to the load need in order to maintain the settled pressure level in the system. The pressure controller can be either mechanically (Figure 14B) or electrically controlled (Figure 14C). The former is similar to the pressure relief valve in the aspect that the system pressure level is

adjusted according to the highest load pressure needed. The lower pressures have to be realized by throttling the pump flow, which naturally causes the efficiency level to drop. When using electrically controlled controller the system pressure level can be adjusted to the load need, which enables higher efficiency level.

The pressure control can also be realized with fixed displacement pump if the rotation speed of the pump can be controlled, which is possible with inverter (Figure 14D). Because the inverter controls the speed of the motor, the system has to be equipped with electric pressure transducer and electric controller in order to create a pressure control system. The system pressure level and the pump flow are possible to adjust to the load need. The main advantage of this type of control is the high efficiency, but the disadvantages are the higher realization costs and slower control compared with other control methods.

4.3 Main system components

The significantly higher energy efficiency of pump control compared to valve control makes it very attractive particularly in high power hydraulic systems. The pump control has its restrictions though. The dynamic properties of a variable displacement pump have a considerable effect on the dynamics of the system connected to it, which in turn can lead to instability of the system. This is particularly true with systems that have long pipelines between the pump and the load, where the delays caused by long lines affect system controllability.

Especially pressure control has been observed to be easily troubled with stability and oscillation problems and therefore the use of it necessitates careful planning and good knowledge of the properties of the system components. In order to accomplish a reliable pressure-controlled system, the system designer should have accurate models of pump, controller and the rest of the system in his use.

The effect of pipeline dynamics has until recent years been either totally neglected in the system models or modeled in a coarse way due to absence of accurate and simple to use pipe models. This naturally causes distortion in simulation results. Owing to the pipe model research work that has recently been done, the fluid power systems can now be modeled more accurately.

The problems that arise when using pressure-controlled pumps with long pipelines have so far not been investigated in the literature either theoretically or in form of measurement data. The special properties of large-scale systems may emerge for example in form of noise, vibration and control problems.

- The system characteristics of the studied large-scale system are:
- High requirements for accuracy and reliability
- Long power transmission lines
- System oscillation risk
- High efficiency demand.

The aim of the study was to create simulation tools for the complete system. Also the means to diminish pressure pulsations by using hydraulic filters were examined during the project. For these purposes reliable models are needed for all of the system components. The key components of the system are

- Pressure-controlled pump
- Pipeline
- Load.

4.4 Research methods

In order to compose reliable component models to be used in system simulations the characteristics of the components had to be known. The measurements that were made to achieve this object also gave comparative knowledge of different control types concerning efficiency and technical properties. This data can be used along with the costs comparison when resolving the most suitable control type for a particular case.

4.5 Measurements

Two test systems were constructed to study the behavior of a pressure-controlled pump, long pipeline and a load in steady state and dynamic situations and to obtain the data needed for modeling. The investigated controller types were hydro-mechanical controller and electro-hydraulic controller. The system in Figure 15 was used to measure the static characteristics of the pressure-controlled pump (1) and to study the interaction between a pressure-controlled pump and a long pipeline (2). The controller shown in this figure is the hydro-mechanical one.

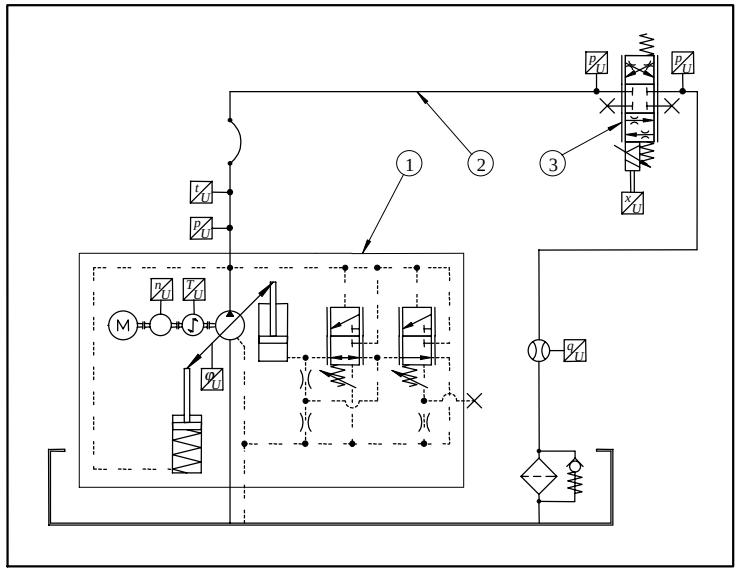

Figure 15. A test rig, which can be used to study the oscillations of a pressure-controlled pump and a long pipeline.

The second system in Figure 16 was used to study the interaction between pump, long pipeline and load i.e. actuator (4) and especially to study the load response to sinusoidal disturbances. The controller shown in this figure is the electro-hydraulic one. In both cases the system was excitated with control valve (3).

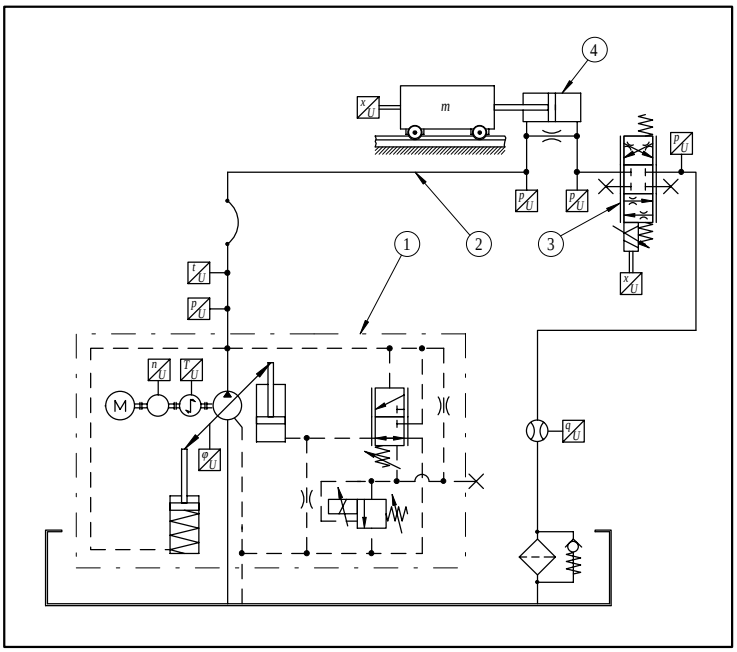

Figure 16. A test rig, which can be used to study the influence of the oscillation of a pressure-controlled pump and a long pipeline to the position of hydraulic cylinder.

The system input in dynamic measurements was the spool position or the flow area of the control valve. The outputs were the system pressures, the swashplate angle of the pump and the cylinder position. The excitation frequency range in these measurements was 0–200 Hz.

4.6 Modeling and simulation

The dynamical models of the hydraulic components can be developed along two routes. First route is to split up the system into subsystems whose essential hydraulic and mechanical properties are described by electrical network analogies i.e. capacitances, resistances and inductances. These properties can be attained by measuring or approximating the physical dimensions, inertial masses, spring constants and the resistances of the subsystems. The equations governing these systems are then joined and a non-linear state-space model of the whole system is obtained. This procedure is commonly called as *analytic*

modeling. The disadvantages and advantages associated to this approach are listed in Figure 17.

+	Model parameters have physical interpretation in the real world
+	Model designer gains more insight of the function of the component and is able to study the effect of changes in component construction by varying the corresponding parameter value
+	The model can be used to describe various components with the same principal of operation by simply changing the parameter values to suit the new component
−	Parameters of the system are not easily attainable without taking the component apart
−	Parameters are not readily attainable from the component manufacturer
−	The level of complexity of the individual subsystems can be chosen too high or low with regard to the essential dynamical behavior of the component or the overall system
−	Some essential dynamics may go unnoticed and is thereby omitted in the final component model

Figure 17. The advantages and disadvantages of analytic modeling method.

The second route is based on experimentation. Input and output signals from the system are recorded and subjected to data analysis in order to obtain a model. This route is called *system identification* or *black-box modeling*. The disadvantages and advantages associated to this approach are listed in Figure 18.

Both of the above mentioned methods were used when modeling a pressure-controlled pump. Comparison of the models revealed that their structures were very much alike. Analytic modeling is often to be preferred when the studied system is simple enough to be analyzed with reasonable effort. The pump

studied in this case had physical phenomena of varying degree of complexity thus the risk of omitting some essential dynamics was considerable. In this case both of the methods proofed to be successful though.

Analytic modeling method was found to be more suitable when modeling a membrane-type pressure accumulator studied in this project. The accumulator, being a relatively simple construction, was modeled by using lumped parameter dynamic elements like hydraulic capacitances and inductances. Furthermore a non-linear model of accumulator was created by taking into account also the pressure dependency of the elasticity of the accumulator gas volume and the turbulent flow at the accumulator inlet throat.

+	Gives a linear model with the best fit between measured and simulated output
±	Time used in modeling the component consists essentially of the time used in carrying out the measurements
−	Data analysis requires some knowledge of the theory of system identification and some familiarity with dynamical systems and stochastic processes
−	Set of obtainable models is limited to linear models. If linear model is inadequate some knowledge about the interconnections of the system variables is needed in order to proceed with the analysis. This is often referred as *gray-box modeling* or *semi-physical modeling*
−	All interesting variables can not be measured without difficulty and there might be restrictions imposed on the input signals applied to the system
−	System might be operating in feedback loop, which can not be opened during measurements. This affects the identifiability of the parameters

Figure 18. The advantages and disadvantages of system identification method.

A schematic presentation of the simulation model of the pump and the test system is shown in Figure 19. The input of the system is the flow area of the control valve used in the measurements and the output is the flow rate of the pump.

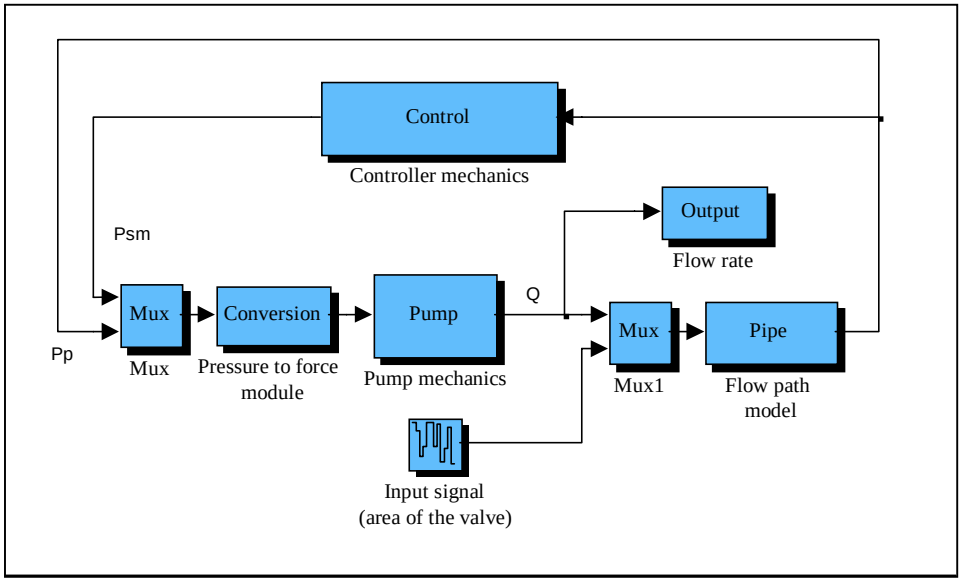

Figure 19. Simulation model of the pressure-controlled pump.

Figure 20 represents a simulation model for the system depicted in Figure 15. The spool position of the control valve is the system input and the output is the pressure at the inlet of the valve. A linearized model for the valve was used since the model was used mainly for frequency domain calculation of small amplitude oscillations. The system model contains also a sub-model for the pressure-controlled pump and a pipeline model taking account the distributed nature of the pipeline dynamics.

As well as other hydraulic components also the pipeline system has dynamic properties of it's own, the importance of which emphasize especially if the line lengths are increased.

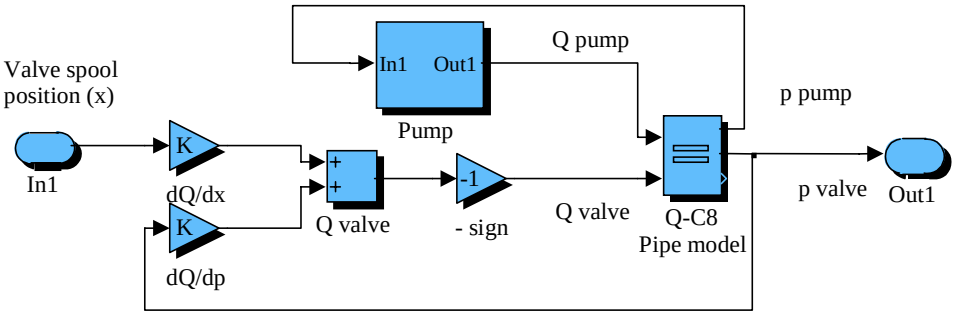

Figure 20. A model for a system with a pressure-controlled pump, a pipeline and a control valve as a load.

Usually the dynamics of the hydraulic pipelines are taken into account as compressible liquid volumes or resistive components producing pressure loss. These simplified models do not contain the effect of the acoustical properties of the pipe. The limited speed of the pressure waves determines the natural frequencies of the pipeline, which become lower as the lengths of the lines increase. In the studied large-scale case, where the line lengths are remarkable the simplified lumped dynamic models have been found inadequate to describe the dynamics of the system.

Satisfactory results in simulating long pipelines are attainable only by using models that are based on distributed parameter flow models. These models take into account all the important phenomena involved in the pipe flow.

4.6.1 Experiences

Modeling and simulation of the hydraulic system was accomplished by modeling the key components separately. Only after gaining sufficiently accurate and reliable models for each of them the component models were joined together to give a model of the total system.

The test installation used in identifying the pressure-controlled pump was similar to the one depicted in Figure 15, with the exception that the pipeline connecting the pump and the control valve was made as short as possible. This was done in

order to reduce the capacitance of the pipeline so that the excitation pressure generated by the valve would have energy content up to sufficiently high frequency.

In Figure 21 the pump and the rest of the measurement system is simulated with a linear model obtained by identification. The input signal is the flow area of the control valve and the output signal is the swash-plate angle of the pump, which is approximately linearly dependent on the flow rate produced by the pump. The results show, that the linear model, which response is plotted in green in the figure, is capable of describing the pump-system behavior accurately. The model derived from analytical mathematical description of the pump gave corresponding results.

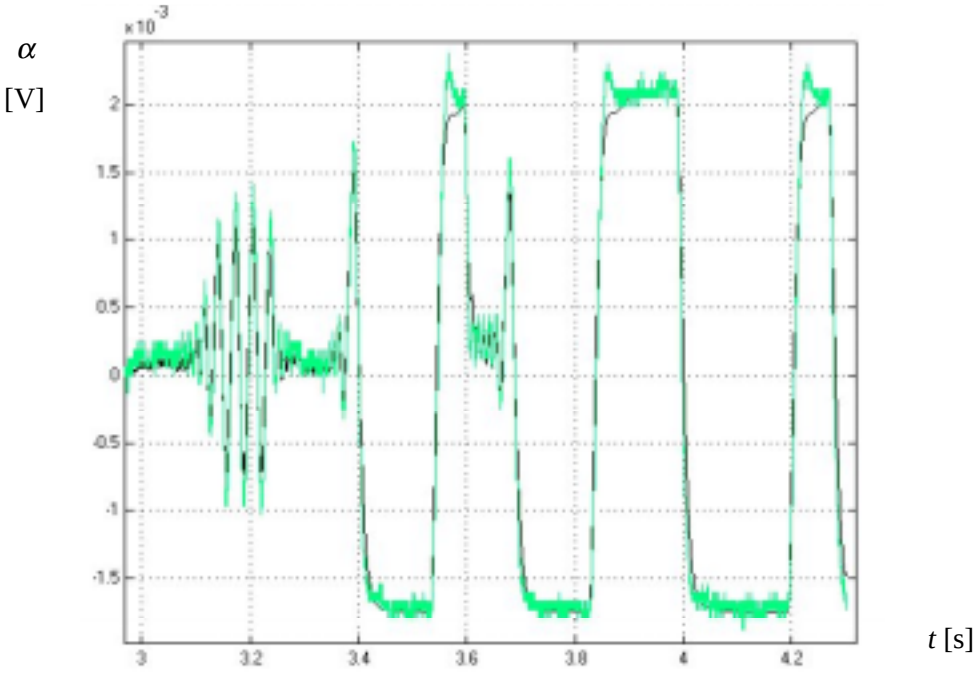

Figure 21. Measured and simulated responses of swash-plate angle of the pressure-controlled pump for a random frequency excitation

In the literature the measurement results related with pipeline dynamics are generally made with pipeline systems including straight pipes and minimum

amount of fittings. The pipelines of the measurement systems used in this project were equipped with industrial standard fittings and the layout of the piping was designed to correspond to a normal industrial system including also curved pipes and sharp bends.

A comparison of a simulated frequency response and identified frequency response is shown in Figure 22. The simulation was made with the model depicted in Figure 20 and the identified curve derives from a measurement made with a system depicted in Figure 15. The Figure 22 represents the output of the system, which is the gain of the pressure oscillation at different frequencies. At very low frequencies the pressure-controlled pump is able to compensate the changes in the flow resistance, which are caused by changing the spool position of the control valve. As a consequence of that the amplitudes of pressure fluctuations are very low near 0 Hz.

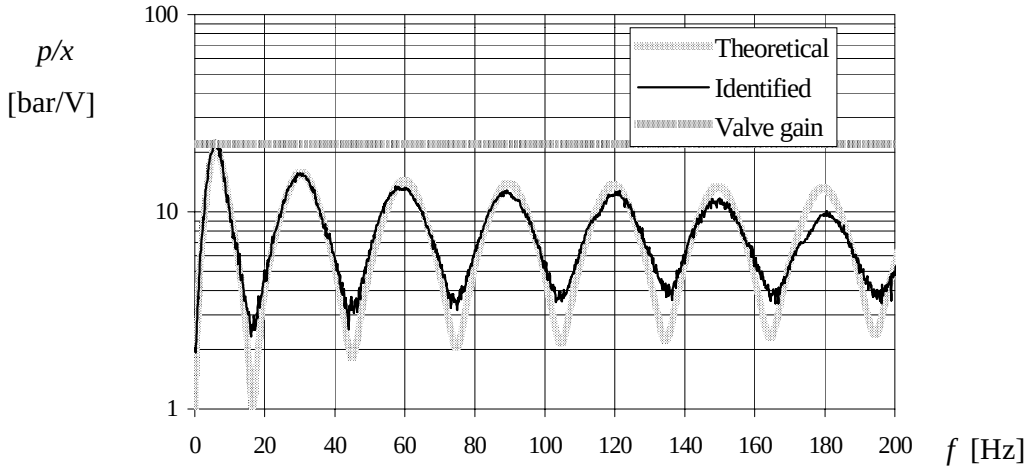

Figure 22. Measured and simulated frequency response, system pressure at measurement initiation 79 bar.

The pressure pulsations are strongest at the resonant frequencies of the system (e.g. 60, 90 and 120 Hz). At the antiresonance frequencies (e.g. 45, 75 and 105 Hz) the amount of oscillation is substantially weaker. Noteworthy is also the somewhat greater damping of the identified curve, the resonance peaks are lower

and the gains at antiresonance frequencies are smaller than what the theoretical model predicts.

The resonant frequencies of the pipeline system depend on the sonic velocity of the hydraulic fluid and the pipeline length. Experimentally it was found that the speed of sound in the liquid is both dependent on pressure level and temperature.

In addition to measuring and modeling the key components of the studied system depicted in Figure 16, the components that suppress the pressure oscillations i.e. hydraulic filters were tested and the results were compared with the models found in the literature. These models were further improved on basis of experience gained by measurements.

Figure 23 shows a measured frequency response of a system consisting of a pressure-controlled pump, a long pipeline and a membrane-type pressure accumulator and two simulations made by using the corresponding system model. The accumulator essentially decreases the amplitudes of oscillation and the damping of the accumulator is most effective near 44 Hz, which is the resonant frequency of the studied accumulator.

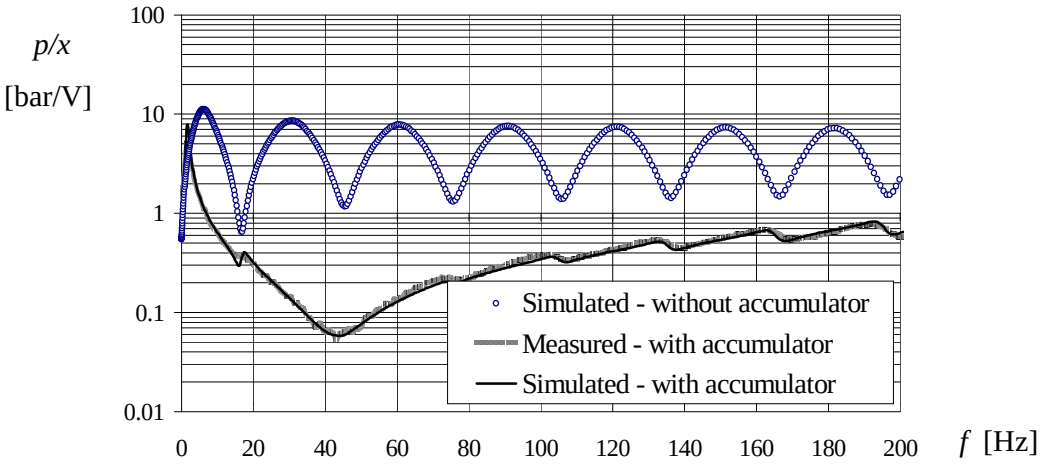

Figure 23. The system pressure oscillation at different frequencies.

4.6.2 Discussion and future research topics

The trend in system design is to shorten the time used in the planning phase and to reduce the number of prototypes needed to reach the final product. This is possible by computer-based simulation, but to be effective, it requires accurate and reliable component models.

The objective of this project was to enable simulation based design in the area of large-scale hydraulic systems. By means of the accurate models created in the project this work this can now be done more reliably.

The next phase in the project is to develop and model alternative methods to realize pressure control. The focus in this work will be in increasing the system efficiency and in cutting down the system costs. The component models created this far will be utilized along with new models in comparing the system alternatives.

Another issue that will be investigated is the attenuation of pressure pulsations. The effects of different type attenuators and attenuator locations will be clarified and design tools will be created.

5. Summary

Virtual testing of hydraulically driven machines can be of great advantage in the R&D process of both mobile working machines and industrial process machines. Basically the environmental conditions and working cycles of these machines are very different but the research and work to be done for virtual testing of these systems are quite similar. Mathematical models of both the mechanics and fluid power system and its cotrol must be made. Virtual testing can be exploited also as a marketing tool. Virtual testing can save many prototype phases in the R&D process and designers can also make some tests that are impossible or unsafe with a prototype.

There are however some hazards that must be avoided before companies can take advantage of virtual testing. First of all the attitude in the company to

virtual testing must be positive. There has to be enough knowledge of modelling and simulation work in the company.

There are some big difficulties in the modelling and simulation of fluid power systems. They contain many nonlinearities. It is also usually very difficult to find proper parameter data of the components and other parts of the system. The basic nature of fluid power systems causes mathematical stiffness in the calculation process.

This chapter presented virtual testing carried out both in one mobile and one industrial hydraulic case. Modelling and simulation is very suitable work to be done by university research groups. Companies can fully take advantage of this kind of research in their R&D work as was shown. A model must be made of the whole mobile or process machine before great time and costs save can be expected in the design process.

References

1. Palmberg, J., Krus, P. & Janssen, A. Early Prototyping in Fluid Power Technology. The 4th Scandinavian Conference on Fluid Power, 26–29 September 1995, Tampere, Finland, pp. 272–286.

Other literature

Käppi, T., Ellman, A. & Pichè, R. Implementation of Rosenbrock Integration Algorithm with Adaptive Step Size Control in Time-Domain Simulation of Fluid Power Systems. Published in proceedings of ASME'98 Fluid Power Systems Technology Symposia FPST-Vol.5. ASME IMECE, Anaheim, USA, November 16–20, 1998, pp. 35–40.

Esqué, S., Käppi, T. & Ellman, A. "Importance of the Mechanical Flexibility on Behaviour of a Hydraulic Driven Log Crane", Proceedings of the 2nd International Conference on Recent Advances in Mechatronics, Istanbul, Turkey, May 1999, pp. 359–365.

Käppi, T. & Ellman, A. Modelling and Simulation of Proportional Mobile Valves.15.–17.11.1999. Tokyo, Japan. Proceedings of the Fourth JHPS International Symposium on Fluid Power. pp. 531–536.

Esqué, S., Ellman, A. & Nykänen, T. "Aspects of The Management of Information in Modelling Multidomain Physical Systems", Proceedings of the 7th European Concurrent Engineering Conference, 17–19 April 2000, Leicester, UK, pp. 156–160.

Kajaste, J. Experiences in simulating pipeline dynamics in large-scale mechatronic fluid power systems. Tampere University of Technology. Proceedings of the ICMA'98, Tampere, Finland, September 15–18, 1998. Tampere, Finland, 1998. P. 789–803. ISBN 952-15-0036-0. (The second international conference on machine automation.)

Kajaste, J. Comportamento dinamico dei sistemi tubieri. Oleodinamica Pneumatica. April 1999, p. 80–89.

Kajaste, J. Pipeline models for large-scale fluid power systems, analysis and validation. Tampere University of Technology. Proceedings of the conference Tampere, Finland, May 26–28, 1999. Tampere, Finland, 1999. P. 529–543. ISBN 952-15-0181-2. (The Sixth Scandinavian Conference on Fluid Power.)

Kauranne, H., Kajaste, J. & Heiskanen, K. Problems in using pressure controlled pumps with long pipelines? Tampere University of Technology. Proceedings of the conference Tampere, Finland, May 26–28, 1999. Tampere, Finland, 1999. P. 545–558. ISBN 952-15-0181-2. (The Sixth Scandinavian Conference on Fluid Power.)

Käppi, T. & Ellman, A. Analytical method for defining pressure compensator dynamics. To be published in proceedings of IMECE'00. November 15–18, 2000, Orlando, USA.

Käppi, T. Modelling and Simulation Utilized in Research and Development of Mobile Hydraulics. To be published in proceedings of FPNI'00. September 20–22, 2000, Hamburg, Germany.

Käppi, T. & Ellman, A. Modelling and Simulation Utilized in Research and Development of Mobile Hydraulics. To be published in proceedings of The Fifth International Conference on Fluid Power Transmission and Control. April 3–5, 2001. Hangzhou, P.R.China.

Ellman, A., Käppi, T. & Kauranne, H. Simulation oriented R & D of hydraulically driven machines. To be published in Smart-book. 35 p.

Kajaste, J. Of the capability of component models to predict the response of a fluid power system with a long pipeline and an accumulator. Dissertation**.** Acta Polytechnica Scandinavica, Mechanical Engineering Series No. 139, Espoo 1999, 116 p. Published by the Finnish Academy of Technology. ISBN 951-666-517-9. ISSN 0001-687X.

Käppi, T. “Modelling and Simulation Utilized in Research and Development of Mobile Hydraulics”. 78 p. Dissertation. Acta Polytechnica Scandinavica, Mechanical Engineering Series, Espoo 2001, 84 p. To be published January 2001 by the Finnish Academy of Technology.

Published by

Vuorimiehentie 5, P.O.Box 2000, FIN-02044 VTT, Finland
Phone internat. +358 9 4561
Fax +358 9 456 4374

Series title, number and report code of publication

VTT Symposium 209
VTT-SYMP-209

Author(s)
Timo Holopainen (ed.)

Title

Modelling and simulation of multitechnological machine systems

Abstract

The Smart Machines and Systems 2010 (SMART) technology programme 1997–2000 aimed at supporting the machine and electromechanical industries in incorporating the modern technology into their products and processes. The public research projects in this programme were planned to accumulate the latest research results and transfer them for the benefit of industrial product development.

The major research topic in the SMART programme was called Modelling and Simulation of Multitechnological Mechatronic Systems. The behaviour of modern machine systems and subsystems addresses many different types of physical phenomena and their mutual interactions: mechanical behaviour of structures, electromagnetic effects, hydraulics, vibrations and acoustics etc. together with associated control systems and software.

The actual research was carried out in three separate projects called Modelling and Simulation of Mechtronic Machine Systems for Product Development and Condition Monitoring Purposes (MASI), Virtual Testing of Hydraulically Driven Machines (HYSI), and Control of Low Frequency Vibration of a Mobile Machine (AKSUS). This publication contains the papers presented at the final seminar of these three research projects, held on November 30th at Otaniemi Espoo.

Keywords
smart machines, mechatronics, simulation, models, condition monitoring, machinery, vibration, noise reduction, sound transmission, hydraulic equipment

Activity unit
VTT Manufacturing Technology, Maritime and Mechanical Engineering,
Tekniikantie 12, P.O. Box 1705, FIN–02044 VTT, Finland

ISBN			Project number
951–38–5712–3 (soft back ed.) 951–38–5713–1 (URL: http://www.inf.vtt.fi/pdf/)			V7SU01349
Date	Language	Pages	Price
January 2001	English	175 p.	D
Name of project Modelling and simulation of mechatronic machine systems for product development and condition monitoring purposes		Commissioned by The National Technology Agency (Tekes), VTT Manufacturing Technology, Industry	
Series title and ISSN VTT Symposium 0357–9387 (soft back ed.) 1455–0849 (URL: http://www.inf.vtt.fi/pdf/)		Sold by VTT Information Service P.O.Box 2000, FIN–02044 VTT, Finland Phone internat. +358 9 456 4404 Fax +358 9 456 4374	

VTT SYMPOSIUM

189 RETU. The Finnish Research Programme on Reactor Safety 1995–1998. Final Symposium. Espoo 24.11.1998. Ed. by Timo Vanttola. Espoo 1998. 206 p. + app. 62 p.

190 RATU2. The Finnish Research Programme on the Structural Integrity of Nuclear Power Plants. Synthesis of achievements 1995–1998. Espoo 7.12.1998. Ed. by Jussi Solin, Matti Sarkimo, Merja Asikainen & Åsa Åvall. Espoo 1998. 333 p. + app. 42 p.

191 SIHTI 2. Energia- ja ympäristöteknologia. Tutkimusohjelman vuosikirja 1998. Projektiesittelyt. Toim. Maija Korhonen & Rabbe Thun. Espoo 1999. 487 s.

192 Power Production from Biomass III. Gasification and Pyrolysis R&D&D for Industry. Ed. by Kai Sipilä & Maija Korhonen. Espoo 1999. 416 s. + liitt. 6 s.

193 30th R3-Nordic Contamination Control Symposium. Ed. by Gun Wirtanen, Satu Salo & Antti Mikkola. Espoo 1999. 503 p.

194 Proceedings of the 2nd CSNI Specialist Meeting on Simulators and Plant Analysers. Ed. by Olli Tiihonen. Espoo 1999. 600 p.

195 International Conference on Product Focused Software Process Improvement. Oulu, Finland, June 22 - 24, 1999. Ed. by Markku Oivo & Pasi Kuvaja. Espoo 1999. 662 p. + app. 4 p.

196 Käyttövarmuus ja käyttökunnon hallinta. Espoo, 18.11.1999. Toim. Kenneth Holmberg. Espoo 1999. 154 s. + liitt. 15 s.

197 15th European TRIGA Conference. Espoo, June 15 - 17, 1998. Seppo Salmenhaara (ed.). Espoo 1999. 229 p.

198 4th Workshop Demonstration of the Nutritional Functionality of Probiotic Foods. FAIR CT96-1028. Functional Foods for EU Health in 2000. Rovaniemi, Finland, February 25 - 28, 2000. Ed. by Minna Alander & Tiina Mattila-Sanholm. Espoo 1999. 106 p.

199 Maritime Research Seminar ´99. Espoo, Finland, March 17th, 1999. Ed. by Tapio Nyman. Espoo 2000. 141 p.

200 9th Nordic Symposium on Tribology. NORDTRIB 2000. Vol. 1. Porvoo, Finland, 11 - 14 June, 2000. Ed. by Peter Andersson, Helena Ronkainen & Kenneth Holmberg. Espoo 2000. 308 p.

201 9th Nordic Symposium on Tribology. NORDTRIB 2000. Vol. 2. Porvoo, Finland, 11 - 14 June, 2000. Ed. by Peter Andersson, Helena Ronkainen & Kenneth Holmberg. Espoo 2000. 308 p.

202 9th Nordic Symposium on Tribology. NORDTRIB 2000. Vol. 3. Porvoo, Finland, 11 - 14 June, 2000. Ed. by Peter Andersson, Helena Ronkainen & Kenneth Holmberg. Espoo 2000. 450 p.

203 Developing & Marketing Future Foods. The Challenge of Communication. Helsinki, Finland, 7 – 9 June 2000. Ed. by Liisa Lähteenmäki, Kaisa Poutanen & Paula Bergqvist. Espoo 2000. 45 p.

204 International Conference on Practical Applications in Environmental Geotechnology. ECOGEO 2000. Helsinki, Finland, 4 - 6 September, 2000. Ed. by Markku Tammirinne. Espoo 2000. 477 p. + app. 2 p.

205 Puuenergian teknologiaohjelman vuosikirja 2000. Puuenergian teknologiaohjelman vuosiseminaari. Jyväskylä, 29.–30.8.2000. Toim. Eija Alakangas. Espoo 2000. 295 s.

206 Käyttövarmuussuunnittelu ja diagnostiikka. Espoo, 21.11.2000. Toim. Kenneth Holmberg. Espoo 2000. 104 s. + liitt. 23 s.

207 2nd European Symposium on Enzymes in Grain Processing. ESEPG-2. Helsinki, Finland, 8 - 10 December, 1999. Ed. by Taina Simoinen & Maija Tenkanen. Espoo 2000. 337 p.

208 Nordic Treasure Hunt: Extracting Energy from Forest Residues. Jyväskylä, 30th August 2000. Ed. by Eija Alakangas. Espoo 2000. 125 p.

209 Modelling and simulation of multitechnological machine systems. Espoo, 30.11.2000. Ed. by Timo Holopainen. Espoo 2001. 175 p.

210 Virtual prototyping. VTT Research Programme 1998–2000. Espoo, Finland, February 1st, 2001. Ed. by Mikko Lehtonen. Espoo 2001. 81 p.